

## PRECISE RADIAL VELOCITIES OF 2046 NEARBY FGKM STARS AND 131 STANDARDS<sup>1</sup>

CARLY CHUBAK<sup>2</sup>, GEOFFREY W. MARCY<sup>2</sup>, DEBRA A. FISCHER<sup>5</sup>, ANDREW W. HOWARD<sup>2,3</sup>,  
HOWARD ISAACSON<sup>2</sup>, JOHN ASHER JOHNSON<sup>4</sup>, JASON T. WRIGHT<sup>6,7</sup>

(Received; Accepted)  
*Draft: Submitted to ApJ Supp.*

### ABSTRACT

We present radial velocities with an accuracy of 0.1 km s<sup>-1</sup> for 2046 stars of spectral type F,G,K, and M, based on ~29000 spectra taken with the Keck I telescope. We also present 131 FGKM standard stars, all of which exhibit constant radial velocity for at least 10 years, with an RMS less than 0.03 km s<sup>-1</sup>. All velocities are measured relative to the solar system barycenter. Spectra of the Sun and of asteroids pin the zero-point of our velocities, yielding a velocity accuracy of 0.01 km s<sup>-1</sup> for G2V stars. This velocity zero-point agrees within 0.01 km s<sup>-1</sup> with the zero-points carefully determined by Nidever et al. (2002) and Latham et al. (2002). For reference we compute the differences in velocity zero-points between our velocities and standard stars of the IAU, the Harvard-Smithsonian Center for Astrophysics, and l'Observatoire de Geneve, finding agreement with all of them at the level of 0.1 km s<sup>-1</sup>. But our radial velocities (and those of all other groups) contain no corrections for convective blueshift or gravitational redshifts (except for G2V stars), leaving them vulnerable to systematic errors of ~0.2 km s<sup>-1</sup> for K dwarfs and ~0.3 km s<sup>-1</sup> for M dwarfs due to subphotospheric convection, for which we offer velocity corrections. The velocities here thus represent accurately the radial component of each star's velocity vector. The radial velocity standards presented here are designed to be useful as fundamental standards in astronomy. They may be useful for Gaia (Crifo et al. 2010; Gilmore et al. 2012) and for dynamical studies of such systems as long-period binary stars, star clusters, Galactic structure, and nearby galaxies, as will be carried out by *SDSS*, *RAVE*, *APOGEE*, *SkyMapper*, *HERMES*, and *LSST*.

*Subject headings:* stars: fundamental parameters — techniques: radial velocities — techniques: spectroscopic — stars: kinematics — stars: late-type — reference systems — Galaxy:kinematics and dynamics — binaries: spectroscopic

### 1. INTRODUCTION

Doppler shifts of stellar spectra provide information about the line-of-sight component of the velocity vector of the target stars in the frame of the telescope. When transformed to the frame of the center of mass of the Solar System, those "barycentric" radial velocities represent the star's velocity component measured relative to a well defined, and commonly adopted, inertial frame within our Milky Way Galaxy, suitable for studying the motions of stars in a wide variety of astronomical settings.

Barycentric radial velocities enable study of the kinematics, structure, and mass distribution of the Milky Way Galaxy, including the disk components, bulge, nu-

cleus, and halo. Doppler measurements also provide a primary tool for detecting and characterizing binary stars in many environments such as in the general field, open clusters, star forming regions, planet-hosting stars, globular clusters, and the Galactic center. Radial velocities also serve to measure the dynamics and mass content, both luminous and dark, of star clusters and galaxies. Moreover, radial velocities are vital for measuring the infalling extragalactic matter into our Galaxy, as well as the dynamically important motions of stars within other galaxies in the local group.

When combined with the proper motion and positions measured using, e.g., the Hipparcos telescope or the upcoming Gaia space telescope, one can measure the three dimensional velocity vectors of stars and stellar systems. Such three dimensional velocity measurements offer information about the origin, history, future, and mass distribution of the components of the Galaxy. Precise radial velocities measured over time can reveal the acceleration of stars, caused surely by gravitational forces exerted by unseen nearby objects including orbiting planets, brown dwarfs, and stars, as well as by nearby compact objects such as white dwarfs, neutron stars, and black holes.

Many new observational facilities are now, or soon will be, providing kinematic and positional information about stars in the Galaxy. The *RA*dial *VE*locity *EX*periment (*RAVE*) is studying the properties and origin of the structure in the Galactic disc (Wilson et al. 2011) by measuring velocities with an accuracy of ~2 km s<sup>-1</sup> for up to 500,000 stars. The Sloan Digital Sky

gmarcy@berkeley.edu

<sup>1</sup> Based on observations obtained at the W.M. Keck Observatory, which is operated jointly by the University of California and the California Institute of Technology, and on observations obtained at the Lick Observatory which is operated by the University of California.

<sup>2</sup> Department of Astronomy, University of California, Berkeley, CA USA 94720

<sup>3</sup> Townes Fellow, Space Sciences Laboratory, University of California, Berkeley, CA 94720, USA

<sup>4</sup> Department of Astrophysics, California Institute of Technology, Pasadena, CA 91125, USA

<sup>5</sup> Department of Astronomy, Yale University, New Haven, CT 06511, USA

<sup>6</sup> Department of Astronomy & Astrophysics, The Pennsylvania State University, University Park, PA 16802, USA

<sup>7</sup> Center for Exoplanets and Habitable Worlds, The Pennsylvania State University, University Park, PA 16802, USA

Survey and the *Sloan Extension for Galactic Understanding and Exploration* (SEGUE), with its imaging and radial velocity capability (with  $10 \text{ km s}^{-1}$  accuracy) are performing extraordinary measurements on the kinematics of the Galaxy and its halo (Schoenrich *et al.* 2010). Some groups are combining spectroscopy with these kinematic measurements to gain unprecedented information about the coupled chemical and kinematic properties of the solar neighborhood in the Galactic context (Casagrande *et al.* 2011). The Gaia-ESO Survey with VLT/Flames will be particularly valuable with its spectroscopy of 100,000 stars in all stellar populations and will nicely complementing the measurements of Gaia (Gilmore *et al.* 2012).

Radial velocity standard stars of a wide range of stellar types provide useful Doppler calibrators for the many different instruments doing this kinematic work. The radial velocity standard stars provide touchstones of comparisons for both zero-points and the velocity scales of the different instruments and observatories.

Despite these current and future uses of radial velocities, one might wonder whether highly precise, absolute radial velocities have value in the modern era. After all, it is relative velocities not absolute barycentric velocities that are used to discover orbiting exoplanets, measure orbits of binary stars, measure velocity dispersions in virialized systems of stars, and to measure masses of compact objects including supermassive black holes. Moreover accurate radial velocities could be obtained by using carefully chosen reference template spectra, either observed (of asteroids, for example) or synthetic. These arguments for the obsolescence of absolute velocities may have some validity for those specialists performing radial velocity measurements. But for the majority of astronomers there remains a widespread need to measure radial velocities as part of a larger project for which exhaustive calibration is not practical. Radial velocity standards offer a sound method at the telescope to place one's Doppler measurements on a well established scale and to learn their accuracy by observing multiple standard stars with one's particular (and sometimes peculiar) instrument. Further, new spectrometers on the ground or in space often come online with uncertain wavelength scales, structural and thermal instabilities, or errors that depend on stellar temperature, all of which can be mitigated by a real-time determination of the velocity zero-point and scale. Radial velocity standard stars offer that metric to establish and demonstrate accuracy and internal precision.

Some information about radial velocity standards is maintained by the International Astronomical Union (IAU), Commission 30 found at <http://sb9.astro.ulb.ac.be/iauc30/>. The IAU has constructed a precise definition of "radial velocity" described by Lindegren & Dravins (2003).

The old standard source of radial velocities was the General Catalog of Stellar Radial Velocities (BCRV) prepared at the Mount Wilson Observatory in Pasadena, California (Wilson 1953). The modern era of radial velocity standards occurred with the work by the Geneva group led by Michel Mayor and Stephane Udry, the University of Victoria group led by Collin Scarfe and Robert McClure, and the group at the Harvard-Smithsonian

Center for Astrophysics led by David Latham and Robert Stefanik (Mayor & Maurice 1985; Scarfe *et al.* 1990; Latham *et al.* 1991, 2002). An excellent summary of the history of radial velocity standards through 1999 is provided by Stefanik *et al.* (1999).

Three excellent radial velocity programs provided standards with high accuracy and integrity (Stefanik *et al.* 1999; Udry *et al.* 1999a,b), all of them constituting a modern velocity zero-point with accuracy better than  $0.3 \text{ km s}^{-1}$ . Additional excellent stellar radial velocity measurements were made by Nordström *et al.* (2004); Famaey *et al.* (2005) at accuracies of  $\sim 0.3 \text{ km s}^{-1}$ , and also by the Fick Observatory at Iowa State University, and at the Mt. John University Observatory in Christchurch, New Zealand (Beavers & Eitter 1986; Hearnshaw & Scarfe 1999). The Pulkova Radial Velocity Catalog compiles the mean velocities for over 35000 Hipparcos stars (Gontcharov 2006). The velocities come from over 200 publications, yielding a median accuracy of  $0.7 \text{ km s}^{-1}$ .

The largest modern catalog of radial velocity standard stars was established by Nidever *et al.* (2002) who measured the radial velocities of 889 FGKM-type stars with an accuracy of  $0.1 \text{ km s}^{-1}$  in the solar system barycentric frame. Nidever *et al.* (2002) made multiple radial velocity measurements with the Keck 1 telescope and High Resolution Echelle Spectrometer (Vogt *et al.* 1994) over a typical time span of 3-7 years, thereby revealing any velocity variability. Use of an iodine cell to impose a wavelength scale yielded relative radial velocities with a precision of  $0.003 \text{ km s}^{-1}$  (RMS, with no zero-point) able to detect tiny velocity variability at the level of  $0.01 \text{ km s}^{-1}$  on time scales of years. Thus, the radial velocity standard stars in Nidever *et al.* (2002) met the highest standard for constancy in velocity. We adhere to that standard here.

Nidever *et al.* (2002) contained more stellar radial velocities at the highest viable accuracy of  $0.1 \text{ km s}^{-1}$  than any previous radial velocity survey, and they provided statistically robust comparisons of the zero-points of other radial velocity surveys. The radial velocity measurements of Nidever *et al.* (2002) thus uphold high integrity for a wide range of spectral types and provide standard stars at all RA and northward of declination  $-30 \text{ deg}$ .

Here we extend the work of Nidever *et al.* (2002) with 9 additional years of radial velocity measurements from the same Keck 1 telescope and spectrometer. These measurements supersede those in the Nidever *et al.* paper by providing more velocity measurements over a longer time baseline, and we include more stars. We include only those 2046 stars for which we obtained Keck-HIRES spectra using the modern CCD detector in HIRES that was installed in June 2004, as we use only the near-IR portion of the spectrum made available at that time. Thus some stars listed in Nidever *et al.* are not included here. We establish 131 standard stars, with radial velocities measured relative to the barycenter of the solar system for spectral types FGKM that are stable at the level of  $0.01 \text{ km s}^{-1}$  during a decade, and we provide barycentric velocities for 2046 FGKM stars. The final velocities have an precision of typically better than  $0.1 \text{ km s}^{-1}$ , and they reside on the Nidever *et al.* velocity scale. We compare these velocities to extant velocities

by other groups.

## 2. SPECTROSCOPIC OBSERVATIONS AND VELOCITY MEASUREMENTS

We obtained spectra using the HIRES echelle spectrometer on the 10-m Keck 1 telescope between 2004 August and 2011 January, as part of the California Planet Survey (CPS) to detect exoplanets by the Doppler technique, using iodine to calibrate both wavelength and the instrumental profile spectrometer at each wavelength (Marcy et al. 2008; Johnson et al. 2011). Before each observing night we positioned the CCD so that the (observatory-frame) wavelengths land on the same pixels within 1/2 pixel as on all previous observing nights. This produced a nearly identical wavelength scale on all nights. At the beginning and end of each observing night, we took spectra of a thorium-argon lamp, providing the linear and non-linear portion of the wavelength scale information, but not the zero-point of the wavelength scale which was instead established by absorption lines formed in the Earth’s atmosphere (see below). We found that the wavelength dispersion of HIRES varies by about 1 part in 2000 over the course of months and years, presumably due to slow mechanical and thermal changes in the spectrometer optics and to changes in air pressure. All 29000 spectra of the 2046 stars and all calibration spectra are available on the Keck Observatory Archive (after the nominal proprietary period of 18 months), made possible by a NASA-funded collaboration between the NASA Exoplanet Science Institute (NExSci) and the W. M. Keck Observatory<sup>8</sup>.

We employed an exposure meter to set exposure times for each observation, promoting uniform and high signal-to-noise spectra during the seven years of observations (Kibrick et al. 2006). The spectra had a typical S/N  $\sim 150$  per pixel at 720 nm, which is near the center of the near-IR wavelength domain, 654 - 800 nm, used in this paper. The spectral resolution was,  $R = 55,000$  and the pixel spacing corresponds to a Doppler shift of 1.3 km s<sup>-1</sup> per pixel at the blaze wavelength of all spectral orders. The dispersion was found to vary by  $\sim 10\%$  along the free spectral range of each order. The spectrometer instrumental profile had a typical FWHM of  $\sim 4.2$  pixels, varying by 10-20% as a function of wavelength. In this current work, we used both types of spectra obtained as part of the CPS planet-search program, namely those with the iodine cell in front of the spectrometer slit for which the starlight passed through the molecular iodine gas (Marcy & Butler 1992) and those with the iodine cell not in the beam that contain no iodine lines. The presence of iodine cell has little effect on the Doppler measurements because the iodine lines are less than 1% deep in the near-IR wavelength regions used here.

We carefully determined a wavelength scale for each spectrum. We first fit a fifth-order polynomial to the positions of the thorium lines, with their associated wavelengths, to determine a first-approximation to the wavelength scale (called "thid" files). We used a spline to map the spectra onto a logarithmic wavelength scale, based on the original wavelength scale from the thorium-argon spectra. The new array pixels were designed to be separated by equal intervals in  $\Delta \ln \lambda$ . This loga-

rithmic wavelength scale offers the advantage that a certain difference in radial velocity,  $\Delta v$ , causes the spectrum to be displaced by the same distance in units of pixels at all wavelengths, given by  $\Delta v = c \Delta \ln \lambda$ . The typical pixel size for a Keck HIRES spectrum corresponds to a Doppler shift of 1.3 km s<sup>-1</sup>, and this thorium-based wavelength scale determined the *relative* wavelength scale to 6 significant digits ( $\sim 0.1$  pixel), based on the scatter in the fits. The wavelength zero-point remained to be set accurately (using telluric lines, as described below). Instead of cross-correlation, we used the chi-square statistic to determine the relative shifts between a template spectrum and observed spectrum. To measure fractional pixel shifts, we oversampled, at 0.01 km s<sup>-1</sup> per pixel, a subarray around the minimum of each chi-squared function and interpolated with a spline function.

To determine a secure wavelength zero-point for each spectrum, we followed the suggestion of Griffin (1973) by using telluric lines to determine the wavelength scale. We used the telluric A and B absorption bands, at wavelengths of 759.4-762.1 nm and 686.7-688.4 nm respectively, due to absorption by molecular oxygen in the Earth’s atmosphere. We again used a  $\chi^2$  minimization method to find the displacement of the telluric lines in the program star relative to those in the reference B-type star spectrum of HD 79439. Figure 1 shows the telluric lines in both that reference spectrum and in the representative spectrum of a program star, HD 182488. The program star spectrum has telluric lines clearly displaced by a fraction of a pixel (redward), in this case by +0.437 pixels, an amount representative of the typical shifts in wavelength zero-point from observation to observation over the time scale of days, months, and years covered by the spectra presented here. This measurable displacement of telluric lines provides the key correction to the wavelength zero-point that accounts for small changes (typically less than 1 km s<sup>-1</sup>) in the CCD position, the spectrometer optics, and (importantly) for the non-uniform illumination of the starlight on the entrance slit of the spectrometer.

This approach corrects for the dominant systematic errors that often compromise normal radial velocity measurements that do not use an absorbing gas to establish the wavelength scale of a slit-fed (rather than fiber-fed) spectrometer. We subtracted this displacement from the apparent shift of the stellar lines in order to find the net (true) Doppler shift. In this way we found the radial velocity determined by the Doppler shift of stellar absorption lines, including a correction for the shift in the wavelength zero-point. Using telluric lines to set the wavelength zero-point leaves systematic errors of  $\sim 0.01$  km s<sup>-1</sup> caused by typical winds in the Earth’s atmosphere. Also, the telluric lines we used (the A and B bands) are not distributed in wavelength coincident with the stellar lines we employed. An additional Doppler error may accrue due to unaccounted for nonlinear errors in the wavelength scale. We find such errors to be several tens of meters per second.

We chose four wavelength segments in the near-IR that are rich in stellar absorption lines in FGKM stars, but nearly free of telluric lines. Using a spectrum of the A5 star, HR 3662, we determined which regions of the spectra in the near-IR of HIRES spectra are largely unpol-

<sup>8</sup> <http://ssd.jpl.nasa.gov/>

luted by telluric lines. The resulting four wavelength regions were 679.5-686.7 nm, 706.7-714.6 nm, 739.8-748.9 nm, and 751.8-759.3 nm. In these wavelength regions, we carried out Doppler measurements by using standard chi-square minimization as a function of Doppler shift between the spectra of the program star and template reference star. We averaged the velocities from the four wavelength segments of the spectrum, and we recorded that average value as the star's radial velocity. We employed two template spectra. For the FGK stars, we used a spectrum of sun-light reflected off Vesta as a solar proxy. As Vesta is unresolved, its use ensured that the spectrometer optics were illuminated in nearly the same way as by the program stars. For M dwarfs we used a spectrum of HIP 80824 (spectral type M3.5). We applied a barycentric correction to the velocity for each spectrum in the frame of the solar system barycenter.

The resulting "raw" radial velocities were systematically different from those of Nidever *et al.* (2002) by an arbitrary constant amount due to the radial velocity and barycentric correction of the template spectrum. We calculated this constant by taking a sample of 110 standard FGKM stars in Nidever *et al.* (2002) and comparing those velocities to our measured raw velocities for those stars. We determined the average difference between our raw velocities and those of Nidever *et al.* (2002), constituting the constant to be applied to all of our velocity measurements. This automatically forces our radial velocities to have the same zero-point as those of Nidever *et al.* (2002).

Thus our velocity measurements reside on the scale of Nidever *et al.* (2002) by construction. These radial velocities of stars are measured relative to a hypothetical inertial frame located at the barycenter of the Solar System. This transformation is accomplished by using the JPL ephemeris of the Solar System to determine the velocity vector of the Keck 1 telescope at the instant of the photon-weighted midpoint of the exposure of the spectrum (accurate to within a few seconds). Our transformation to the barycentric frame is performed using the JPL ephemeris<sup>9</sup>, accessed and interpreted with utilities from the IDL Astronomy User's Library<sup>10</sup> and custom driver codes written by the California Planet Survey. We carried out extensive tests of our barycentric transformation code, finding discrepancies of  $0.1 \text{ m s}^{-1}$  in comparison with TEMPO 1.1 which is similar to that of TEMPO 2 (Edwards *et al.* 2006). Errors of that magnitude,  $10^{-4} \text{ km s}^{-1}$ , are negligible compared to other sources of error in this present work.

As usual for such transformations to the Solar System barycenter, we do not include the effects of the solar gravitational potential at that location (near the surface of the Sun) that would cause a (meaningless) gravitational blueshift. Similarly, we do not account for the gravitational blueshift caused by starlight falling into the potential well of the Sun at the location of the Earth, a  $\sim 3 \text{ m s}^{-1}$  effect. We also do not take into account the gravitational redshift as light departs the photosphere of the star, an effect of hundreds of  $\text{m s}^{-1}$  that depends on stellar mass and radius.

We further ignore the convective blueshift of the

starlight caused by the Doppler asymmetry between the upwelling hot gas and the downflowing cool gas. Convective blueshift depends on spectral type (Dravins 1999), and we do not include any theoretical estimates of this photospheric hydrodynamic effect here. Both gravitational redshift and convective blueshift amount to a few tenths of a kilometer per second, and while they are opposite in sign they may not cancel each other. However see Section 4 for a quantitative discussion of these two effects, that appear to largely cancel each other. We note that several efforts have been successful at measuring the convective blueshift in a few stars, especially for the Sun and the alpha Centauri system (Ramírez *et al.* 2010; Dravins 2008; Nordlund 2008; Pourbaix *et al.* 2002).

### 2.1. Radial Velocity Standard Stars

We identified standard stars from among the 2046 total sample of stars based on several criteria. We examined the iodine-based relative velocities, having a precision of  $\sim 3 \text{ m s}^{-1}$ , for each of the 2046 stars. We established a severe criterion of stability during 10 years in order for a star to be qualified as a "radial velocity standard star". All standard stars must exhibit an RMS of their iodine-based relative velocities under  $0.03 \text{ km s}^{-1}$  (Marcy & Butler 1992) and a duration of such velocity measurements of at least 10 years. Figure 2 displays the iodine-based relative velocities for three representative standard stars. The absolute radial velocity relative to the Solar System sets the zero-point and the relative velocities come from the iodine-based Doppler measurements. The velocities of the three representative cases exhibit an RMS of under  $0.010 \text{ km s}^{-1}$  ( $10 \text{ m s}^{-1}$ ) and span over 10 years, typical of the standard stars, promoting their integrity as standard stars at the more relaxed level of  $0.1 \text{ km s}^{-1}$ .

Thus, our radial velocity standard stars must demonstrate constant velocity during a decade within a tolerance of  $30 \text{ m s}^{-1}$  RMS during that time. We required that at least 3 spectra be obtained over a 10 year time period to demonstrate the decade-long stability. We identified 131 standard stars based on these criteria. Among them, only 12 exhibit an RMS scatter in their iodine-based RVs of more than  $0.01 \text{ km s}^{-1}$ , and none over  $0.03 \text{ km s}^{-1}$ , during 10 years of observations. Thus, the 131 standard stars all exhibit radial velocity stability during a decade at the level of  $0.03 \text{ km s}^{-1}$ .

The barycentric radial velocities for the 131 standard stars are reported in Tables 1 and 2. In Table 1, primary and alternate star names are given in the first three columns, and the spectral type is given in column 4. Columns 5, 6, and 7 give the Julian dates of the first and last observations, and the duration of observations in years. Column 8 lists the radial velocity of the star relative to the solar system barycenter given by Nidever *et al.* (2002). Column 9 lists the unweighted average of all radial velocity measurements from this current work. In the next two columns we list the standard deviation of the multiple velocities we measured here for the star and the number of spectra used. We report the final velocity for each standard star as the average of the Nidever *et al.* (2002) and present velocities. We consider this final radial velocity to be robust as both sets of velocities have high integrity and we do not rank one set significantly higher in integrity than the other. Impor-

<sup>9</sup> <http://ssd.jpl.nasa.gov/>

<sup>10</sup> <http://idlastro.gsfc.nasa.gov/>

tantly, the Nidever et al. velocities and these new velocities were determined using completely different Doppler algorithms and different wavelength regions. Thus the Nidever and present radial velocities offer considerable resistance to unexpected errors associated with any particular method or wavelength. The Nidever et al. velocities had a wavelength scale rooted in the iodine lines and measured using the 500-600 nm wavelength region, quite different from the wavelength scale here rooted in telluric lines at 670 and 760 nm and measured using the near IR spectrum.

The radial velocity uncertainty recorded in Tables 1 and 2 is the largest of three values: the difference between our present velocity and Nidever's, the uncertainty in the mean, or  $0.03 \text{ km s}^{-1}$ , which we deemed our base accuracy, to prevent artificially low uncertainties. Table 2 lists the same standard stars, but in a format more suitable for observing. We give the primary name, position in RA and DEC, magnitude, spectral type, final absolute radial velocity, and uncertainty.

Establishing and maintaining a single, well-defined velocity scale, including zero-point accuracy and precision, is important to make the radial velocities more useful. The velocity scale must be compared to other well-known scales. In particular, our velocities are compared here to those from Geneva, Harvard-Smithsonian, and the California Planet Survey<sup>11</sup>.

We compared our "present" velocities to those of the standard stars of Udry et al. (1999a). The average of the differences (i.e. zero-point difference) is:

$$\langle V_{\text{present}} - V_{\text{Udry}} \rangle = +0.063 \text{ km s}^{-1}.$$

Thus there is a statistically significant difference in the zero-points. That this difference is less than  $0.1 \text{ km s}^{-1}$  offers some scale to the integrity of the discrepancies in the two systems of radial velocities. The RMS of the differences is  $0.072 \text{ km s}^{-1}$  (RMS) for the 30 standard stars in common, as shown in Figure 3. Thus the two sets of velocities agree within  $0.1 \text{ km s}^{-1}$  in zero point and scatter. However, the differences in the velocities appear to be correlated with stellar B-V color, suggesting a systematic error. Inspection of Figure 3 shows that it is the M dwarfs, with  $B-V > 0.9$  where the systematic difference resides of (present - Udry) =  $+0.10 \text{ km s}^{-1}$ . Thus, while the FGK stars of Udry et al. and the present set have different velocity zero-points by  $0.063 \text{ km s}^{-1}$ , the M dwarfs differ by  $0.10 \text{ km s}^{-1}$ .

We also compared our velocities to those of Stefanik et al. (1999). Considering the 25 standard stars in common, as seen in Figure 4, the average of the differences is:

$$(V_{\text{present}} - V_{\text{Stefanik}}) = +0.15 \text{ km s}^{-1}.$$

The differences in the 25 velocities have a scatter of  $0.13 \text{ km s}^{-1}$  (RMS). Thus the present velocities differ in zero-point from those of Stefanik et al. (1999) by a statistically significant amount (see Section 4 for the explanation).

A useful compilation of velocities was provided by Crifo et al. (2010) based on various past surveys. They show that the velocities from Nidever et al. (2002) are

valuable because of the accuracy ( $< 0.1 \text{ km s}^{-1}$ ), the large number of observations, and the long duration of the velocity time series. They compare the Nidever et al. velocities to those from past CORAVEL measurements that have typical accuracy of  $0.3 \text{ km s}^{-1}$ , finding good agreement within errors. They offer a preliminary list of standard stars drawn heavily from Nidever et al. (2002). Thus the zero-point and scale of the velocities in Crifo et al. naturally agree with those here.

We also compare our measurements of M dwarfs to those of Marcy et al. (1987). We find that the velocity differences scatter by  $0.26 \text{ km s}^{-1}$  (RMS) and our zero-points are different by

$$\langle V_{\text{present}} - V_{\text{Marcy}} \rangle = 0.007 \text{ km s}^{-1}$$

for the 17 stars in common (see Figure 5). As the velocities from Marcy et al. (1987) are expected to carry precision of only  $\sim 0.2 \text{ km s}^{-1}$ , this scatter of  $0.26 \text{ km s}^{-1}$  RMS is consistent with most of the error residing in Marcy et al. (1987) and only  $\sim 0.1 \text{ km s}^{-1}$  residing in the errors in the present velocities of M dwarfs.

The differences in the velocities between those of Nidever et al. (2002) and those of both Udry et al. (1999a) and Stefanik et al. (1999) exhibited a scatter of less than  $0.1 \text{ km s}^{-1}$  (RMS), and our present velocities differ from those previous standard measurements within a margin of  $0.1 \text{ km s}^{-1}$  (RMS). *Thus, the velocities reported here agree with the best established standard stars to within  $0.1 \text{ km s}^{-1}$  in precision, with modest zero-point differences of comparable magnitude.*

We show in section 2.3, that the radial velocities measured here for 428 stars in common with Nidever et al. (2002) agree within  $\sim 0.13 \text{ km s}^{-1}$  (RMS) and that there is little dependence on the color of the stars. This comparison of 428 stars offers further weight to the suggestion that the standard stars in Tables 1 and 2 have integrity at the level of  $0.1 \text{ km s}^{-1}$ . We also show in Section 4 that the zero-point of the velocity scale has integrity at the level of  $0.1 \text{ km s}^{-1}$ .

## 2.2. Uncertainty in the Velocities of Standard Stars

We compute the uncertainty of the radial velocity for each of the 131 standard stars by considering two separate estimates of the uncertainty. The first estimate is the uncertainty of the mean velocity measurement, defined as  $\sigma/N_{\text{obs}}^{1/2}$ , where  $\sigma$  is the standard deviation of the ensemble of velocities for a particular star. This estimate offers a measure of the internal uncertainty revealed by the scatter in the individual velocity measurements. As a second estimate of uncertainty we compute the difference between the radial velocity measured here and the radial velocity published in Nidever et al. (2002). This difference in radial velocities offers a measure of agreement in the two radial velocity measurements despite two different methods used to compute them and two different sets of spectra used to measure them in the two papers. The largest of these two uncertainty estimates, but not less than  $0.030 \text{ km s}^{-1}$ , is listed in Tables 1 and 2 as the final estimate of the 1-sigma uncertainty for the radial velocity of each standard star. We adopted this floor  $0.030 \text{ km s}^{-1}$  for the stated uncertainty because this was the uncertainty of the velocities given in Nidever et al.

<sup>11</sup> <http://exoplanets.org>

(2002). Any fortuitous agreement between the current velocities and those in Nidever *et al.* that happens to be smaller than  $0.030 \text{ km s}^{-1}$  could well be spurious. This adopted floor at  $0.030 \text{ km s}^{-1}$  prevents our quoted measurement uncertainty from dropping lower than the level below which we have no useful comparison with the Nidever *et al.* velocities.

To broaden the scope of this uncertainty assessment for the standard stars, we compared the measured radial velocities here to those in common with Nidever *et al.* (2002) among the full set of 2046 stars, not just the standard stars. We display the difference between our present radial velocities and those of Nidever *et al.* (2002) in Figure 6 for FGK stars and Figure 7 for the M dwarfs. For the 428 FGK stars in common, the differences have an RMS of  $0.13 \text{ km s}^{-1}$ . Thus the combined errors in the present work and in Nidever *et al.* amount to  $0.13 \text{ km s}^{-1}$  for the FGK stars, as described in more detail in Section 2.3. For the 52 M dwarfs in common, the differences exhibit an RMS of  $0.13 \text{ km s}^{-1}$  (with three outliers near  $0.4 \text{ km s}^{-1}$ ) indicating the level of combined errors among M dwarfs in the two studies. The errors in the final velocities for the standard stars will be smaller than quoted above for the entire set of 2046 stars because the standards typically have more observations and have constant radial velocities by their selection.

### 2.3. Radial Velocities of 2046 Stars

Table 3 reports the radial velocities of all 2046 stars (including the standards) relative to the solar system barycenter. The same technique that was used to determine the radial velocities of the standard stars was used to determine the radial velocities for all 2046 stars. In Table 3, the primary star name is given in column 1, and the template type in column 2. The symbol "V" represents the Vesta spectrum (solar), and "M" represents the constructed M-dwarf template described above. The 3rd column gives the unweighted mean of the Julian Dates of our observations, and the 4th column gives the number of days between the first and last observation. For each star, we compute the unweighted average of all radial velocity measurements from all spectra we obtained for that star. The 5th column gives that average radial velocity for the star, measured in the frame of the barycenter of the solar system. The 6th column gives the number of radial velocity observations, and the 7th column gives the standard deviation of all radial velocity measurements of that star, a measure of both the uncertainty and of the intrinsic variation of the radial velocities.

Examination of Table 3 shows that among the 2046 stars with measured radial velocities, some stars have only one or two velocity measurements while others have over 30 measurements. The time span between the first and last spectrum is typically over a year, and often many years. The standard deviation of the velocities given in the last column is a measure of the combined errors and acceleration of the star during the time span of observations. The median standard deviation is  $0.12 \text{ km s}^{-1}$ , representing the uncertainty of our individual velocity measurements, but increased slightly by the actual velocity variations of the stars.

One measure of the 1-sigma errors of the radial velocities in Table 3 is given by the uncertainty in the mean,

namely,  $\sigma_{\text{RV}}/N_{\text{Obs}}$ . However, because of systematic errors caused by convection of  $\sim 0.1 \text{ km s}^{-1}$  described in Section 4, we prefer to avoid stating the formal uncertainties that could be misinterpreted as useful uncertainties. Also, some stars exhibit intrinsic velocity variation caused by unseen orbiting companions, thus artificially augmenting the formal uncertainty in the mean.

Nonetheless, examination of  $\sigma_{\text{RV}}$  in the last column of Table 3 shows scatter of typically  $0.15 \text{ km s}^{-1}$  for individual velocity measurements, serving as an upper limit to the typical errors. Thus any values of  $\sigma_{\text{RV}}$  in Table 3 greater than  $0.45 \text{ km s}^{-1}$  (3 sigma) are likely "real", i.e. indicating actual changes in the radial velocity of that star by an amount given by that standard deviation on a time scale constrained by the time span of the observations.

We have compared the present velocities to those of Nidever *et al.* (2002). Nidever *et al.* used the iodine lines and the visible portion of the spectrum to measure Doppler shifts, a method quite independent of that used here. Thus a comparison of the two sets of the velocities for stars in common offers a method of identifying random and systematic errors that stem from the Doppler methods themselves. Figure 6 shows the difference between the present velocities and those of Nidever *et al.* (2002) as a function of stellar color, B-V, for all 428 stars in common classified as F, G, or K spectral type. The plot shows that the differences in the velocities are typically less than  $0.2 \text{ km s}^{-1}$ , with an RMS of the differences of  $0.13 \text{ km s}^{-1}$ , and there is no evidence of a dependence on stellar color. (We removed HD 217165 from the RMS calculation, which is a binary star.) This suggests that the accuracy and zero-points of the present and Nidever *et al.* velocities are similar within  $\sim 0.13 \text{ km s}^{-1}$  (RMS).

However, Figure 6 reveals six stars (with one off scale) for which the difference between present and Nidever *et al.* velocities are over  $0.5 \text{ km s}^{-1}$  ( $>3$  sigma differences). These stars are HD 87359 ( $+0.81 \text{ km s}^{-1}$ ), HD 114174 ( $+0.58 \text{ km s}^{-1}$ ), HD 180684 ( $+0.61 \text{ km s}^{-1}$ ), HD 196201 ( $+0.65 \text{ km s}^{-1}$ ), HD 91204 ( $-0.74 \text{ km s}^{-1}$ ), and HD217165 ( $-2.2 \text{ km s}^{-1}$ ). Examination of the iodine-based relative velocities (precise to  $0.002 \text{ km s}^{-1}$  RMS) for these six stars reveals all of them to exhibit long-term trends of velocity of over  $0.5 \text{ km s}^{-1}$ . These are certainly long period binary stars. The difference between the present velocities and those of Nidever *et al.* (2002) is simply due to the orbital motion that has occurred since the spectra were taken for the work of Nidever *et al.* (prior to 2002) and those here that were taken after 2004 June. Thus, the present velocities offer a sieve for binary stars,

Figure 7 shows a similar comparison of present velocities and those of Nidever *et al.* (2002) for the 52 M dwarfs in common. The RMS of the differences of  $0.13 \text{ km s}^{-1}$  indicates larger errors for the M dwarfs than for the FGK-type stars. This error is reminiscent of that seen in Figure 4 for which the difference between the present velocities and those of Udry *et al.* (1999a) among the M dwarfs was  $0.15 \text{ km s}^{-1}$ . These metrics suggests that the M dwarf velocities in general, from all surveys, remain uncertain at the level of  $0.2 \text{ km s}^{-1}$  (RMS) and harbor uncertain zero points at the level of  $0.15 \text{ km s}^{-1}$ .

Figure 8 shows the location of the stars in equatorial

coordinates in a Mollweide projection on the sky. The broad distribution at all RA, and northward of DEC = -50 offers a set of secondary standard stars. The dots are color-coded with blue representing stars approaching and red representing stars receding from the barycenter of the solar system. The size of the dots is proportional to the square root of the absolute value of the radial velocity, an arbitrary functional form for ease in display. The solar apex is shown as a cross, the direction of the motion of the sun relative to the G dwarfs in the solar neighborhood (Abad et al. 2003). Analysis of such all-sky measurements of Doppler shifts can, in principle and after removal of the solar apex motion, reveal effects from gravitational redshift including tests of general relativity (Hentschel 1994).

Those stars exhibiting a standard deviation of their measured velocities less than  $0.1 \text{ km s}^{-1}$  as listed in Table 3 (last column) and having a time span of observations over a few years constitute secondary standard stars. Their lack of radial velocity variation above  $0.1 \text{ km s}^{-1}$  during several years indicates a constant velocity suitable for many purposes. In contrast, the standard stars listed in Tables 1 and 2 met a higher standard of constant radial velocity within  $0.1 \text{ km s}^{-1}$  during a time span of a full 10 years and all of them also exhibited precise radial velocities (using iodine as wavelength reference) constant to within  $0.025 \text{ km s}^{-1}$ , thereby ensuring their integrity as standard stars.

### 3. BINARY STARS

We compared our radial velocities with those previously published, noting a subset of stars that show differences of over  $2 \text{ km s}^{-1}$ , indicating likely binary stars. We made great use of the Pulkovo Catalog of Radial Velocities (Gontcharov 2006). The Pulkovo catalog gives the weighted mean absolute velocities for over 35000 Hipparcos stars drawn from over 200 publications. Despite the inhomogeneous sources, the median accuracy of the final radial velocities in the Pulkovo Catalog is  $0.7 \text{ km s}^{-1}$ , adequate to identify binaries in comparison with the absolute velocities presented here. The times of observations from the Pulkovo Catalog were typically 10-30 years ago, offering a time difference of typically over 10 years between those measurements and the radial velocities presented here. Thus, binary stars with periods over a decade can be identified. Thanks are due to Charles Francis and Erik Anderson for their critical evaluation of the velocities in this work compared to those in the Pulkovo Catalog of Radial Velocities.

Among the 2046 stars reported here in Table 3, we identified those having a difference between the present velocities and those in the Pulkovo Catalog of more than  $3 \sigma$ , i.e.  $2 \text{ km s}^{-1}$ . Velocity differences of over  $2 \text{ km s}^{-1}$  offer a sign, but not convincing evidence, of long term binary motion with orbital periods over a year. For binaries with periods of between a year and several decades, the velocity variation will be many  $\text{km s}^{-1}$  on time scales of a decade, allowing some of them to be detected.

Table 4 gives a list of the stars showing differences of over  $2 \text{ km s}^{-1}$  between the present and Pulkovo velocities, indicating a possible binary. The first and second columns give the HD and Hipparcos identities of the star. The third column gives the radial velocity

from the present work, and the fourth column give the radial velocity from the Pulkovo Catalog (Gontcharov 2006). For each of the stars in Table 4, we examined the relative, precise iodine-based radial velocities (precision of  $\sim 2 \text{ m s}^{-1}$ ) to detect any obvious velocity variations. Indeed, for many of the stars in Table 4, the precise, iodine-based RVs reveal large velocity variations of over  $1 \text{ km s}^{-1}$ , confirming the binary nature. For them, we note the measured time derivative of the variation of precise radial velocities ("PRV var") in the last column of Table 4 under "Comments". For the remaining stars in Table 4, we do not have precise relative RVs, and must rely on the difference between the present and Pulkovo velocities as the indicator of a binary star. Certainly a few of these entries may be false binaries, due to unavoidable errors in the Pulkovo compilation. But we suspect that the vast majority of the stars in Table 4 are actual binaries, and we are alerting the community to this likelihood. In addition, we discovered several double-line spectroscopic binaries among our target stars, so indicated in the Comments in Table 4.

### 4. VELOCITY ZERO POINT

The present velocities share, by construction, the zero-point of the velocity scale with that of Nidever et al. (2002). The Nidever zero-point in velocity was determined by using spectra of both the day sky and of the asteroid, Vesta, yielding a zero-point accurate to within  $0.01 \text{ km s}^{-1}$  for G2V stars. The present velocities have a similarly accurate zero-point for G2V stars.

However one must consider the effects of general relativistic gravitational redshifts upon departure of the light from the star (but we do include the general relativistic blueshift caused by entry of light into the potential wells of the solar system, an effect of only  $0.003 \text{ km s}^{-1}$ ). One must also consider the "convective blueshift" caused by the hydrodynamic effects in the photospheres of FGKM stars (Dravins 2008). We emphasize that our present velocities were constructed to have the correct velocity for the Sun and Vesta, thus automatically accounting for gravitational redshift and convective blueshift for G2V stars. Here we estimate these two effects on the velocity zero-point as a function of stellar mass along the main sequence.

The gravitational redshift of light upon departure from stars is  $K = 0.635(M/R)$  where  $K$  is given in  $\text{km s}^{-1}$  and  $M$  and  $R$  are the stellar mass and radius given in solar units. As  $R$  is nearly proportional to  $M$  along the main sequence, the gravitational redshift varies little among the main sequence stars, and remains  $\sim 0.6 \text{ km s}^{-1}$  for FGKM stars.

But the convective velocities decrease substantially for the lower mass stars that have lower luminosities, requiring lower convective velocities to carry the energy. Scaling the convective energy transport with stellar mass suggests that convective velocities will vary linearly with stellar mass. Indeed, the RV "jitter" decreases from  $2 \text{ m s}^{-1}$  for G dwarfs to less than  $1 \text{ m s}^{-1}$  for M dwarfs, in part caused by the decrease in sub-photospheric convective hydrodynamics, not necessarily due to spots. We note that convective blueshift depends on the technique used to measure radial velocity because it stems from a net displacement and distortion of the absorption line profiles. These displacements and shapes of the lines

arise from the integrated velocity field with depth in the photosphere, implying that each radial velocity technique with its particular set of absorption lines will sample a different portion of that velocity field. Given this physical situation, it is noteworthy that the present velocities and those of Nidever *et al.* (2002) show negligible discrepancies as they sample the near-IR and green/optical portions of the spectrum, respectively.

One may anticipate that M dwarfs of  $\sim 0.5$  solar masses will suffer a convective blueshift that is only half that of solar type stars, and hence half that necessary to cancel the gravitational redshift. This suggests that the radial velocities of M dwarfs presented here may suffer from a net surplus of gravitational redshift compared to convective blueshift of  $\sim 0.3 \text{ km s}^{-1}$ .

To quantify this imbalance of convective blueshift against gravitational redshift, Nidever *et al.* (2002) draw from hydrodynamic models of stellar atmospheres of Dravins (1999) to estimate the resulting systematic errors. Based on them and on computed gravitational redshifts, we estimate that our present radial velocities are too low by  $\sim 0.56 \text{ km s}^{-1}$  for F5V stars. For those stars convective blueshift causes a greater blueshift than the gravitational redshift. For G2V stars, our present radial velocities have a zero-point accurate to within  $0.01 \text{ km s}^{-1}$ , by construction (using the Sun and Vesta). For K0V and M0V stars, our present velocities are probably too high by  $\sim 0.15$  and  $0.30 \text{ km s}^{-1}$ , respectively.

We caution that the asymmetries in absorption lines leading to convective blueshift vary from line to line depending on the velocity fields at their depth of formation, with variations of  $\sim 0.1 \text{ km/s}$ . The asymmetries also vary with time during a magnetic cycle as the surface fields influence the convective flow patterns. Moreover, the convective blueshift will be a function of spectral resolution and of the algorithm used to measure it, *i.e.* cross-correlation or other, that implicitly apply weights along the line profile.

*Thus, to obtain kinematically robust measures of radial velocity,  $dr/dt$ , we recommend applying the corrections listed above, to the velocities in Tables 1, 2, and 3, *i.e.* adding  $0.56 \text{ km s}^{-1}$  to our velocities of F5V stars, zero for G2V, subtracting  $0.15 \text{ km s}^{-1}$  for K0V, and subtracting  $0.3 \text{ km s}^{-1}$  for M0V.* A useful linear relation that approximately represents the correction (in  $\text{km s}^{-1}$ ) to be applied is:

$$V_{\text{Corr}} = 1.3 \times 10^{-4}(T_{\text{eff}} - 5780K)$$

This correction to our radial velocities is pinned to the zero-point established by the spectra of the Sun and asteroids, and applies only to main sequence stars.

We check the velocity zero-point assessment described above, as follows. A careful assessment of gravitational redshifts is provided by Pasquini *et al.* (2011). They compared the radial velocities of main sequence stars and giants within the open cluster, M67, expecting to find a larger gravitational redshift from the main sequence stars due to their smaller radii. Remarkably, their radial velocities of main sequence stars and giants showed no difference in systemic velocities of the two stellar populations. Pasquini *et al.* (2011) find an upper limit of  $0.1 \text{ km s}^{-1}$  in the net difference in the systemic radial velocities between main sequence stars and giants. This lack

of RV difference indicates that the spectral lines in main sequence stars are sufficiently blueshifted, compared to those in giant stars (that suffer only a small gravitational redshift due to their large radii), such that the gravitational redshift and convective blueshift nearly cancel each other in FGK main sequence stars, at the level of  $0.1 \text{ km s}^{-1}$ . This cancellation provides some assurance that our velocity zero-point, which is forced to be zero for G2V stars, is not highly sensitive to changes in convective blueshift along the main sequence.

We further check our velocity zero-point by comparison with Center for Astrophysics (CfA) radial velocity results that targeted asteroids having known ephemerides to establish the instantaneous velocity vectors relative to the observatory (Latham *et al.* 2002). This effort is similar to that employed by Nidever *et al.* (2002) who used Vesta to set their zero-point. The CfA group finds that their native radial velocities require a correction of  $+0.139 \text{ km s}^{-1}$  to achieve agreement with the actual dynamical orbital velocities of the asteroids (Latham *et al.* 2002).

This asteroid-derived correction of  $+0.139 \text{ km s}^{-1}$  to the CfA radial velocities may be combined with the measured zero-point difference between the present radial velocities and those from the CfA. In Section 2.1 we noted that the velocities of the present standard stars differed from those of the CfA (Stefanik *et al.* 1999), with a zero-point difference:  $(V_{\text{present}} - V_{\text{Stefanik}}) = +0.15 \text{ km s}^{-1}$ . But the CfA radial velocities should be corrected by  $+0.139$  based on their asteroid reference. Doing so reduces the difference between the present and (corrected) CfA velocity zero point to  $0.15 - 0.139 \text{ km s}^{-1} = 0.011 \text{ km s}^{-1}$ . *Thus, the radial velocities presented here differ from the dynamically derived velocity zero-point at the CfA by only  $0.011 \text{ km s}^{-1}$ .*

The lines of evidence presented in this section indicate that the radial velocities presented here are accurate measures of the time rate of change of the distance of the star from the solar system barycenter for solar type stars. In summary, our velocity zero-point was pinned to Nidever *et al.* (2002) that stemmed from spectra of the Sun and Vesta. Pasquini *et al.* (2011) show that gravitational redshift and convective blueshift nearly cancel for main sequence FGK stars. The asteroid measurements at the CfA (Latham *et al.* 2002) yield a zero-point of the velocity scale that agrees with that here, within  $0.01 \text{ km s}^{-1}$ . Thus, the present velocities represent the actual time rate of change of distance,  $dr/dt$ , of the solar-type stars. For other spectral types, corrections to velocities should be applied for convective blueshift, as noted above. We caution that even after applying such corrections, the present radial velocities may carry systematic errors of  $0.1 \text{ km s}^{-1}$  or more, especially for spectral types far from G2V.

## 5. DISCUSSION

We have provided barycentric radial velocities with an internal precision of  $\sim 0.1 \text{ km s}^{-1}$  for 2046 stars, of which 131 are standards. The error estimates come from both the internal errors found from our measurements and from the comparison with the standard velocities of Nidever *et al.* (2002), Stefanik *et al.* (1999) and Udry *et al.* (1999a). Our absolute radial velocities were constructed to share the velocity zero-point



defined by Nidever et al. (2002) and apparently the resulting velocity scale differs by only  $0.063 \text{ km s}^{-1}$  from that of Udry et al. (1999a), by  $0.15 \text{ km s}^{-1}$  from that of Stefanik et al. (1999), and  $0.007 \text{ km s}^{-1}$  from that of Marcy et al. (1987), which adds confidence to the zero points of all four sets of velocities.

The 1-sigma errors of the radial velocities in Table 3 are  $\sim 0.12 \text{ km s}^{-1}$ . Any stars exhibiting a scatter among their individual velocity measurements, listed as  $\sigma_{RV}$  in the last column of Table 3, that is greater than  $0.36 \text{ km s}^{-1}$  represents a 3-sigma departure from a constant velocity. Such scatter likely indicates physical changes in the radial velocity of that star by an amount given by that standard deviation and occurring on a time scale constrained by (shorter than) the time span of the observations. In such cases of velocity variability, the individual radial velocities and their times of observation offer information about the coherence, if any, and the time scale of the acceleration of the star. Certainly long term trends and periodicities in the radial velocities offer information on the cause of the velocity variation and on the orbital or physical behavior.

Such accelerations are likely caused by gravitational forces within a multiple star system. Other possible causes are gravitational forces exerted by orbiting giant planets, passing stars including compact objects, structural pulsations in the star itself, rapid rotation coupled with surface inhomogeneities such as starspots, Rossiter McLaughlin effect from orbiting objects, or stochastic surface velocities from magnetic events such as flares.

The precise barycentric radial velocities presented here may serve as useful reference measurements for calibrations of other spectroscopic programs. They may be used to construct velocity metrics for studies of the kinematics of the Galaxy or of other galaxies. We intended for these velocities to be useful to surveys of Galactic kinematics and dynamics such as *Gaia*, *SDSS*, *RAVE*, *APOGEE*, *SkyMapper*, *HERMES*, and *LSST*. They may assist in Doppler searches for long-period binary stars. Indeed, these velocities will help identify long period orbiting or passing companions to the 2046 stars themselves, most of which reside within 100 pc thus making them interesting targets for future high contrast imaging.

We are indebted to the University of California and NASA for allocation of telescope time on the Keck telescope. We thank Charles Francis and Erik Anderson for a critical review of the velocities compared to past measurements. We thank Guillermo (Willie) Torres and Dimitri Pourbaix for valuable suggestions that improved the manuscript. This work benefited from valuable discussions about radial velocity standard stars with Dave Latham, Stephane Udry, and Dainis Dravins. We are grateful to UCLA for hospitality during the writing of some of the paper. This work made use of the Exoplanet Orbit Database and the Exoplanet Data Explorer at [www.exoplanets.org](http://www.exoplanets.org). All 29000 spectra are archived and publicly available, thanks to the Keck Observatory Archive made possible by a NASA-funded collaboration between the NASA Exoplanet Science Institute and the W. M. Keck Observatory. We acknowledge support by NASA grants NAG5-8299, NNX11AK04A, NSF grants AST95-20443 (to GWM) and AST-1109727 (to JTW),

and by Sun Microsystems. This research was made possible by the generous support from the Watson and Marilyn Albert SETI Chair fund (to GWM) and by generous donations from Howard and Astrid Preston. The Center for Exoplanets and Habitable Worlds is supported by the Pennsylvania State University, the Eberly College of Science, and the Pennsylvania Space Grant Consortium. This research has made use of NASA's Astrophysics Data System and the SIMBAD database, operated at CDS, Strasbourg, France. We thank R. Paul Butler and Steven Vogt for help making observations. We thank the staff of the W.M Keck Observatory and Lick Observatory for their valuable work maintaining and improving the telescopes and instruments, without which the observations would not be possible. We appreciate the State of California for its support of operations at both observatories. We thank the University of California, Caltech, the W.M. Keck Foundation, and NASA for support that made the Keck Observatory possible. We appreciate the indigenous Hawaiian people for the use of their sacred mountain, Mauna Kea.

## REFERENCES

- Abad, C., Vieira, K., Bongiovanni, A., Romero, L., & Vicente, B. 2003, *A&A*, 397, 345
- Beavers, W. I., & Eitter, J. J. 1986, *ApJS*, 62, 147
- Burkart, J., Quataert, E., Arras, P., & Weinberg, N. N. 2012, *MNRAS*, 421, 983
- Casagrande, L., Schoenrich, R., Asplund, M., Cassisi, S., Ramirez, I., Melendez, J., Bensby, T., & Feltzing, S. 2011, [arXiv:1103.4651](https://arxiv.org/abs/1103.4651)
- Crifo, F., Jasniewicz, G., Soubiran, C., et al. 2010, *A&A*, 524, A10
- Dravins, D. 1999, *IAU Colloq. 170: Precise Stellar Radial Velocities*, 185, 268
- Dravins, D. 2008, *A&A*, 492, 199
- Edwards, R. T., Hobbs, G. B., & Manchester, R. N. 2006, *MNRAS*, 372, 1549
- Famaey, B., Jorissen, A., Luri, X., et al. 2005, *A&A*, 430, 165
- Gilmore, G., Randich, S., Asplund, M., et al. 2012, *The Messenger*, 147, 25
- Gontcharov, G. A. 2006, *Astronomy Letters*, 32, 759
- Griffin, R. & Griffin, R. 1973, *Mon. Not. R. astr. Soc.* 162, 243-253.
- Griffin, R. 1973, *MNRAS*, 162, 243
- Hearnshaw, J. B., & Scarfe, C. D. 1999, *IAU Colloq. 170: Precise Stellar Radial Velocities*, 185,
- Hentschel, K. 1994, *Archive for History of Exact Sciences*, 47, 143
- Holmberg, J., Nordström, B., & Andersen, J. 2009, *A&A*, 501, 941
- Johnson, J. A., Clanton, C., Howard, A. W., et al. 2011, *ApJS*, 197, 26
- Kibrick, R. I., Clarke, D. A., Deich, W. T. S., & Tucker, D. 2006, *Proc. SPIE*, 6274,
- Latham, D. W., Stefanik, R., Torres, G., Davis, R. J., & Mazeh, T. 1991, *Montreal International Astronautical Federation Congress*,
- Latham, D. W., Stefanik, R. P., Torres, G., et al. 2002, *AJ*, 124, 1144
- Lindegren, L., & Dravins, D. 2003, *A&A*, 401, 1185
- Marcy, G. W., Lindsay, V., & Wilson, K. 1987, *PASP*, 99, 490
- Marcy, G. W., & Butler, R. P. 1992, *PASP*, 104, 270
- Marcy, G. W., Butler, R. P., Vogt, S. S., et al. 2008, *Physica Scripta Volume T*, 130, 014001
- Mayor, M., & Maurice, E. 1985, *Stellar Radial Velocities*, 299
- Nidever, D. L., Marcy, G. W., Butler, R. P., Fischer, D. A., & Vogt, S. S. 2002, *ApJS*, 141, 503
- Nordlund, Å. 2008, *Physica Scripta Volume T*, 133, 014002
- Nordström, B., et al. 2004, *A&A*, 418, 989
- Pasquini, L., Melo, C., Chavero, C., et al. 2011, *A&A*, 526, A127
- Pourbaix, D., et al. 2002, *A&A*, 386, 280
- Ramírez, I., Collet, R., Lambert, D. L., Allende Prieto, C., & Asplund, M. 2010, *ApJ*, 725, L223
- Scarfe, C. D., Batten, A. H., & Fletcher, J. M. 1990, *Publications of the Dominion Astrophysical Observatory Victoria*, 18, 21
- Schoenrich, R., Asplund, M., & Casagrande, L. 2010, [arXiv:1012.0842](https://arxiv.org/abs/1012.0842)
- Stefanik, R. P., Latham, D. W., & Torres, G. 1999, *IAU Coll 170*, 354
- Udry, S., Mayor, M., & Queloz, D. 1999a, *IAU Coll 170*, 367
- Udry, S., et al. 1999b, *IAU Coll 170*, 383
- Welsh, W. F., Orosz, J. A., Aerts, C., et al. 2011, *ApJS*, 197, 4
- Wilson, R. E. 1953, *Carnegie Institute Washington D.C. Publication*, 0
- Wilson, M. L., et al. 2011, *MNRAS*, 260

TABLE 1  
RADIAL VELOCITIES OF STANDARD STARS

HD#	HIP	Gliese	Spec. Type	JD <sub>Init</sub> (-2440000)	JD <sub>Fin</sub> (-2440000)	$\Delta t$ (yr)	RV <sub>Nidever</sub> <sup>a</sup> (km/s)	RV <sub>Present</sub> <sup>b</sup> (km/s)	$\sigma_{RV}$ <sup>c</sup> (km/s)	$N_{Obs}$ <sup>d</sup>	RV <sub>Final</sub> <sup>e</sup> (km/s)	Unc <sup>f</sup> (km/s)
166	544	5	K0	6960	15252	23	-6.537	-6.350	0.118	12	-6.444	0.187
283	616	9003	K0	10367	14457	11	-43.102	-43.247	0.077	7	-43.174	0.145
3651	3093	27	K0	7048	15251	22	-32.961	-32.919	0.108	63	-32.940	0.042
3765	3206	28	K2	10462	15252	13	-63.202	-63.179	0.119	62	-63.191	0.030
4256	3535	31.4	K2	10367	15172	13	9.460	9.393	0.104	49	9.426	0.067
4628	3765	33	K2	7047	15252	22	-10.230	-10.228	0.121	79	-10.229	0.030
8389	6456	57.1	K0	10367	15016	13	34.647	34.606	0.110	58	34.626	0.041
9562	7276	59.2	G2	10367	15230	13	-14.989	-14.990	0.132	7	-14.990	0.050
10002	7539	62	K0	10463	14431	11	11.562	11.494	0.045	5	11.528	0.068
10145	7902	9059	G5	10462	15110	13	17.838	17.938	0.158	4	17.888	0.100
10476	7981	68	K1	7048	15172	22	-33.647	-33.650	0.103	137	-33.648	0.030
10700	8102	71	G8	7047	15232	22	-16.619	-16.640	0.121	466	-16.629	0.030
12051	9269	82.1	G5	10419	15257	13	-35.102	-35.163	0.146	117	-35.133	0.061
13043	9911	9073	G2	10367	15232	13	-39.333	-39.326	0.102	122	-39.329	0.030
14412	10798	95	G5	10366	15232	13	7.383	7.297	0.129	73	7.340	0.086
16141	12048	9085	G5	10366	15230	13	-50.971	-50.909	0.109	18	-50.940	0.062
18803	14150	120.2	G8	10367	15135	13	9.878	9.847	0.092	69	9.862	0.031
20165	15099	9112	K1	10366	15173	13	-16.676	-16.667	0.164	28	-16.672	0.031
20619	15442	135	G1.5	10366	15135	13	22.689	22.637	0.130	40	22.663	0.052
22484	16852	147	F9	7049	15261	22	28.080	28.253	0.073	3	28.167	0.173
22879	17147	147.1	F9	10366	15173	13	120.356	120.325	0.107	31	120.340	0.031
23439	17666	1064	K1	10463	15134	13	50.704	50.572	0.119	25	50.638	0.132
24365	18208	3254	G8	10463	15172	13	19.278	19.274	0.083	6	19.276	0.034
24238	18324	15	K0	10463	15257	13	38.809	38.736	0.136	31	38.772	0.073
26794	19788	165.2	K3	10420	14456	11	56.573	56.402	0.112	7	56.487	0.171
26965	19849	166A	K1	7049	15261	22	-42.331	-42.344	0.118	83	-42.337	0.030
28187	20638	-	G3	10366	14024	10	18.321	18.324	0.137	3	18.322	0.079
31253	22826	-	F8	10839	14807	11	12.184	12.285	0.167	14	12.235	0.101
31560	22907	2037	K3	10366	14780	12	6.203	6.208	0.112	8	6.205	0.040
32147	23311	183	K3	7047	15286	23	21.552	21.536	0.115	126	21.544	0.030
34721	24786	198	G0	10366	15081	13	40.448	40.503	0.130	32	40.475	0.055
34411	24813	197	G0	7049	15322	23	66.511	66.482	0.135	88	66.497	0.030
36003	25623	204	K5	10367	15109	13	-55.527	-55.588	0.111	69	-55.558	0.061
36395	25878	205	M1.5	10420	15257	13	8.665	8.687	0.169	13	8.676	0.047
245409	26335	208	K7	10420	15257	13	22.046	22.333	0.273	6	22.190	0.287
37124	26381	209	G4	10420	15230	13	-23.076	-23.032	0.094	28	-23.054	0.044
38858	27435	1085	G4	10419	15262	13	31.543	31.471	0.093	76	31.507	0.072
39881	28066	224	G5	10366	14865	12	0.333	0.307	0.085	14	0.320	0.030
42581	29295	229A	M1	10420	15199	13	4.724	4.753	0.115	14	4.738	0.031
42618	29432	3387	G4	10366	15322	14	-53.501	-53.499	0.127	164	-53.500	0.030
45184	30503	3394	G2	10366	15199	13	-3.856	-3.863	0.119	117	-3.859	0.030
48682	32480	245	G0	7049	15343	23	-23.933	-23.881	0.101	33	-23.907	0.052
265866	33226	251	M3	10784	15173	12	22.914	22.969	0.165	24	22.942	0.055
51866	33852	257.1	K3	10462	15134	13	-21.624	-21.688	0.128	33	-21.656	0.064
52711	34017	262	G4	7049	15230	22	24.604	24.566	0.115	95	24.585	0.038
-	36208	273	M3.5	7049	15290	23	18.216	18.203	0.095	20	18.210	0.030
65583	39157	295	G8	10419	15345	13	14.832	14.760	0.114	61	14.796	0.072
67767	40023	-	G7	10419	15345	13	-44.318	-44.225	0.091	5	-44.272	0.093
71334	41317	306.1	G4	10462	14130	10	17.286	17.493	0.148	3	17.389	0.207
73667	42499	315	K1	10462	15290	13	-12.088	-12.159	0.102	29	-12.123	0.071
84035	47690	365	K5	10462	15199	13	-12.225	-12.317	0.104	23	-12.271	0.092
84737	48113	368	G0.5	6960	15351	23	4.900	4.862	0.128	32	4.881	0.038
88230	49908	380	K5	7195	15017	21	-25.729	-25.692	0.118	18	-25.710	0.037
88371	49942	-	G2	10463	14811	12	82.497	82.430	0.070	4	82.463	0.067
88725	50139	9322	G1	10463	14131	10	-22.045	-21.987	0.187	3	-22.016	0.108
89269	50505	3593	G5	10419	15351	14	-7.551	-7.563	0.125	94	-7.557	0.030
-	-	388	M4.5	8020	15198	20	12.420	12.486	0.104	30	12.453	0.066
90156	50921	3597	G5	10419	15352	14	26.934	26.902	0.147	70	26.918	0.032
90711	51257	3603	K0	10462	14642	11	29.940	29.867	0.090	21	29.903	0.073
95735	54035	411	M2	6959	15343	23	-84.689	-84.678	0.136	149	-84.683	0.030
96700	54400	412.2	G2	10419	14928	12	12.769	12.805	0.170	5	12.787	0.076
97101	54646	414	K8	8649	15351	18	-16.376	-15.942	0.107	24	-16.159	0.434
97343	54704	3648	G8	10419	15352	14	39.794	39.783	0.132	66	39.789	0.030
97658	54906	3651	K1	10463	15352	13	-1.654	-1.758	0.122	151	-1.706	0.104
98281	55210	423.1	G8	10462	15352	13	13.330	13.294	0.128	70	13.312	0.036
99491	55846	429A	K0	10419	15320	13	4.190	4.151	0.134	109	4.171	0.039
100180	56242	3669A	G0	10419	15351	14	-4.854	-4.867	0.118	39	-4.860	0.030
100623	56452	432A	K0	10419	15352	14	-21.959	-21.970	0.111	54	-21.964	0.030
101259	56830	3679	G6	10462	14808	12	96.905	96.718	0.156	3	96.812	0.187
104067	58451	1153	K2	10462	15315	13	15.021	14.963	0.110	40	14.992	0.058
105631	59280	3706	K0	10463	15231	13	-2.428	-2.516	0.121	120	-2.472	0.088
106156	59572	3715	G8	10463	15174	13	-7.415	-7.256	0.069	4	-7.336	0.159
111515	62607	3752	G8	10463	14549	11	2.548	2.578	0.069	7	2.563	0.030
116442	65352	3781A	G5	10463	15315	13	28.421	28.401	0.151	37	28.411	0.030

TABLE 1 — *Continued*

HD#	HIP	Gliese	Spec. Type	JD <sub>Init</sub> (-2440000)	JD <sub>Fin</sub> (-2440000)	$\Delta t$ (yr)	RV <sub>Nidever</sub> <sup>a</sup> (km/s)	RV <sub>Present</sub> <sup>b</sup> (km/s)	$\sigma_{RV}$ <sup>c</sup> (km/s)	$N_{Obs}$ <sup>d</sup>	RV <sub>Final</sub> <sup>e</sup> (km/s)	Unc <sup>f</sup> (km/s)
116443	65355	3782B	G5	10463	15320	13	27.416	27.351	0.117	82	27.383	0.065
-	65859	514	M0.5	10546	14964	12	14.556	14.506	0.107	25	14.531	0.050
119850	67155	526	M1.5	10546	15257	13	15.809	15.748	0.110	20	15.778	0.061
120467	67487	529	K4	10546	15315	13	-37.806	-37.450	0.089	21	-37.628	0.356
122120	68337	535	K5	10546	15285	13	-57.444	-57.440	0.105	45	-57.442	0.030
122652	68593	-	F8	10832	15232	12	1.409	1.558	0.107	5	1.484	0.149
125184	69881	541.1	G5	10277	13985	10	-12.377	-12.285	0.117	12	-12.331	0.092
125455	70016	544	K1	10276	15315	14	-9.806	-9.906	0.117	26	-9.856	0.100
132142	73005	31.4	K1	10546	15345	13	-14.771	-14.806	0.104	32	-14.789	0.035
136713	75253	1191	K2	10277	15256	14	-6.037	-6.067	0.127	93	-6.052	0.030
136834	75266	1192	K3	10276	13935	10	-26.374	-26.460	0.018	3	-26.417	0.086
139323	76375	591	K3	10546	15261	13	-67.101	-67.108	0.131	123	-67.105	0.030
141004	77257	598	G0	6960	15315	23	-66.416	-66.363	0.126	179	-66.390	0.053
144585	78955	-	G5	10547	14295	10	-14.067	-13.961	0.116	17	-14.014	0.106
146233	79672	616	G2	10284	15352	14	11.748	11.763	0.124	114	11.756	0.030
151541	81813	637.1	K1	10546	15285	13	9.475	9.470	0.131	39	9.473	0.030
151288	82003	638	K5	10602	15343	13	-31.357	-31.341	0.121	35	-31.349	0.030
154345	83389	54.2	G8	10547	15351	13	-46.930	-46.959	0.122	88	-46.945	0.030
154363	83591	653	K5	10276	15322	14	34.146	34.044	0.118	34	34.095	0.102
157214	84862	672	G0	6958	15351	23	-78.546	-78.572	0.119	40	-78.559	0.030
157881	85295	673	K5	10276	15081	13	-23.199	-23.037	0.065	3	-23.118	0.162
159222	85810	56.3	G5	10547	15322	13	-51.605	-51.506	0.121	90	-51.556	0.099
-	86162	687	M3.5	10604	15016	12	-28.779	-28.660	0.109	73	-28.720	0.119
-	86287	686	M1	10605	15043	12	-9.515	-9.483	0.112	37	-9.499	0.032
161848	87089	9605	K1	10276	13935	10	-94.929	-94.982	0.124	3	-94.955	0.072
-	87937	699	M4	6958	14930	22	-110.506	-110.326	0.132	75	-110.416	0.180
164922	88348	700.2	K0	10276	15321	14	20.248	20.224	0.098	100	20.236	0.030
165222	88574	701	M1	6959	15352	23	32.671	32.571	0.160	58	32.621	0.100
166620	88972	706	K2	6959	15261	23	-19.418	-19.512	0.107	42	-19.465	0.094
170493	90656	715	K3	10276	15043	13	-54.752	-54.801	0.109	44	-54.776	0.049
170657	90790	716	K1	9201	15322	17	-43.131	-43.142	0.161	13	-43.137	0.045
172051	91438	722	G5	10284	15136	13	37.103	37.087	0.121	43	37.095	0.030
173701	91949	725.1	K0	10548	14987	12	-45.602	-45.658	0.093	31	-45.630	0.056
175541	92895	736	G8	10284	15352	14	19.698	19.650	0.112	41	19.674	0.048
176982	93518	740.1	G5	10284	14024	10	-6.793	-6.856	0.062	3	-6.825	0.063
182488	95319	758	G8	11005	15319	12	-21.508	-21.462	0.134	55	-21.485	0.046
182572	95447	759	G8	10367	15319	14	-100.292	-100.285	0.126	61	-100.289	0.030
187923	97767	4126	G0	10277	15319	14	-20.611	-20.626	0.138	99	-20.619	0.030
188512	98036	771A	G8	6960	15319	23	-40.109	-40.039	0.122	20	-40.074	0.070
190404	98792	778	K1	10276	15016	13	-2.527	-2.543	0.155	30	-2.535	0.030
191785	99452	783.2	K1	10277	15111	13	-49.286	-49.291	0.119	28	-49.289	0.030
196761	101997	796	G8	10277	15318	14	-41.987	-41.873	0.115	46	-41.930	0.114
197076	102040	797A	G5	10366	15318	14	-35.409	-35.395	0.110	160	-35.402	0.030
-	102401	806	M1.5	7374	15015	21	-24.702	-24.692	0.116	41	-24.697	0.030
199305	103096	809	M0.5	10602	14984	12	-17.161	-17.127	0.133	19	-17.144	0.034
202751	105152	825.3	K2	10366	15111	13	-27.427	-27.468	0.104	39	-27.448	0.041
204587	106147	830	K5	10366	15084	13	-84.186	-84.021	0.103	20	-84.103	0.165
210302	109422	849.1	F6	11342	15136	10	-16.259	-16.049	0.194	36	-16.154	0.210
216259	112870	-	K0	10276	14809	12	1.291	1.192	0.125	63	1.241	0.099
216899	113296	880	M1.5	10666	14809	11	-27.317	-27.194	0.156	24	-27.255	0.123
217357	113576	884	K5	10366	15135	13	16.420	16.502	0.105	49	16.461	0.082
217877	113896	-	F8	11006	15019	11	-12.676	-12.800	0.100	3	-12.738	0.124
218566	114322	4313	K3	10367	15198	13	-37.804	-37.846	0.119	31	-37.825	0.042
219538	114886	4320	K2	10462	15111	13	9.990	9.943	0.108	46	9.967	0.047
220339	115445	894.5	K2	10367	15173	13	34.001	33.966	0.112	41	33.984	0.035
221356	116106	9829	F8	10277	15017	13	-12.713	-12.537	0.327	4	-12.625	0.176
-	117473	908	M2	7047	15199	22	-71.147	-71.022	0.169	52	-71.084	0.125
223498	117526	4366	G7	10367	14839	12	-23.985	-24.025	0.037	3	-24.005	0.040

<sup>a</sup> Radial velocities from Nidever *et al.* (2002)<sup>b</sup> Radial velocities from the measurements made here.<sup>c</sup> Standard deviation of all RVs measured here for this star.<sup>d</sup> Number of observations (spectra) used for this star.<sup>e</sup> Unweighted average of the Nidever RV and the RV measured here. This is the recommended RV for use as a standard star.<sup>f</sup> Uncertainty in the Final RV (see text).

TABLE 2  
RADIAL VELOCITY STANDARD STARS WITH COORDINATES

Star Name	RA (2000)	DEC (2000)	$V_{\text{mag}}$	Spectral Type	Final RV ( $\text{km s}^{-1}$ )	Unc ( $\text{km s}^{-1}$ )
HD 166	0 6 36.8	29 1 17.4	6.13	K0	-6.444	0.187
HD 283	0 7 32.5	-23 49 7.4	8.70	K0	-43.174	0.145
HD 3651	0 39 21.8	21 15 1.7	5.80	K0	-32.940	0.042
HD 3765	0 40 49.3	40 11 13.8	7.36	K2	-63.191	0.030
HD 4256	0 45 4.9	1 47 7.9	8.03	K2	9.426	0.067
HD 4628	0 48 23.0	5 16 50.2	5.75	K2	-10.229	0.030
HD 8389	1 23 2.6	-12 57 57.8	7.84	K0	34.626	0.041
HD 9562	1 33 42.8	-7 1 31.2	5.76	G2	-14.990	0.050
HD 10002	1 37 8.6	-29 23 35.7	8.13	K0	11.528	0.068
HD 10145	1 41 37.7	66 54 35.8	7.70	G5	17.888	0.100
HD 10476	1 42 29.8	20 16 6.6	5.20	K1	-33.648	0.030
HD 10700	1 44 4.1	-15 56 14.9	3.50	G8	-16.629	0.030
HD 12051	1 59 6.6	33 12 34.8	7.14	G5	-35.133	0.061
HD 13043	2 7 34.3	0 -37 2.7	6.87	G2	-39.329	0.030
HD 14412	2 18 58.5	-25 56 44.5	6.34	G5	7.340	0.086
HD 16141	2 35 19.9	-3 33 38.2	6.78	G5	-50.940	0.062
HD 18803	3 2 26.0	26 36 33.3	6.62	G8	9.862	0.031
HD 20165	3 14 47.2	8 58 50.9	7.83	K1	-16.672	0.031
HD 20619	3 19 1.9	-2 50 35.5	7.10	G1.5	22.663	0.052
HD 22484	3 36 52.4	0 24 6.0	4.28	F9	28.167	0.173
HD 22879	3 40 22.1	-3 13 1.1	6.74	F9	120.340	0.031
HD 23439	3 47 2.1	41 25 38.2	8.18	K1	50.638	0.132
HD 24365	3 53 37.7	28 8 53.2	7.87	G8	19.276	0.034
HD 24238	3 55 3.8	61 10 0.5	7.85	K0	38.772	0.073
HD 26794	4 14 30.3	3 1 19.4	8.81	K3	56.487	0.171
HD 26965	4 15 16.3	-7 39 10.3	4.41	K1	-42.337	0.030
HD 28187	4 25 23.8	-35 40 32.0	7.80	G3	18.322	0.079
HD 31253	4 54 43.7	12 21 7.9	7.14	F8	12.235	0.101
HD 31560	4 55 41.9	-28 33 50.1	8.12	K3	6.205	0.040
HD 32147	5 0 49.0	-5 45 13.2	6.22	K3	21.544	0.030
HD 34721	5 18 50.5	-18 7 48.2	5.96	G0	40.475	0.055
HD 34411	5 19 8.5	40 5 56.6	4.70	G0	66.497	0.030
HD 36003	5 28 26.1	-3 29 58.4	7.64	K5	-55.558	0.061
HD 36395	5 31 27.4	-3 40 38.0	7.92	M1.5	8.676	0.047
HD 245409	5 36 31.0	11 19 40.3	8.89	K7	22.190	0.287
HD 37124	5 37 2.5	20 43 50.8	7.68	G4	-23.054	0.044
HD 38858	5 48 34.9	-4 5 40.7	5.97	G4	31.507	0.072
HD 39881	5 56 3.4	13 55 29.7	6.60	G5	0.320	0.030
HD 42581	6 10 34.6	-21 51 52.7	8.14	M1	4.738	0.031
HD 42618	6 12 0.6	6 46 59.1	6.87	G4	-53.500	0.030
HD 45184	6 24 43.9	-28 46 48.4	6.37	G2	-3.859	0.030
HD 48682	6 46 44.3	43 34 38.7	5.25	G0	-23.907	0.052
HD 265866	6 54 49.0	33 16 5.4	9.89	M3	22.942	0.055
HD 51866	7 1 38.6	48 22 43.2	8.00	K3	-21.656	0.064
HD 52711	7 3 30.5	29 20 13.5	5.93	G4	24.585	0.038
GJ 273	7 27 24.5	5 13 32.8	9.89	M3.5	18.210	0.030
HD 65583	8 0 32.1	29 12 44.5	6.94	G8	14.796	0.072
HD 67767	8 10 27.2	25 30 26.4	5.73	G7	-44.272	0.093
HD 71334	8 25 49.5	-29 55 50.1	7.82	G4	17.389	0.207
HD 73667	8 39 50.8	11 31 21.6	7.64	K1	-12.123	0.071
HD 84035	9 43 25.7	42 41 29.6	8.12	K5	-12.271	0.092
HD 84737	9 48 35.4	46 1 15.6	5.10	G0.5	4.881	0.038
HD 88230	10 11 22.1	49 27 15.3	6.61	K5	-25.710	0.037
HD 88371	10 11 48.1	23 45 18.7	8.43	G2	82.463	0.067
HD 88725	10 14 8.3	3 9 4.7	7.74	G1	-22.016	0.108
HD 89269	10 18 51.9	44 2 54.0	6.65	G5	-7.557	0.030
GJ 388	10 19 36.3	19 52 11.9	9.43	M4.5	12.453	0.066
HD 90156	10 23 55.3	-29 38 43.9	6.95	G5	26.918	0.032
HD 90711	10 28 12.1	-6 36 2.1	7.90	K0	29.903	0.073
HD 95735	11 3 20.2	35 58 11.5	7.49	M2	-84.683	0.030
HD 96700	11 7 54.4	-30 10 28.4	6.54	G2	12.787	0.076
HD 97101	11 11 5.2	30 26 45.7	8.31	K8	-16.159	0.434
HD 97343	11 12 1.2	-26 8 12.0	7.04	G8	39.789	0.030
HD 97658	11 14 33.2	25 42 37.4	7.78	K1	-1.706	0.104
HD 98281	11 18 22.0	-5 4 2.3	7.31	G8	13.312	0.036
HD 99491	11 26 45.3	3 0 47.2	6.49	K0	4.171	0.039
HD 100180	11 31 44.9	14 21 52.2	6.20	G0	-4.860	0.030
HD 100623	11 34 29.5	-32 49 52.8	5.98	K0	-21.964	0.030
HD 101259	11 39 0.4	-24 43 15.9	6.42	G6	96.812	0.187
HD 104067	11 59 10.0	-20 21 13.6	7.93	K2	14.992	0.058
HD 105631	12 9 37.3	40 15 7.4	7.47	K0	-2.472	0.088
HD 106156	12 12 57.5	10 2 15.8	7.92	G8	-7.336	0.159
HD 111515	12 49 44.8	1 11 16.9	8.10	G8	2.563	0.030
HD 116442	13 23 39.2	2 43 24.0	7.06	G5	28.411	0.030
HD 116443	13 23 40.8	2 43 31.0	7.36	G5	27.383	0.065

TABLE 2 — *Continued*

Star Name	RA (2000)	DEC (2000)	$V_{\text{mag}}$	Spectral Type	Final RV ( $\text{km s}^{-1}$ )	Unc ( $\text{km s}^{-1}$ )
GJ 514	13 29 59.8	10 22 37.8	9.04	M0.5	14.531	0.050
HD 119850	13 45 43.8	14 53 29.5	8.46	M1.5	15.778	0.061
HD 120467	13 49 44.8	-22 6 39.9	8.16	K4	-37.628	0.356
HD 122120	13 59 19.4	22 52 11.1	9.04	K5	-57.442	0.030
HD 122652	14 2 31.6	31 39 39.1	7.17	F8	1.484	0.149
HD 125184	14 18 0.7	-7 32 32.6	6.50	G5	-12.331	0.092
HD 125455	14 19 34.9	-5 9 4.3	7.58	K1	-9.856	0.100
HD 132142	14 55 11.0	53 40 49.2	7.73	K1	-14.789	0.035
HD 136713	15 22 36.7	-10 39 40.0	7.99	K2	-6.052	0.030
HD 136834	15 22 42.5	1 25 7.1	8.30	K3	-26.417	0.086
HD 139323	15 35 56.6	39 49 52.0	7.56	K3	-67.105	0.030
HD 141004	15 46 26.6	7 21 11.1	4.43	G0	-66.390	0.053
HD 144585	16 7 3.4	-14 4 16.6	6.32	G5	-14.014	0.106
HD 146233	16 15 37.3	-8 22 10.0	5.50	G2	11.756	0.030
HD 151541	16 42 38.6	68 6 7.8	7.56	K1	9.473	0.030
HD 151288	16 45 6.4	33 30 33.2	8.11	K5	-31.349	0.030
HD 154345	17 2 36.4	47 4 54.8	6.74	G8	-46.945	0.030
HD 154363	17 5 3.4	-5 3 59.4	7.73	K5	34.095	0.102
HD 157214	17 20 39.6	32 28 3.9	5.40	G0	-78.559	0.030
HD 157881	17 25 45.2	2 6 41.1	7.54	K5	-23.118	0.162
HD 159222	17 32 1.0	34 16 16.1	6.56	G5	-51.556	0.099
GJ 687	17 36 25.9	68 20 20.9	9.15	M3.5	-28.720	0.119
GJ 686	17 37 53.3	18 35 30.2	9.62	M1	-9.499	0.032
HD 161848	17 47 42.1	4 56 22.7	8.91	K1	-94.955	0.072
GJ 699	17 57 48.5	4 41 36.2	9.54	M4	-110.416	0.180
HD 164922	18 2 30.9	26 18 46.8	6.99	K0	20.236	0.030
HD 165222	18 5 7.6	-3 1 52.8	9.37	M1	32.621	0.100
HD 166620	18 9 37.4	38 27 28.0	6.37	K2	-19.465	0.094
HD 170493	18 29 52.4	-1 49 5.2	8.05	K3	-54.776	0.049
HD 170657	18 31 19.0	-18 54 31.7	6.82	K1	-43.137	0.045
HD 172051	18 38 53.4	-21 3 6.7	5.87	G5	37.095	0.030
HD 173701	18 44 35.1	43 49 59.8	7.52	K0	-45.630	0.056
HD 175541	18 55 40.9	4 15 55.2	8.03	G8	19.674	0.048
HD 176982	19 2 44.4	0 -42 40.4	8.35	G5	-6.825	0.063
HD 182488	19 23 34.0	33 13 19.1	6.36	G8	-21.485	0.046
HD 182572	19 24 58.2	11 56 39.9	5.16	G8	-100.289	0.030
HD 187923	19 52 3.4	11 37 42.0	6.10	G0	-20.619	0.030
HD 188512	19 55 18.8	6 24 24.3	3.71	G8	-40.074	0.070
HD 190404	20 3 52.1	23 20 26.5	7.28	K1	-2.535	0.030
HD 191785	20 11 6.1	16 11 16.8	7.33	K1	-49.289	0.030
HD 196761	20 40 11.8	-23 46 25.9	6.37	G8	-41.930	0.114
HD 197076	20 40 45.1	19 56 7.9	6.45	G5	-35.402	0.030
GJ 806	20 45 4.1	44 29 56.7	10.79	M1.5	-24.697	0.030
HD 199305	20 53 19.8	62 9 15.8	8.54	M0.5	-17.144	0.034
HD 202751	21 18 3.0	0 9 41.7	8.23	K2	-27.448	0.041
HD 204587	21 30 2.8	-12 30 36.3	9.10	K5	-84.103	0.165
HD 210302	22 10 8.8	-32 32 54.3	4.92	F6	-16.154	0.210
HD 216259	22 51 26.4	13 58 11.9	8.30	K0	1.241	0.099
HD 216899	22 56 34.8	16 33 12.4	8.66	M1.5	-27.255	0.123
HD 217357	23 0 16.1	-22 31 27.6	7.89	K5	16.461	0.082
HD 217877	23 3 57.3	-4 47 41.5	6.68	F8	-12.738	0.124
HD 218566	23 9 10.7	-2 15 38.7	8.60	K3	-37.825	0.042
HD 219538	23 16 18.2	30 40 12.7	8.09	K2	9.967	0.047
HD 220339	23 23 4.9	-10 45 51.3	7.80	K2	33.984	0.035
HD 221356	23 31 31.5	-4 5 14.7	6.49	F8	-12.625	0.176
GJ 908	23 49 12.5	2 24 4.4	8.98	M2	-71.084	0.125
HD 223498	23 50 5.7	2 52 37.8	8.41	G7	-24.005	0.040

TABLE 3  
ABSOLUTE RADIAL VELOCITIES FOR 2046 STARS

Star Name	Template <sup>a</sup>	<JD> -2450000	$\Delta T$ (days)	<RV> (km s <sup>-1</sup> )	Obs	$\sigma_{RV}$ (km s <sup>-1</sup> )
HD 224983	V	4176	1619	-17.486	8	0.136
HD 225021	V	4646	832	-6.225	7	0.176
HD 225118	V	3810	594	10.869	9	0.069
HD 225261	V	3585	692	7.493	2	0.022
HIP 428	M	4292	1933	-0.287	13	0.175
HD 225213	M	4290	1474	25.379	34	0.094
HD 38b	M	4219	1480	-1.700	18	0.101
HD 38a	M	4172	1482	1.654	10	0.142
HD 105	V	3955	1778	2.162	4	0.200
HD 166	V	4128	1326	-6.444	12	0.118
HD 283	V	4153	1219	-43.174	7	0.077
HD 377	V	3670	1961	1.321	19	0.175
HD 457	V	3604	0	-19.447	1	...
HD 533	V	3605	0	24.101	1	...
HD 531a	V	3422	367	13.338	2	0.149
HD 531b	V	3422	367	14.525	2	0.157
HIP 916	V	4723	4	-11.418	4	0.302
HD 691	V	4241	1776	-2.864	4	0.043
HD 745	V	5379	0	-2.357	1	...
HD 804	V	3695	3	-47.871	4	0.077
HD 834	V	4294	405	5.199	3	0.112
HIP 1055	V	4736	87	-36.137	7	0.317
HD 1100	V	4663	795	22.749	7	0.132
HIP 1294	V	4779	2	-0.325	4	0.079
HD 1205	V	4944	1355	6.561	14	0.183
HD 1293	V	4652	507	45.140	10	0.082
HIP 1368	M	3972	2137	2.822	4	0.223
HD 1388	V	3856	1487	28.574	3	0.157
HD 1384	V	4987	973	-35.185	30	0.135
HD 1326	M	4037	1796	11.817	44	0.110
HD 1326b	M	3928	0	10.960	1	...
HD 1461	V	4330	2143	-10.158	437	0.116
HIP 1532	V	5042	476	-10.994	22	0.146
HD 1497	V	3867	525	-7.488	2	0.210
HD 1502	V	4988	1037	-10.024	43	0.114
HD 1605	V	4371	1632	9.775	18	0.104
WASP-1	V	4345	6	-13.430	37	0.089
HIP 1734	M	3702	150	16.928	3	0.076
HIP 1780	V	3695	2	-47.094	3	0.045
HD 1835	V	5232	0	-2.280	1	...
HD 1832	V	3585	692	-30.492	2	0.034
HD 2025	V	4052	2140	3.094	4	0.153
HD 2085	V	4024	0	-47.402	2	0.950
HD 2331	V	3928	6	-16.702	5	0.055
HIP 2247	V	4816	468	2.913	5	0.188
HD 236427	V	4747	832	-12.479	6	0.081
HD 2589	V	3754	0	13.743	2	0.026
HD 2946	V	4682	795	10.460	11	0.174
HD 2992	V	4024	0	-16.150	1	...
HD 3074a	V	4201	1412	29.412	3	0.064
HD 3141	V	4136	679	0.606	4	0.108
HD 3404	V	4411	317	5.770	6	0.080
HD 3458	V	4585	507	-4.607	6	0.365
HD 3545	V	4773	1174	-24.951	28	0.107
HD 3592	V	3695	2	7.395	3	0.034
HD 3578	V	3695	2	3.187	3	0.034
GJ 26	M	3966	1776	-0.383	14	0.115
HD 3651	V	3949	2140	-32.940	63	0.109
HD 3684	V	4158	295	-23.238	3	0.064
HIP 3143	M	3766	354	12.249	4	0.169
HD 3700	V	3689	893	-1.356	3	0.141
HD 3795	V	4515	1844	-45.481	4	0.278
HD 3765	V	4160	2137	-63.191	60	0.107
HD 3861	V	4258	0	-14.786	3	0.023
HD 4113	V	4242	677	4.944	7	0.096
HIP 3418	V	4816	469	-36.313	5	0.192
HD 4208	V	4843	1566	56.785	5	0.074
HD 4203	V	4452	1657	-14.092	14	0.131
HD 4075	V	3642	693	-9.485	3	0.110
HD 4256	V	4387	1980	9.426	52	0.109
HD 4313	V	4927	1038	14.482	30	0.113
HD 4395	V	4710	795	-0.439	7	0.158
HD 4406	V	4007	1223	2.431	13	0.353
HD 4628	V	4859	1319	-10.229	79	0.121
HD 4614	V	5017	789	8.397	37	0.117

TABLE 3 — *Continued*

Star Name	Template <sup>a</sup>	<JD> -2450000	$\Delta T$ (days)	<RV> (km s <sup>-1</sup> )	Obs	$\sigma_{RV}$ (km s <sup>-1</sup> )
HD 4614b	M	4862	1147	11.196	26	0.107
HD 4747	V	4506	1960	10.078	23	0.117
HD 4635	V	4349	1443	-31.508	5	0.107
HD 4813	V	4516	1292	8.303	3	0.135
HD 4917	V	5039	916	-11.482	31	0.114
HD 4915	V	4687	1448	-3.729	49	0.129
HIP 3998	V	5189	2	6.693	4	0.036
HD 4741	V	3495	513	11.513	2	0.017
HD 5035	V	3931	0	-7.177	1	...
HD 5133	V	4408	1239	-13.071	4	0.072
HD 232301	V	3693	7	-15.072	4	0.094
HD 5294	V	4065	615	-8.202	3	0.029
HD 5319	V	4289	2013	0.344	44	0.105
HIP 4353	V	4722	2	7.727	4	0.154
HD 5372	V	3931	0	0.698	1	...
HIP 4454	V	5101	112	-51.402	5	0.072
HD 5891	V	5006	916	-96.564	22	0.241
HD 5946	V	3983	2	-2.850	4	0.057
GJ 47	M	4654	1445	7.599	2	0.094
HD 6019	V	4827	459	-23.812	5	0.247
HIP 4845	M	4879	478	9.538	6	0.149
GJ 48	M	4475	1771	1.377	15	0.122
GJ 49	M	4136	409	-5.895	2	0.114
HD 6268	V	3983	0	38.966	1	...
HIP 5004	V	3422	367	45.432	2	0.169
HD 6512	V	4257	405	10.246	3	0.038
HD 6558	V	3422	367	8.839	2	0.127
HIP 5247	V	4861	413	2.661	5	0.034
HD 6697	V	4226	405	-24.752	2	0.001
HD 6734	V	4661	1625	-94.606	8	0.103
HD 6715	V	3999	1192	-23.680	5	0.080
HD 6872b	V	3996	1486	-35.158	3	0.626
HD 6872a	V	3586	694	-34.681	2	0.121
HD 6963	V	4307	1950	-31.840	6	0.090
HIP 5643	M	3605	0	27.840	1	...
HIP 5663	V	5041	478	-4.765	22	0.145
HD 7530	V	4717	734	55.245	6	0.073
HD 7510	V	4072	447	-35.616	5	0.097
HIP 5938	V	4461	1994	8.327	6	0.133
HD 7931	V	4661	794	11.248	6	0.049
HD 8038	V	3422	367	9.606	2	0.112
HIP 6276	V	4302	1935	10.549	5	0.099
HD 8110	V	3697	0	9.519	1	...
HIP 6344	V	4816	470	-20.485	5	0.163
HD 8250	V	5257	0	5.364	1	...
HD 7924	V	4620	2046	-22.711	374	0.122
HD 8407	V	4664	794	-6.833	7	0.064
HD 8389	V	4387	1778	34.626	57	0.109
HD 8446	V	4210	405	19.785	5	0.123
HD 8328	V	3599	720	-3.874	2	0.076
HD 8467	V	4394	1958	14.712	7	0.111
HD 8508	V	4930	916	9.086	18	0.149
HD 8553	V	4036	1193	6.898	7	0.112
HD 8574	V	4609	1958	19.041	6	0.094
HD 8648	V	4067	1787	0.859	3	0.099
HD 8765	V	3728	60	-23.399	11	0.076
HD 8859	V	3610	743	24.586	2	0.102
HD 8828	V	4256	1437	13.603	27	0.104
HIP 6778	V	3575	6	-0.659	3	0.138
HD 8912	V	3610	743	24.512	2	0.138
HD 8907	V	4379	1957	8.966	5	0.169
HD 8939	V	4024	0	-5.838	1	...
HD 9113	V	4073	825	-32.621	4	0.120
HD 9081	V	4226	405	28.668	2	0.049
HD 9070	V	3601	721	11.805	2	0.049
HD 9218	V	4662	794	11.171	6	0.056
HD 9156	V	4749	736	28.918	8	0.095
HD 9331	V	3600	722	-19.961	2	0.043
HD 9540	V	4672	0	2.598	1	...
HD 9540a	V	3490	745	2.456	4	0.154
HD 9554	V	4630	507	-18.085	6	0.136
HD 9472	V	4657	1265	11.443	4	0.091
HD 9562	V	4410	1992	-14.990	7	0.132
HD 9625	V	4890	892	-26.883	12	0.640
HD 9407	V	4668	2046	-33.313	309	0.124
HD 9672	V	4724	0	-2.838	1	...



TABLE 3 — *Continued*

Star Name	Template <sup>a</sup>	<JD> -2450000	$\Delta T$ (days)	<RV> (km s <sup>-1</sup> )	Obs	$\sigma_{RV}$ (km s <sup>-1</sup> )
HD 9518a	V	3600	722	-17.100	2	0.066
s11844	V	4080	1100	-17.089	6	0.133
HD 9782	V	3749	891	11.408	4	0.078
HD 9826	V	4085	0	-28.351	1	...
HD 10002	V	3945	1193	11.528	5	0.045
WASP18	V	5232	0	2.780	2	0.042
HD 10008	V	3971	620	11.689	5	0.026
HD 9986	V	4749	1776	-20.984	38	0.145
HD 10015	V	3983	2	2.281	4	0.105
HIP 7728	V	3695	2	-15.350	3	0.092
HD 10013	V	4072	447	-61.891	5	0.057
HIP 7830	V	5189	2	10.162	4	0.076
HD 10353	V	3695	2	-6.463	3	0.078
HD 10383	V	4947	1041	20.676	11	0.153
HD 10336	V	3689	0	-13.548	1	...
HD 10145	V	4257	1871	17.888	4	0.158
HIP 7924	V	3575	6	1.397	3	0.124
HD 10442	V	4827	1355	7.804	17	0.108
HD 10479	V	5106	704	2.045	15	0.191
HD 10195	V	3689	0	10.076	1	...
HD 10476	V	3966	2139	-33.648	136	0.103
HIP 8051	M	4528	1961	-25.945	18	0.212
HD 10436	V	4032	1541	-50.946	9	0.063
HD 10700	V	4309	1994	-16.629	460	0.121
HD 10697	V	4723	2139	-45.919	7	0.132
HD 10823	V	4940	916	25.650	19	0.138
HD 11020	V	3622	784	22.739	3	0.079
HIP 8361	V	5191	0	8.351	1	...
HD 10780	V	4045	1871	2.814	13	0.086
HD 11131	V	3753	53	-4.394	12	0.111
HD 11170	V	3798	596	-10.803	6	0.139
HD 10790	V	4564	1993	-25.689	7	0.122
HD 11271	V	4223	827	9.276	4	0.098
HD 11506	V	4633	2012	-7.421	55	0.117
HD 11373	V	3621	723	-27.449	5	0.191
HD 11616	V	3689	0	-11.790	1	...
HIP 8920	V	3933	0	-41.325	1	...
HD 11731	V	3804	436	-22.767	4	0.108
HIP 8943	V	3399	2	-4.714	2	0.051
HD 11791	V	3695	2	18.130	3	0.084
HD 11850	V	4369	1933	1.941	5	0.153
HD 11964a	V	4049	2023	-9.306	76	0.150
HD 11997	V	3695	1	29.297	2	0.067
HD 12039	V	5092	424	6.341	4	0.273
HD 11970	V	4747	832	-14.377	6	0.734
HD 12051	V	4492	2017	-35.133	117	0.146
HD 12165	V	3695	2	-15.730	3	0.065
HD 12164	V	4718	735	-18.252	6	0.148
HD 12235	V	5257	0	-18.243	1	...
GJ 83.1	M	4003	1158	-28.308	6	0.192
HD 12137	V	4701	830	-12.799	7	0.192
g244-047	M	3837	1073	-84.256	3	0.116
HD 12484	V	4344	1537	4.960	9	0.101
HAT-P-32	V	4616	1039	-22.489	25	0.741
HD 12661	V	4566	1992	-47.309	20	0.141
HIP 9788	V	4920	541	-10.703	16	0.151
HD 12846	V	4297	1957	-4.694	86	0.105
HD 13043	V	4593	1994	-39.329	122	0.102
HD 13167	V	4886	892	15.780	11	0.075
HD 13361	V	4024	0	6.802	1	...
HIP 10072	M	5151	118	17.642	3	0.066
HD 13345	V	4024	0	22.362	1	...
s92823	V	3622	784	26.000	3	0.075
HD 13357	V	3622	784	25.145	3	0.093
HD 13382	V	4386	1779	20.026	7	0.112
HD 13483	V	3641	693	-12.077	3	0.152
GJ 87	M	4627	1238	-2.655	37	0.152
HD 13612b	V	3605	729	-5.422	2	0.156
HD 13555	V	4085	0	5.771	1	...
HD 13584	V	3604	0	6.212	1	...
HIP 10337	V	4997	452	3.058	19	0.186
HIP 10416	V	4976	484	-8.576	7	0.081
HD 13747	V	5261	0	18.603	1	...
HIP 10449	V	3605	729	27.893	2	0.223
HD 13773	V	4172	295	9.193	2	0.068
HD 13836	V	3642	693	1.076	3	0.121

TABLE 3 — *Continued*

Star Name	Template <sup>a</sup>	<JD> -2450000	$\Delta T$ (days)	<RV> (km s <sup>-1</sup> )	Obs	$\sigma_{RV}$ (km s <sup>-1</sup> )
HD 13579	V	3899	1059	-12.859	3	0.121
HD 13999	V	3695	1	18.536	2	0.133
HD 13997	V	3793	1193	-20.788	6	0.112
HD 13931	V	4815	2022	30.586	27	0.139
HD 14223	V	3604	0	31.544	1	...
HD 14412	V	4062	1993	7.340	73	0.129
HD 14374	V	3623	783	25.195	3	0.315
HD 14655	V	3899	1863	0.787	37	0.108
HIP 11000	V	4933	539	26.409	9	0.102
HD 14651	V	3793	1104	53.685	5	0.427
HIP 11048	M	4457	1896	-37.964	18	0.151
HD 14787	V	4863	892	-8.220	10	0.077
HD 15337	V	3814	420	-3.995	2	0.089
HD 11437	V	5259	6	25.574	3	0.133
HD 15336	V	4756	734	-30.453	6	0.186
HD 15391	V	4899	582	28.682	6	0.192
HD 15367	V	3604	0	-64.275	1	...
HD 15335	V	3722	724	41.202	3	0.095
HD 15928	V	4778	916	11.064	7	0.129
HD 16141	V	4387	1992	-50.940	17	0.112
HD 16160	V	4695	1299	25.756	62	0.142
HD 16249	V	3695	2	6.924	3	0.018
HD 16297	V	4311	1204	-1.032	4	0.032
HD 16178	V	4664	796	-24.585	7	0.107
G.J 105b	M	4104	1896	26.159	9	0.194
HD 16417	V	4673	8	11.096	18	0.102
HD 16175	V	5256	0	21.949	1	...
HD 16275	V	3831	1436	-7.552	4	0.057
HD 16397	V	3587	693	-99.654	2	0.115
HD 16623	V	3551	744	17.541	3	0.097
HD 16559	V	5261	0	-12.757	1	...
HIP 12493	V	4817	470	72.885	5	0.119
HIP 12635	V	5049	0	-3.455	1	...
HD 16760	V	4126	1092	-3.566	18	0.372
HIP 12709	V	4740	69	34.053	4	0.171
HD 16984	V	4664	796	69.677	7	0.258
G.J 107b	M	3601	722	25.784	2	0.012
G.J 109	M	4479	1896	30.458	11	0.149
HD 17152	V	3241	0	27.857	1	...
HD 17354	V	3320	158	16.794	2	0.851
HD 17190	V	4341	523	14.045	5	0.052
HD 17230	V	4619	2042	11.006	32	0.110
HD 17311	V	4778	916	18.516	7	0.114
HD 17449	V	3694	0	-48.965	1	...
HD 17075	V	3695	2	-34.298	3	0.044
HD 17382	V	3833	407	5.841	4	0.441
HD 17620	V	4826	798	1.340	7	0.099
HD 17156	V	4197	1425	-3.207	38	0.110
HD 17660	V	4248	1540	-28.997	7	0.118
HIP 13342	V	4961	541	0.313	17	0.129
HIP 13375	M	4945	540	-49.470	8	0.095
HIP 13447	V	3695	2	-1.291	3	0.038
HD 18015	V	4778	916	19.008	7	0.140
HD 18131	V	5261	0	14.493	1	...
HD 18143	V	4543	1475	31.970	44	0.145
HD 18436a	V	3642	323	30.598	3	0.058
HD 18445	V	3839	1004	50.465	5	0.487
HD 18645	V	4714	794	-2.656	7	0.122
HD 18632	V	3541	743	28.924	3	0.144
HD 18667	V	4702	528	3.660	8	0.364
HD 18742	V	4868	916	-13.831	18	0.106
HD 18702	V	3820	1189	71.313	5	0.162
HD 18747	V	4489	1628	49.424	6	0.105
HD 18752	V	3562	269	20.248	2	0.391
HIP 14113	V	3762	269	40.386	4	0.065
HD 18803	V	3909	1796	9.862	68	0.093
HD 18975	V	3676	613	35.268	2	0.073
HD 19034	V	3551	744	-20.281	3	0.051
HD 19019	V	4148	1896	24.867	7	0.122
HD 18916	V	3654	729	-51.057	3	0.139
HD 18993	V	4159	375	-19.391	4	0.119
HD 19056	V	3695	2	41.549	3	0.029
HD 19467	V	3607	744	7.002	4	0.090
HD 19308	V	3551	744	32.828	3	0.168
HD 19522	V	4727	834	57.359	7	0.118
HD 19659	V	3828	556	1.974	7	0.077

TABLE 3 — *Continued*

Star Name	Template <sup>a</sup>	<JD> -2450000	$\Delta T$ (days)	<RV> (km s <sup>-1</sup> )	Obs	$\sigma_{RV}$ (km s <sup>-1</sup> )
HD 19373	V	4001	1957	49.400	128	0.114
HAT-P-10	V	4748	643	4.779	10	0.153
HD 19676	V	4636	0	-41.965	1	...
HD 19668	V	4148	1896	14.664	7	0.062
HD 19638	V	4428	0	-1.124	1	...
HD 19618	V	3984	3	-26.551	4	0.094
HD 19617	V	4073	447	-27.372	5	0.133
HIP 14729	V	4928	483	39.134	6	0.080
HD 19502	V	4024	0	-8.604	1	...
HD 19773	V	4029	1001	21.789	11	0.116
HIP 14809	V	3694	0	5.203	1	...
HIP 14810	V	4202	1591	-4.971	64	0.300
HD 20155	V	3320	158	-7.949	2	0.070
HIP 15095	V	5002	484	15.315	8	0.153
HD 20165	V	4510	1803	-16.672	28	0.164
HD 19961	V	3695	1	-11.626	2	0.092
HD 20439	V	3813	209	32.234	10	0.133
HD 20619	V	4588	1895	22.663	40	0.130
HD 20618	V	5261	0	-4.708	1	...
HD 20781	V	3604	0	40.135	1	...
HIP 15563	V	5212	70	31.102	4	0.114
HD 20678	V	3705	62	35.051	5	0.154
HD 20675	V	4584	1230	23.029	2	0.487
HIP 15673	V	4856	386	-40.148	5	0.072
HD 20670	V	4416	785	15.573	2	0.050
HD 21019a	V	3970	2016	41.737	4	0.207
HIP 15904	V	3779	1104	86.643	4	0.047
HD 21197	V	3472	744	-13.023	5	0.130
HD 21340	V	4861	357	21.900	4	0.096
HD 21316	V	3695	2	40.584	3	0.065
HD 21313	V	3969	0	-20.188	1	...
HIP 16134	V	4724	1	34.050	3	0.020
HD 21581	V	4726	734	152.943	6	0.119
HD 21449	V	3870	706	-5.328	14	0.123
HD 21774	V	3983	0	-3.116	1	...
HIP 16404	V	3604	731	-161.665	2	0.134
HD 21847	V	3540	746	30.289	3	0.094
HD 22049	V	5217	151	16.428	8	0.087
HD 21742	V	4055	678	-36.126	3	0.093
HD 22072	V	3542	744	11.039	3	0.107
HD 22233	V	4747	916	19.434	7	0.127
HD 22282	V	3512	745	-4.945	4	0.145
HD 22484	V	5209	150	28.167	3	0.073
HD 22657	V	4887	892	65.610	11	0.115
HD 22670	V	3709	57	9.937	4	0.078
HD 22879	V	4317	1934	120.340	31	0.107
HD 22778	V	4172	414	-24.909	3	0.082
HD 23134	V	4747	916	18.831	7	0.091
HIP 17346	V	4928	483	16.023	6	0.078
HD 22844	V	5062	912	-26.972	8	0.107
HD 23249	V	4040	2016	-6.189	38	0.177
HD 23221	V	3695	2	46.649	3	0.047
HII 152	V	5087	450	5.807	3	0.044
HD 23356	V	4257	1858	25.278	30	0.114
HIP 17496	V	4861	412	83.869	5	0.115
HII 514	V	5087	450	4.976	3	0.070
HII 1101	V	5087	450	5.563	3	0.357
HD 23439	V	4425	1896	50.638	25	0.119
HD 23486	V	3985	0	-19.860	1	...
HD 23825	V	4832	945	-16.793	7	0.080
HD 24148	V	4876	946	49.483	8	0.101
HD 24040	V	4086	1833	-9.379	18	0.077
HD 24316	V	4934	892	52.272	12	0.103
HD 24213	V	3541	747	-39.627	3	0.141
HD 281309	V	3695	2	20.526	3	0.088
HD 24365	V	4089	1934	19.276	6	0.083
HD 24521	V	3969	0	-0.159	1	...
HD 24496	V	4586	2046	18.869	118	0.138
s130811	V	4645	2047	62.441	25	0.190
HD 24341	V	3611	746	142.692	2	0.100
HD 24505	V	4081	1747	-12.696	6	0.179
HD 24238	V	4559	1856	38.772	30	0.138
HD 24727	V	3540	744	-18.076	3	0.136
HD 24612	V	3985	0	33.976	1	...
HD 24892	V	3600	743	45.545	4	0.250
HD 24916	V	3412	783	3.585	7	0.234

TABLE 3 — *Continued*

Star Name	Template <sup>a</sup>	<JD> -2450000	$\Delta T$ (days)	<RV> (km s <sup>-1</sup> )	Obs	$\sigma_{RV}$ (km s <sup>-1</sup> )
HD 24451	V	4264	1441	17.585	7	0.081
HD 25311	V	4012	1833	-40.043	11	0.075
HD 25565	V	4044	1470	-27.168	3	0.098
HD 25457	V	3997	2017	17.846	10	0.196
HD 25445	V	3695	2	7.638	3	0.034
HD 25329	V	4327	1772	-25.845	33	0.107
HD 25622	V	4827	917	-1.817	7	0.096
HD 25682	V	3554	785	-30.338	3	0.161
HD 26007	V	4870	946	9.167	7	0.089
HD 281540	V	4264	561	110.315	2	0.106
HD 25825	V	3555	784	37.625	3	0.139
HIP 19165	V	4019	2022	25.068	22	0.111
HD 25894	V	3779	2	-15.393	3	0.080
HD 26151	V	4438	2017	-6.752	7	0.151
HD 25998	V	5057	424	26.066	3	0.234
HD 26257	V	3387	61	33.841	5	0.083
HD 25665	V	4406	1795	-13.556	18	0.121
HD 26161	V	3984	0	12.870	1	...
HD 26140	V	4748	972	-6.970	7	0.142
HIP 19472	V	5188	0	45.412	1	...
HD 26634	V	4790	917	8.476	7	0.118
HD 26633	V	5262	0	91.484	1	...
HD 26756	V	3778	1	38.162	2	0.001
HD 26794	V	4019	1216	56.487	7	0.112
HD 26736	V	4276	1061	37.430	13	0.118
FP Tau	V	5229	58	4.617	3	0.289
HD 26965	V	4174	2021	-42.337	83	0.118
HD 26874	V	3399	0	61.401	1	...
HD 27063	V	4034	101	-9.580	2	0.093
HD 284253	V	4336	0	38.183	1	...
HIP 19946	V	3695	2	145.427	3	0.015
HIP 19981	V	5204	72	27.994	5	0.064
HD 27297	V	4846	922	42.493	6	0.136
HD 27250	V	3778	1	38.520	2	0.003
HD 27282	V	3765	55	37.949	8	0.107
HD 281934	V	4413	1862	16.294	7	0.644
HD 27530	V	4084	1469	42.209	7	0.098
HD 27371	V	4336	0	38.581	1	...
HIP 20218	V	4162	1958	18.253	7	0.093
HD 27496	V	3785	238	27.783	8	0.083
HIP 20359	V	5208	72	-78.582	4	0.130
XO-3	V	4876	420	-10.702	43	0.532
HD 27697	V	4336	0	37.470	1	...
HD 27732	V	4016	715	38.507	3	0.035
HD 284414	V	4336	0	39.585	1	...
HD 27771	V	4336	0	39.601	1	...
HD 27956	V	4793	917	45.984	7	0.131
HD 27859	V	4493	0	37.692	1	...
HAT-P-15	V	4558	857	31.668	25	0.155
HD 28187	V	3554	784	18.322	3	0.137
HD 27990	V	4336	0	42.593	1	...
HD 27748	V	3695	2	-23.892	3	0.019
HIP 20705	V	3767	288	23.394	4	0.041
HD 28185	V	3884	1089	50.253	2	0.298
HD 28099	V	4016	715	38.431	3	0.018
HD 28192	V	3778	1	-4.138	2	0.005
HD 28137	V	3779	2	18.922	3	0.092
HD 28005	V	4448	1627	34.729	21	0.108
HD 28388	V	4481	388	20.406	4	0.462
HD 28237	V	4162	1957	39.690	7	0.147
HD 28258	V	4336	0	40.436	1	...
HD 28307	V	4336	0	39.281	1	...
HD 28305	V	4336	0	38.442	1	...
HD 28437	V	3806	598	26.731	3	0.453
HD 28097	V	3884	710	8.375	6	0.120
HD 28343	M	4466	1797	-35.000	17	0.158
HD 283704	V	3779	1	38.509	2	0.142
HD 285773	V	4336	0	39.992	1	...
HD 28462	V	3778	1	40.090	2	0.022
HIP 21091	V	3710	60	14.402	4	0.101
HD 28593	V	3778	1	39.666	2	0.046
HD 28678	V	4968	973	61.465	13	0.152
HD 28737	V	4770	922	-5.702	6	0.203
HD 28946	V	3875	1059	-46.327	8	0.101
HD 28992	V	3778	1	40.214	2	0.074
DN Tau	V	5200	96	18.462	3	0.061

TABLE 3 — *Continued*

Star Name	Template <sup>a</sup>	<JD> -2450000	$\Delta T$ (days)	<RV> (km s <sup>-1</sup> )	Obs	$\sigma_{RV}$ (km s <sup>-1</sup> )
HD 232979	M	4153	1526	34.269	24	0.131
HIP 21556	M	4641	1273	-6.831	9	0.080
HD 29461	V	4680	1146	40.326	3	0.239
LkCa15	V	5259	54	18.187	2	0.011
HD 29528	V	3554	783	-18.789	3	0.254
HD 29621	V	3779	2	35.022	3	0.102
HD 285968	M	4725	1886	26.244	39	0.139
HD 29980	V	4084	1116	32.286	6	0.089
HD 29883	V	4198	1951	17.776	25	0.111
HD 30128	V	4798	917	20.863	7	0.149
HD 29818	V	3696	1	46.573	2	0.017
HD 30286	V	3779	2	18.334	3	0.113
HD 30090	V	3697	0	23.377	1	...
HD 30246	V	3778	1	41.721	2	0.029
HIP 22288	V	4987	456	27.274	9	0.092
HD 30166	M	4701	794	-32.300	6	0.114
HD 30339	V	3696	2	8.686	3	0.561
HD 30572	V	3778	1	32.450	2	0.051
HD 30663	V	3715	83	-15.485	4	0.063
HD 30856	V	4901	916	35.457	11	0.130
HD 30712	V	4130	1	42.593	2	0.174
HD 30708	V	3985	0	-55.696	1	...
HD 30649	V	4977	509	32.241	2	0.067
HIP 22627	M	4844	1278	-8.865	21	0.080
HD 31018	V	3892	1002	-4.147	12	0.107
HIP 22762	M	4727	1450	-14.554	25	0.132
HD 30882	V	4915	974	-39.511	7	0.089
HD 31392	V	4419	1917	29.447	8	0.114
HD 31253	V	4152	1566	12.235	14	0.167
gmaur	V	4385	1891	16.180	6	0.994
HD 31560	V	4159	1440	6.205	8	0.112
HD 31412	V	4876	391	42.118	5	0.226
HD 31452	V	3360	30	15.151	3	0.106
HD 31543	V	4669	590	-6.940	8	0.144
HD 31693	V	4686	922	29.318	6	0.170
HD 31609	V	3695	2	42.825	3	0.074
HD 31451	M	4794	859	0.644	7	0.108
HD 31664	V	5314	0	-8.368	1	...
HD 31966	V	3532	743	-17.897	3	0.214
HD 32147	V	4496	1946	21.544	125	0.112
HD 32259	V	3779	2	28.075	3	0.093
HD 31675	V	4546	1	16.049	2	0.063
HIP 23512	M	3661	645	15.432	2	0.095
HIP 23516	V	4779	2	122.509	4	0.130
HD 31864	V	3992	705	-26.445	6	0.095
HD 32483	V	5262	0	9.115	1	...
HD 32673	V	4024	0	-6.714	1	...
HD 32923	V	4673	1339	20.594	48	0.115
HD 33142	V	4971	973	33.525	27	0.126
HD 33021	V	4655	1262	-22.388	2	0.132
HD 33240	V	4938	946	10.465	18	0.133
HD 32963	V	4913	1911	-62.295	19	0.127
HD 33283	V	3981	1917	4.721	30	0.139
HD 33108	V	3695	2	55.861	3	0.050
HIP 24121	V	4862	413	115.339	5	0.032
HD 33334	V	3825	1834	83.122	11	0.122
HD 33298	V	4931	945	-6.983	6	0.139
HIP 24141	V	3694	0	-7.256	1	...
HD 33822	V	3723	1059	-6.639	3	0.173
HD 33636	V	4705	1982	5.710	12	0.138
HD 33844	V	4931	973	36.307	20	0.135
HIP 24284	M	4548	1827	-24.999	15	0.113
HD 34445	V	4712	1973	-78.867	57	0.122
HD 34721	V	4311	1682	40.475	32	0.130
HD 34411	V	4147	1983	66.497	87	0.135
HD 34745	V	3725	597	35.225	2	0.090
HD 34909	V	4736	973	-0.426	6	0.090
HD 34957	V	4560	1567	0.909	31	0.419
HD 34575	V	4309	707	-23.592	5	0.113
HD 34887	V	4346	1975	-25.569	26	0.115
HIP 25220	V	4987	484	38.254	10	0.138
HD 35627	V	3626	597	27.220	3	0.054
HD 35974	V	3725	597	76.502	2	0.045
HD 36003	V	4168	1769	-55.558	69	0.111
DQ Tau	V	3339	0	44.489	1	...
HD 278253	V	3779	2	12.896	3	0.062

TABLE 3 — *Continued*

Star Name	Template <sup>a</sup>	<JD> -2450000	$\Delta T$ (days)	<RV> (km s <sup>-1</sup> )	Obs	$\sigma_{RV}$ (km s <sup>-1</sup> )
HD 36215	V	3849	738	-16.323	7	0.131
HD 36308	V	3662	646	26.064	2	0.111
HD 36395	M	4313	1917	8.676	12	0.170
HD 36387	V	3779	2	37.290	3	0.061
HIP 26080	V	3779	2	-14.572	3	0.044
HD 244992	V	3749	148	11.340	8	0.110
g097-054	M	3870	558	37.572	5	0.114
HIP 26196	V	5154	332	29.980	7	0.176
HD 37213	V	3427	0	12.264	1	...
HD 245409	M	3733	1206	22.190	5	0.200
HD 37124	V	4118	1990	-23.054	27	0.096
HD 36974	V	4646	471	15.106	6	0.847
HD 36130	V	3697	654	-62.445	2	0.145
HD 37484	V	4305	1380	24.019	4	0.483
HD 37445	V	4885	973	38.804	8	0.153
HD 37008	V	3931	1772	-45.861	35	0.116
HD 37250	V	5299	29	43.275	2	0.005
HD 37216	V	4441	1771	11.418	5	0.097
HD 37605	V	4264	1191	-22.197	12	0.286
HD 37962	V	3427	0	2.949	1	...
HD 37394	V	4064	1946	1.323	7	0.114
HD 233153	M	3711	626	2.061	2	0.031
HD 37986	V	3813	1060	59.202	4	0.093
HIP 26857	M	4359	561	106.040	3	0.037
HD 37977	V	3779	2	20.667	3	0.056
HD 38392	V	3517	684	-9.570	5	0.183
HD 38393	V	5116	480	-9.152	3	0.088
HD 38467	V	3999	1091	-17.783	5	0.126
HD 38308	V	3642	349	43.522	3	0.149
HD 38230	V	4128	1886	-29.212	46	0.110
HD 37006	V	4356	1771	-11.556	4	0.154
HD 38529	V	4564	1570	30.247	30	0.177
HD 38505	V	4826	981	75.613	9	0.329
HD 38400	V	3339	0	18.969	1	...
HD 38801	V	4315	1093	-25.370	12	0.184
HD 38949	V	4471	1746	3.485	8	0.136
HD 233165	V	3696	1	27.870	2	0.017
HD 38858	V	3849	1922	31.507	76	0.093
HD 37879	V	3339	0	-28.427	1	...
HD 39142	V	4938	981	8.977	12	0.121
HD 39352	V	3339	0	48.226	1	...
HD 39094	V	4206	447	10.170	10	0.106
HD 39796	V	3724	745	62.824	3	0.105
HD 39251	V	3398	0	-9.594	1	...
HIP 27793	V	3930	1116	7.549	5	0.047
HD 39480	V	3340	0	48.733	1	...
HD 39997	V	4024	0	10.263	1	...
HD 39715	V	3468	385	-33.724	3	0.170
HD 39731	V	4812	981	32.695	7	0.103
HD 39833	V	3817	791	24.891	3	0.064
HD 40126	V	3339	0	35.865	1	...
HD 39828	V	4781	974	28.802	9	0.097
HD 39881	V	4214	1438	0.320	13	0.087
HD 40397	V	3993	1789	143.356	54	0.098
HD 40537	V	4736	886	53.783	8	0.123
HD 40330	V	3779	2	56.603	3	0.059
g192-13	M	4036	1001	1.939	6	0.047
HD 41700	V	4149	1804	27.944	5	0.359
HD 40979	V	4075	1772	32.597	7	0.127
HD 41484	V	3339	0	0.385	1	...
HD 40647	V	4489	1771	-14.112	6	0.287
HD 41593	M	3974	674	-9.644	7	0.133
HIP 29052	M	4016	1029	13.640	9	0.091
HIP 29067	V	5190	1	-1.799	3	0.060
HD 42182	V	3339	0	60.735	1	...
GJ 226	M	4421	1858	-1.682	9	0.070
HD 42698	V	3750	52	18.707	2	0.013
HD 42581	M	4033	1830	4.738	13	0.119
HD 42618	V	4626	1923	-53.500	164	0.127
HIP 29548	V	5207	72	21.739	4	0.088
HD 43162	V	4114	1533	22.089	8	0.092
HD 42250	V	3577	353	19.806	2	0.263
HD 43745	V	3401	0	-2.423	1	...
HD 43691	V	4156	1689	-28.916	4	0.045
HD 43947	V	4377	1798	40.880	6	0.221
HIP 30112	V	5179	332	31.760	10	0.129

TABLE 3 — *Continued*

Star Name	Template <sup>a</sup>	<JD> -2450000	$\Delta T$ (days)	<RV> (km s <sup>-1</sup> )	Obs	$\sigma_{RV}$ (km s <sup>-1</sup> )
HD 43296	V	3779	2	-8.388	3	0.057
HD 44420	V	3713	623	-0.439	2	0.285
HD 44663	V	3369	0	5.919	1	...
HD 44614	V	3484	0	32.807	1	...
HD 45184	V	4113	1800	-3.859	117	0.119
HD 45067	V	3414	26	47.311	2	0.261
HD 44985	V	3401	0	32.481	1	...
HD 256714	V	3779	2	19.505	3	0.090
HD 45210	V	4866	943	53.781	10	0.565
HD 45588	V	3973	1145	36.220	2	0.086
HD 45350	V	4308	1982	-20.649	18	0.089
HD 45652	V	3941	651	-5.021	4	0.188
HIP 30979	V	4856	386	43.193	5	0.055
WASP12	V	5239	125	18.921	14	0.232
HD 45410	V	5273	34	39.477	2	0.139
HD 46375	V	4602	1918	-0.906	6	0.095
HD 46013	V	3779	2	-67.985	3	0.078
HD 45161	V	3780	3	-16.441	3	0.167
HD 47186	V	4618	1947	4.322	11	0.103
HIP 31546	V	3695	2	6.343	3	0.046
GJ 239	M	4633	1921	-58.224	31	0.113
HD 47157	V	4725	1469	25.215	27	0.056
HD 47562	V	4744	886	17.309	8	0.100
HD 47309	V	3779	2	27.765	3	0.049
HD 47752	V	3940	1411	-44.389	10	0.148
HD 47625	V	3441	86	31.181	2	0.237
HD 48122	V	4803	913	2.698	8	0.148
HIP 32132	V	3719	83	16.220	6	0.123
HD 48345	V	5290	0	24.701	1	...
COROT7	V	5321	0	31.020	1	...
HD 48938	V	3401	0	-10.293	1	...
HD 48682	V	4730	1199	-23.907	33	0.101
COROT1	V	5232	0	23.802	1	...
HD 49197	V	4437	1738	10.398	3	0.126
HIP 32769	V	4946	483	-52.417	7	0.103
HIP 32892	V	3695	2	23.587	3	0.073
HD 49674	V	4647	1944	12.034	22	0.148
HIP 32919	V	4868	386	19.244	5	0.134
HD 50499	V	4507	1946	36.883	16	0.206
HD 50281	V	3969	1742	-6.985	3	0.149
GJ 250b	M	4791	1796	-7.280	25	0.120
HD 50275	V	5006	945	84.308	9	0.132
HD 50806	V	3713	623	72.443	2	0.167
HD 50639	V	5099	447	-4.066	3	0.096
HD 50554	V	4637	1916	-3.919	7	0.094
HD 265866	M	4530	1775	22.942	24	0.165
HIP 33241	V	3864	1177	15.007	5	0.162
HD 50692	V	4466	1974	-14.968	64	0.178
HIP 33287	V	5188	0	31.134	1	...
HD 51219	V	3401	0	-7.809	1	...
HD 51419	V	5041	1257	-26.804	89	0.124
HD 51845	V	3601	349	23.616	2	0.089
HD 51046	V	3381	32	0.470	5	0.088
HD 51813	V	3778	1	36.427	2	0.076
HD 0748-01711-1	V	5234	101	8.338	6	0.109
HD 52265	V	3806	1857	53.763	29	0.126
HD 52456	V	3383	87	-12.138	2	0.036
HD 51866	V	4442	1735	-21.656	32	0.118
HD 52919	V	4201	1411	-30.526	6	0.090
HD 52711	V	4599	1861	24.585	95	0.115
HD 51067a	V	3778	0	13.184	1	...
HD 51067b	V	3778	0	13.548	1	...
HD 53665	V	3713	623	-14.543	2	0.200
HD 53532	V	4077	417	42.868	6	0.102
HD 55696	V	4335	1799	19.631	9	0.135
HIP 35093	V	3695	2	-50.685	3	0.053
HD 56083	V	4497	1573	-11.680	7	0.132
HD 55575	V	4923	1214	84.769	47	0.135
HD 56274	V	3383	88	66.529	2	0.134
HD 55647	V	3695	2	-16.717	3	0.084
HD 56303	V	3401	0	8.431	1	...
HD 56957	V	3398	0	54.806	1	...
HD 56122	V	5290	0	24.363	1	...
XO-4	V	5270	29	1.620	2	0.046
HD 57204	V	4165	447	-13.211	8	0.072
GJ 272	M	4778	0	-31.158	1	...

TABLE 3 — *Continued*

Star Name	Template <sup>a</sup>	<JD> -2450000	$\Delta T$ (days)	<RV> (km s <sup>-1</sup> )	Obs	$\sigma_{RV}$ (km s <sup>-1</sup> )
HD 57813	V	3984	3	46.063	4	0.036
GJ 273	M	4278	1921	18.210	20	0.095
HD 58781	V	3383	88	4.920	2	0.115
HD 58727	V	3984	3	-13.584	4	0.047
HD 59062	V	3481	0	46.114	1	...
HIP 36338	M	3659	1176	1.685	6	0.208
HIP 36551	V	4862	385	65.876	5	0.070
HIP 36635	M	5322	0	-17.917	1	...
HAT-P-33	V	4925	524	23.460	18	0.163
HD 60491	V	4154	1888	-9.586	5	0.142
HIP 36834	M	4027	1090	-41.708	13	0.141
HD 60234	V	3590	328	-0.242	2	0.408
HD 61005	V	4910	1177	22.558	5	0.081
HD 60521	V	3725	0	29.355	1	...
HD 60803	V	3697	0	47.102	1	...
HD 60041	V	3481	0	-77.051	1	...
HD 61236	V	3601	349	3.903	2	0.691
HD 60737	V	5149	450	6.448	5	0.045
HD 61447	V	3587	378	89.308	2	0.133
HIP 37217	M	3853	1178	-28.833	4	0.147
HD 61364	V	3705	31	-10.536	3	0.033
HD 61606	V	4154	1888	-18.085	5	0.144
HD 62128	V	4087	1090	107.066	6	0.231
HD 61995	V	5290	0	-36.443	1	...
HD 62068	V	5290	0	-66.510	1	...
HIP 37766	M	4018	1177	26.643	11	0.149
HIP 37798	V	5161	331	-34.465	7	0.229
HD 62857	V	3778	1	13.142	2	0.029
HD 62694	V	3779	2	-30.779	3	0.172
HD 61994	V	4207	1828	-16.429	5	0.920
XO-2	V	4667	884	46.856	3	0.071
HIP 38117	V	5043	420	-7.653	11	0.236
HD 63754	V	3383	88	44.963	2	0.117
HD 56322	V	3778	0	6.295	1	...
HIP 38340	V	4493	0	18.816	2	0.020
HD 64502	V	3558	436	55.165	2	0.048
HD 64413	V	5052	952	15.856	16	0.122
HD 64324	V	4203	1767	17.182	6	0.105
HD 64730	V	4812	952	15.976	9	0.194
HD 64942	V	3935	1538	-8.022	7	0.084
HD 62613	V	4141	1943	-7.861	50	0.137
HD 65080	V	3715	82	-8.280	4	0.120
HD 65277	V	4371	1974	-4.457	25	0.146
HD 65486	V	4010	1827	-8.135	10	0.090
HIP 38969	V	5245	126	53.208	7	0.076
HD 65430	V	4614	1566	-28.568	18	0.322
HD 65368	V	3695	2	-11.239	2	0.078
HD 65583	V	4071	1975	14.796	61	0.114
HD 66221	V	3481	0	26.216	1	...
HD 66428	V	4057	1944	44.143	19	0.119
HD 66485	V	3864	735	25.094	5	0.054
HD 67458	V	3383	88	-15.689	2	0.186
HD 67346	V	3370	0	26.906	1	...
HD 66171	V	3384	28	36.520	2	0.152
HIP 39939	V	3695	2	-8.074	3	0.050
HD 67767	V	4424	1919	-44.272	5	0.091
HD 68017	V	4314	1946	29.496	103	0.139
HD 68168	V	4244	1125	9.076	10	0.086
HD 68165	V	5290	0	-69.928	1	...
HD 68978	V	3536	503	51.726	3	0.126
HIP 40375	V	5036	511	21.316	16	0.106
HD 69076	V	3598	383	-8.894	5	0.491
HD 69056	V	3340	0	20.395	1	...
GJ 2066	M	4524	1921	61.992	19	0.114
HD 69027	V	3779	2	2.670	3	0.391
HIP 40671	V	4923	483	13.385	6	0.123
HD 68988	V	4441	1943	-69.383	20	0.153
HD 69830	V	4988	1261	30.207	143	0.124
HD 69809	V	3507	415	17.486	3	0.100
HIP 40910	V	4879	358	6.992	5	0.129
HD 69960	V	3727	1060	32.292	6	0.117
HD 70573	V	4862	1146	20.133	5	0.049
HIP 41130	V	4879	358	-27.105	5	0.078
HD 70516	V	4335	1804	8.481	5	0.153
HD 71334	V	3751	761	17.389	3	0.148
HIP 41443	V	5027	455	55.036	9	0.117



TABLE 3 — *Continued*

Star Name	Template <sup>a</sup>	<JD> -2450000	$\Delta T$ (days)	<RV> (km s <sup>-1</sup> )	Obs	$\sigma_{RV}$ (km s <sup>-1</sup> )
HD 71479	V	3507	415	60.142	3	0.100
HD 71835	V	3572	349	-1.204	2	0.250
HIP 41689	M	4913	1975	-51.570	21	0.128
HD 71881	V	3426	0	13.699	1	...
HD 71067	V	3778	0	-1.017	1	...
HD 72673	V	3969	1915	14.666	45	0.128
HD 72429	V	4658	798	79.290	7	0.282
HD 72003	V	4830	1134	-6.950	9	0.130
HD 72687	V	5144	450	21.951	5	0.109
HD 72490	V	4992	943	31.512	18	0.121
HD 72659	V	4299	1974	-18.294	27	0.135
HD 72616	V	3481	0	24.101	1	...
HD 72440	V	4871	1096	-33.261	7	0.119
HD 73256	V	4677	1834	29.736	6	0.253
HIP 42220	M	4532	1917	11.309	20	0.290
HD 73226	V	3968	1693	25.670	10	0.120
HD 72905	V	4285	1827	-12.715	8	0.122
HD 73534	V	4355	1765	9.720	32	0.137
HAT-P-13	V	5068	742	14.766	101	0.165
HIP 42491	V	4105	1802	-20.050	5	0.160
HD 73667	V	4515	1920	-12.123	29	0.102
HD 74104	V	3587	320	-4.258	2	0.007
HIP 42567	V	4923	453	54.509	6	0.049
HD 73940	V	3634	323	13.057	3	0.163
G.J 317	M	4543	1862	87.728	29	0.117
HD 74156	V	4818	1947	3.833	27	0.090
HIP 42731	V	3779	2	24.067	3	0.123
HD 73933	V	4131	0	0.598	1	...
HD 74390	V	4870	1134	-58.086	8	0.148
HD 74669	V	5288	52	26.821	2	0.094
HIP 43151	V	3695	2	15.962	3	0.076
HD 74777	V	3696	1	-20.251	2	0.080
HIP 43212	V	4866	920	2.819	7	0.127
HD 75407	V	5321	1	-25.430	2	0.034
HIP 43534	V	4950	483	-22.259	15	0.149
HD 75784	V	4333	1892	45.415	13	0.105
HD 75732	V	4565	2013	27.360	378	0.130
HD 75732b	M	4433	1495	27.356	15	0.104
HIP 43667	V	4949	410	45.614	7	0.082
HD 75898	V	4340	1885	21.790	30	0.122
HD 75576	V	3484	0	-12.343	1	...
HD 76151	V	5232	0	32.276	1	...
HD 76218	V	4252	1766	-12.576	4	0.125
HD 76078	V	3696	1	-34.605	2	0.051
HD 76445	V	4750	913	-16.402	8	0.121
HIP 44072	V	4856	386	-50.545	5	0.051
HD 76780	V	4305	1384	31.129	6	0.145
HD 76617	V	3861	646	5.565	4	0.177
HD 76909	V	3547	355	3.286	2	0.004
HD 77172	V	4997	1162	-15.808	12	0.130
HD 77519	V	3481	0	28.397	1	...
HD 76539	V	3779	2	15.328	2	0.269
HD 77803	V	3695	2	2.006	3	0.048
HD 76974	V	3778	0	-40.520	1	...
HD 77818	V	4764	1096	-44.051	8	0.128
HD 78277	V	3481	0	2.832	1	...
HD 78538	V	3778	1	5.087	2	0.088
HD 78752	V	3481	0	72.179	1	...
HIP 45042	V	4995	235	-27.301	4	0.069
HD 79282	V	3779	2	4.031	3	0.129
HD 79210	M	4069	1829	11.224	8	0.107
HD 79211	M	3722	1176	12.683	6	0.274
HD 79498	V	3481	0	20.023	1	...
HD 80367	V	3985	1086	50.896	6	0.134
WASP13	V	5243	25	9.940	2	0.058
HIP 45839	V	4808	5	36.642	4	0.165
HD 80355	V	3845	407	-6.714	4	0.065
HD 80811	V	4755	913	30.014	8	0.113
HD 80846	V	3779	2	34.993	3	0.160
HD 80903	V	3725	0	41.726	1	...
HD 80606	V	4703	1976	3.948	47	0.241
HD 81110	V	3481	0	30.443	1	...
HIP 46018	V	5190	0	0.645	1	...
HD 81324	V	3779	2	33.418	3	0.134
HIP 46199	V	5237	73	1.016	3	0.082
g161-29	V	3517	383	22.226	3	0.138

TABLE 3 — *Continued*

Star Name	Template <sup>a</sup>	<JD> -2450000	$\Delta T$ (days)	<RV> (km s <sup>-1</sup> )	Obs	$\sigma_{RV}$ (km s <sup>-1</sup> )
HD 81505	V	3481	0	17.279	1	...
HIP 46343	V	4922	412	-6.589	11	0.087
HIP 46417	V	4949	454	-18.190	7	0.175
HD 81856	V	3587	321	17.028	2	0.020
HIP 46627	V	3697	0	18.432	1	...
HD 233641	V	3398	56	36.237	2	0.041
HIP 46655	M	3772	1177	46.107	4	0.228
HIP 46769	M	4330	1916	19.894	15	0.199
HD 82460	V	3779	2	9.579	3	0.115
HD 82943	V	4791	1975	8.111	38	0.137
HD 83024	V	4750	913	4.556	8	0.159
HD 82886	V	4993	1156	12.554	24	0.119
GJ 357	M	4424	1920	-34.484	15	0.092
HD 82905	V	3779	2	5.058	3	0.141
HIP 47201	V	4866	358	-36.400	6	0.077
HD 83443	V	4292	1829	28.990	4	0.112
HIP 47261	V	5190	0	-4.277	1	...
HD 83394	V	4933	1162	40.345	9	0.138
HIP 47455	V	3779	2	27.370	3	0.153
HIP 47513	M	4341	1892	11.493	8	0.109
HD 83983	V	3778	1	30.812	2	0.117
HD 84117	V	4739	2006	34.687	70	0.146
HIP 47650	M	3546	472	6.495	3	0.063
HD 84035	V	4600	1829	-12.271	23	0.104
HD 84501	V	3481	0	2.795	1	...
HD 84453	V	5334	89	-44.436	2	0.125
HD 84703	V	3481	0	22.288	1	...
HD 84737	V	4825	1296	4.881	33	0.134
HIP 48139	V	4893	357	-20.978	6	0.108
HIP 48205	V	3697	0	15.718	1	...
HIP 48411	V	4808	5	21.452	4	0.155
HD 85301	V	4588	1861	15.345	17	0.101
HD 85440	V	4940	1069	-4.184	10	0.127
HD 85725	V	3921	1854	61.744	4	0.201
WASP19	V	5232	0	21.001	1	...
HD 85689	V	4378	1483	8.562	21	0.133
HD 85472	V	4869	1068	-9.954	8	0.100
HD 86081	V	3824	1479	30.882	29	0.184
HIP 48714	M	4118	1440	15.430	6	0.080
HIP 48740	V	5155	332	-4.735	6	0.114
HIP 48855	V	4851	1104	50.236	8	0.154
HD 86359	V	5333	87	17.864	2	0.016
HD 86728	V	4074	2005	55.955	64	0.145
HIP 49091	M	5154	332	51.409	4	0.125
HIP 49197	V	5059	546	30.204	9	0.138
HD 87230	V	4975	1157	42.625	11	0.123
HD 87001	V	3779	2	-26.036	3	0.134
HD 87359	V	4545	1	0.553	2	0.044
HD 87424	M	3705	1178	-11.723	4	0.316
HD 87669	V	4889	1161	8.257	10	0.107
HD 87836	V	4017	1558	-42.128	3	0.116
HD 87883	V	4947	739	9.188	35	0.126
HD 88072	V	3573	350	-17.778	2	0.276
HD 88218	V	3427	0	36.322	1	...
HD 88134	V	4799	1096	21.617	8	0.094
HD 88133	V	4122	1825	-3.454	12	0.119
HD 88230	M	4390	932	-25.710	18	0.170
HD 88371	V	4186	1441	82.463	4	0.070
GJ 382	M	4147	1945	8.021	10	0.162
g195-59	M	3623	380	-3.548	3	0.105
HD 88656	V	4049	1441	8.252	6	0.186
HD 88402	V	3779	2	34.453	3	0.140
HD 88654	V	5055	1159	-6.933	13	0.102
HD 88725	V	3761	733	-22.016	3	0.187
HD 88609	V	4258	0	-38.237	1	...
HD 88775	V	3779	2	-26.633	3	0.131
HD 88986	V	4167	1920	29.106	3	0.033
HIP 50341	M	5337	30	-10.688	2	0.155
HD 89022	V	3779	2	-33.598	3	0.057
HD 89391	V	4608	1096	29.603	12	0.108
HD 89269	V	4745	1981	-7.557	94	0.125
HD 89454	V	3576	356	18.872	2	0.205
GJ 388	M	3803	1859	12.453	30	0.104
HD 89886	V	3425	0	12.990	1	...
HD 89793	V	4051	1090	32.705	4	0.121
HD 90028	V	3479	0	12.098	2	0.005

TABLE 3 — *Continued*

Star Name	Template <sup>a</sup>	<JD> -2450000	$\Delta T$ (days)	<RV> (km s <sup>-1</sup> )	Obs	$\sigma_{RV}$ (km s <sup>-1</sup> )
HD 90043	V	5062	571	7.088	29	0.123
HD 90054	V	4112	950	48.645	3	0.205
HD 90156	V	4567	1954	26.918	70	0.147
HD 90125	V	4325	1980	-13.933	5	0.100
HIP 50960	V	5094	332	19.415	5	0.091
HD 90211	V	3479	0	17.551	1	...
HIP 51007	M	4174	1945	21.800	6	0.371
HD 90323	V	3479	0	10.565	1	...
HD 90383	V	3779	2	-34.012	3	0.087
HD 90711	V	4552	187	29.903	21	0.090
HD 90722	V	3618	440	40.113	2	0.111
HD 90792	V	4784	1069	32.556	8	0.105
HD 90681	V	3779	2	4.241	3	0.112
GJ 393	M	4436	1410	8.294	23	0.085
HD 90905	V	4495	1801	16.726	6	0.118
HIP 51443	V	5114	539	31.476	12	0.120
HD 237903	V	3777	1861	8.885	7	0.143
HD 90875	V	4900	1920	4.968	22	0.109
GJ 397	V	4252	1818	20.613	9	0.152
HD 91148	V	3779	2	-23.126	3	0.124
HD 91204	V	4315	1834	-9.619	2	0.553
HD 91332	V	3779	2	-43.504	3	0.111
HD 91348	V	3779	2	8.193	3	0.145
HD 91331	V	3779	2	-13.428	3	0.119
HD 91275	V	3779	2	-18.634	3	0.138
HD 91702	V	3941	651	-46.684	4	0.145
HD 91856	V	3779	2	46.234	3	0.138
HD 91876	V	3820	456	-2.873	4	0.199
HD 91909	V	3779	2	20.943	3	0.138
HD 92194	V	3778	1	-0.588	2	0.075
HD 92222b	V	3501	377	7.904	6	0.178
HD 92222a	V	3687	384	8.339	6	0.077
HD 92266	V	5320	61	5.744	2	0.013
HD 92320	V	3779	2	2.805	3	0.246
HD 92719	V	4370	1954	-17.924	38	0.120
HD 92788	V	4311	1823	-4.399	7	0.180
HD 92945	V	5073	615	22.900	4	0.057
HD 92885	V	3779	2	14.992	3	0.046
HD 93215	V	3941	651	-15.301	4	0.139
HD 93396	V	4788	1103	34.959	8	0.127
HD 93461	V	4788	1103	13.093	8	0.114
HD 93745	V	3494	326	38.200	4	0.390
HD 93664	V	3839	1003	-1.315	4	0.087
HD 93849	V	3479	0	8.919	1	...
HIP 52942a	V	4357	1945	24.538	13	0.114
HD 93864	V	4809	1097	15.935	8	0.101
HD 93932	V	3479	0	43.653	1	...
HD 93811	V	3778	1	-0.814	2	0.045
HIP 53020	M	3796	1178	-0.794	4	0.295
HD 94151	V	4038	1775	4.553	6	0.180
HD 94178	V	5320	61	9.958	2	0.019
HD 94292	V	3779	2	27.630	3	0.125
HD 94375	V	3479	0	28.754	1	...
HD 94482	V	3479	0	29.395	1	...
HD 94383	V	3779	2	44.596	3	0.137
HIP 53327	V	5116	416	-26.223	4	0.118
HD 94587	V	3779	2	8.757	3	0.108
GJ 406	M	3918	1092	19.321	9	0.145
HIP 53541	V	4808	4	-34.087	4	0.092
HD 94834	V	4940	1164	2.813	11	0.107
HD 95022	V	4052	1090	19.377	4	0.127
bd-103166	V	4838	1983	26.787	4	0.153
HD 95089	V	4932	1157	8.081	25	0.128
HD 95088	V	4345	1483	0.263	17	0.119
HD 95128	V	5096	449	11.293	24	0.108
HD 95188	V	4362	1827	6.023	7	0.083
GJ 408	M	4383	1920	3.181	10	0.131
HD 95456	V	3620	444	-1.227	2	0.148
twhya	V	4962	655	12.600	2	0.334
HD 95526	V	4906	1098	22.059	8	0.183
HD 95622	V	4042	1395	-8.861	11	0.147
HD 95650	M	3806	1915	-13.832	12	0.104
HD 95735	M	4245	2004	-84.683	148	0.136
HD 95900	V	5337	88	4.483	3	0.086
HD 96063	V	5042	1156	-1.373	12	0.104
HD 96108	V	3369	0	-11.083	1	...

TABLE 3 — *Continued*

Star Name	Template <sup>a</sup>	<JD> -2450000	$\Delta T$ (days)	<RV> (km s <sup>-1</sup> )	Obs	$\sigma_{RV}$ (km s <sup>-1</sup> )
HD 96167	V	4057	1805	12.031	41	0.132
GJ 412a	M	4453	1828	68.675	103	0.139
HD 96361	V	4004	650	12.921	5	0.135
HD 96529	V	4148	1090	-14.752	6	0.129
HD 96700	V	4368	1530	12.787	5	0.170
HD 96683	V	4991	836	17.922	8	0.143
HIP 54459	V	5256	452	103.869	9	0.125
HIP 54498	V	3897	473	-11.462	4	0.150
HIP 54532	M	4527	1892	-3.821	12	0.098
HD 96937	V	3479	0	10.474	1	...
HD 97038	V	3479	0	-3.176	1	...
HD 97089	V	3398	0	-26.400	1	...
HD 97101b	M	4567	1916	-15.421	17	0.098
HD 97101	V	4803	1981	-16.159	24	0.102
HIP 54651	V	5143	332	37.054	5	0.119
HD 97343	V	4803	1628	39.789	66	0.132
HIP 54810	V	4808	5	16.435	4	0.145
HD 97645	V	3780	3	-7.324	3	0.127
HD 97658	V	4999	1633	-1.706	178	0.119
HD 97584a	M	3697	732	9.114	4	0.095
HD 97854	V	3849	156	-7.751	7	0.156
HD 98219	V	5044	1160	-10.458	15	0.119
HD 98281	V	4258	1983	13.312	70	0.128
HD 98427	V	3600	351	20.258	2	0.466
HIP 55360	M	4740	1887	60.466	15	0.132
HD 98553	V	4354	1829	-36.612	5	0.059
HIP 55368	V	3779	2	-13.224	3	0.153
HD 98630	V	3992	1470	13.530	6	0.954
HD 98618	V	3574	349	7.078	2	0.247
HD 98736	V	3370	1	-3.411	2	0.189
HIP 55507	V	5230	448	-5.554	14	0.159
HD 98744	V	3574	349	-40.311	2	0.281
HD 99109	V	3980	1975	33.069	16	0.143
HD 99491	V	4329	1896	4.171	110	0.134
HD 99492	V	4236	2038	3.676	73	0.138
HIP 55915	M	5337	30	-3.148	2	0.419
HD 99706	V	4981	916	-30.256	12	0.110
HD 99934	V	3492	436	-9.321	4	0.366
HD 100180	V	4539	2009	-4.860	40	0.117
HD 238008	V	3780	3	-18.913	3	0.185
HD 100337	V	4868	1096	-30.480	8	0.134
HD 100623	V	4376	1950	-21.964	56	0.110
GJ 433	M	4420	1921	17.934	14	0.110
HIP 56630	V	5114	357	-38.943	5	0.239
HD 101165	V	3778	0	18.010	1	...
HD 101259	V	3887	1438	96.812	3	0.156
HD 101348	V	4086	0	11.697	1	...
HD 101444	V	3778	0	-1.443	1	...
HD 101501	V	5052	243	-5.464	2	0.105
HIP 57050	M	4962	1886	-9.006	26	0.113
HIP 57058	V	4808	5	18.225	4	0.118
HIP 57087	M	4680	1982	9.544	169	0.107
HD 101675	V	3897	473	-13.786	4	0.143
HD 101847	V	3758	83	4.100	9	0.133
HD 101959	V	4234	1828	-0.912	6	0.058
HD 101904	V	3846	156	-10.364	9	0.139
HD 102071	V	4228	1828	-10.600	6	0.781
HIP 57274	V	5244	575	29.701	30	0.140
HD 102158	V	3576	354	28.124	2	0.174
HD 102195	V	4075	1605	1.930	18	0.153
HD 102365	V	4497	742	16.911	18	0.070
HD 102283	V	3778	0	-13.092	1	...
HIP 57450	V	3399	0	64.732	1	...
HD 102329	V	5042	1157	14.580	14	0.093
HIP 57493	V	5032	484	0.360	9	0.095
HD 102444	V	4951	1104	23.056	8	0.143
GJ 445	M	4315	1915	-111.750	18	0.110
HIP 57548	M	3428	114	-31.173	5	0.087
HIP 57683	V	4808	4	11.568	3	0.114
GJ 450	M	4434	1887	0.295	10	0.128
HD 102956	V	5181	1164	-26.025	23	0.113
HD 103047	V	5317	55	-4.593	2	0.013
HD 103432	V	3619	437	6.164	2	0.163
HD 103417	V	3937	473	-9.408	3	0.016
HD 103459	V	4372	1830	19.708	15	0.125
HD 103828	V	3898	473	-50.050	4	0.156

TABLE 3 — *Continued*

Star Name	Template <sup>a</sup>	<JD> -2450000	$\Delta T$ (days)	<RV> (km s <sup>-1</sup> )	Obs	$\sigma_{RV}$ (km s <sup>-1</sup> )
HD 103813	V	5333	86	42.203	2	0.170
HD 103847	V	4103	704	5.048	5	0.079
HD 103829	V	4173	1753	-2.162	3	0.481
HD 103890	V	3612	851	31.076	4	0.170
HD 103932	V	4195	1980	48.388	65	0.152
HD 104017	V	4935	1097	-4.577	8	0.134
HD 104067	V	4597	1914	14.992	40	0.110
HD 104263	V	3929	6	42.969	5	0.127
HD 104304	V	4805	1239	0.105	36	0.109
HD 104389	V	4005	474	-11.336	12	0.132
HD 104437	V	3898	473	-18.695	4	0.190
HD 104556	V	3635	354	-10.791	3	0.179
HD 104576	V	4493	0	-10.458	1	...
HD 104588	V	3898	473	-10.058	4	0.159
HD 104800	V	3565	472	10.027	3	0.142
HD 104860	V	3907	1798	-11.660	8	0.149
HD 104985	V	4128	1833	-20.102	3	0.277
HD 238069	V	3897	473	-10.063	4	0.203
HD 105113	V	3834	769	31.913	6	0.054
HD 105279	V	3923	1469	-13.199	5	0.080
HD 105304	V	4329	301	35.585	6	0.079
HD 105546	V	4258	0	18.195	1	...
HD 105618	V	3546	468	7.460	3	0.097
HD 105631	V	4558	1832	-2.472	120	0.121
HD 105811	V	5336	84	-37.612	3	0.138
HD 105844	V	3778	0	0.474	1	...
HIP 59406a	M	3971	1177	-8.924	4	0.247
HIP 59406b	M	3604	468	-9.281	2	0.100
HIP 59431	V	3778	0	-4.003	1	...
HD 105963	V	3778	0	-5.379	1	...
HIP 59496	V	5040	332	-9.977	4	0.119
HD 106088	V	4176	508	-14.107	9	0.112
HD 106116	V	3619	437	14.634	2	0.089
HD 106156	V	4336	1773	-7.336	4	0.069
HD 106279	V	4905	1127	-45.801	8	0.403
HD 106270	V	5016	1156	24.331	14	0.152
HD 106314	V	5332	84	-4.116	2	0.015
HD 106421	V	3666	686	6.222	8	0.078
HIP 59748	M	4957	114	-13.240	5	0.126
HD 106949	V	3481	0	6.936	1	...
HD 107087	V	3616	382	8.635	2	0.448
HD 107146	V	4245	1796	1.904	6	0.196
HD 107148	V	4289	1982	25.287	23	0.128
HIP 60093	M	5002	260	-0.665	7	0.118
HD 107211	V	3937	473	4.802	3	0.056
HIP 60357	M	5358	58	-22.105	4	0.103
HD 107990	V	4839	1097	-6.554	11	0.071
HIP 60559	M	3929	1146	51.096	3	0.306
HIP 60633	V	5358	58	12.841	4	0.078
HD 108189	V	4821	1104	-3.686	7	0.153
HD 108300	V	3778	0	1.004	1	...
HD 108351	V	3849	732	0.529	4	0.154
g60-06	V	3333	184	-17.519	2	0.179
HD 108863	V	5003	1160	-27.984	16	0.109
HD 108874	V	4512	1978	-30.069	23	0.101
HD 108942	V	3937	473	-11.008	3	0.025
HD 108916	V	3778	0	-0.020	1	...
HD 109202	V	3780	3	-9.391	2	0.024
HIP 61205	V	3935	35	-1.029	7	0.110
HD 109159	V	4908	1159	9.348	8	0.114
HD 109218	V	4894	1159	18.423	8	0.091
HD 109286	V	3778	0	-7.587	1	...
HD 109358	V	4278	1952	6.228	70	0.151
HD 109331	V	3954	354	6.143	2	0.105
HD 109409	V	3548	441	18.191	3	0.129
HD 109718	V	3898	473	-16.054	4	0.135
HD 109749	V	3820	1952	-13.135	20	0.122
HD 109929	V	3874	1438	-10.706	13	0.170
HIP 61706	M	5082	423	-4.334	14	0.179
HD 110044	V	4048	473	-6.730	7	0.148
HD 110315	V	4476	1828	24.357	39	0.129
HD 110537	V	3477	414	35.585	8	0.108
HD 110743	V	3927	1	-2.980	3	0.045
HD 110745	V	3779	2	-3.326	2	0.300
HD 110897	V	4667	1801	80.358	36	0.139
HD 111031	V	4751	1922	-20.346	55	0.118

TABLE 3 — *Continued*

Star Name	Template <sup>a</sup>	<JD> -2450000	$\Delta T$ (days)	<RV> (km s <sup>-1</sup> )	Obs	$\sigma_{RV}$ (km s <sup>-1</sup> )
HD 111153	V	3432	114	-24.307	12	0.147
HD 111096	V	3425	0	14.520	1	...
HIP 62406	V	5224	452	2.402	19	0.166
GJ 486	M	4083	1145	19.471	4	0.268
HD 111395	V	4283	1639	-8.911	5	0.107
HD 111484b	V	3413	27	-19.037	4	0.377
HD 111484a	V	3634	376	-20.797	3	0.157
HD 111515	V	4249	1148	2.563	7	0.069
HD 111528	V	3778	0	45.463	1	...
HD 111606	V	3778	0	-27.659	2	0.009
HD 111631	M	4456	1920	5.017	17	0.085
HD 111814	V	4157	1410	-2.185	11	0.121
HIP 62794	V	4929	0	9.818	2	0.106
HIP 62847	V	5023	444	11.596	12	0.106
HD 112019	V	3954	353	25.066	2	0.271
HD 112115	V	5175	832	3.973	10	0.101
HD 112337	V	4250	3	-20.215	3	0.096
HD 112257	V	4297	1772	-39.428	6	0.118
HD 112415	V	4060	474	7.530	4	0.045
HIP 63257	V	5321	2	-7.336	4	0.099
HD 112742	V	5333	86	7.046	2	0.008
HD 112973	V	4818	1097	-34.986	8	0.146
HD 112988	V	4989	1163	-32.842	13	0.184
HD 113039	V	3778	0	-4.714	1	...
HIP 63510	M	4609	997	-13.740	15	0.309
HD 113194	V	3748	0	10.632	1	...
HIP 63762	V	4887	236	-48.729	6	0.361
HIP 63759	V	5321	2	-17.423	4	0.045
HD 113595	V	5350	60	-40.717	2	0.029
HIP 63894	V	5317	8	-6.834	4	0.095
HD 113983	V	3452	151	0.495	4	0.194
HD 113938	V	3778	0	7.395	1	...
HIP 64048	V	5317	8	-8.371	4	0.086
HD 114174	V	3480	0	24.587	2	0.028
HD 114161	V	4893	1100	-7.180	9	0.157
HD 114375	V	4250	3	-39.976	4	0.144
HD 114506	V	3778	0	-26.778	1	...
HIP 64262	V	5331	25	18.703	7	0.078
HD 114659	V	4889	1081	-1.322	8	0.096
HD 114613	V	4476	1039	-13.095	28	0.061
HD 114783	V	4503	2138	-12.012	63	0.096
HD 114729	V	4957	1536	64.905	4	0.084
HD 114826	V	3778	0	-12.843	1	...
HD 114946	V	4552	1655	-48.283	2	0.159
HD 115404a	V	3828	2015	7.853	6	0.209
HD 115589	V	3633	417	-21.193	2	0.544
HD 115617	V	4251	2011	-7.844	184	0.128
HIP 65016	M	5000	333	-11.540	5	0.109
HD 116029	V	4958	1163	-6.923	15	0.181
HD 116321	V	3475	201	-25.119	20	0.106
HD 116442	V	4141	1917	28.411	37	0.151
HD 116443	V	4309	2141	27.383	83	0.117
HD 116956	M	4148	794	-12.183	22	0.096
HD 117122	V	4093	473	0.280	6	0.123
HD 117176	V	4780	1442	4.882	37	0.124
HD 117378	V	3778	0	-9.485	1	...
HD 117207	V	4957	1536	-17.457	4	0.073
HD 117623	V	3530	515	-6.631	15	0.127
GJ 514	M	4519	1565	14.531	25	0.107
HD 117434	V	5334	89	2.879	2	0.039
HD 117497	V	3446	58	-6.618	9	0.064
HD 117576	V	3779	2	-25.532	2	0.275
HD 117762	V	4825	1103	-26.104	8	0.131
HIP 66074	V	5022	333	-30.851	6	0.122
HD 117936	V	3839	1991	-5.864	4	0.212
HD 118034	V	3778	0	-7.958	1	...
HIP 66193	V	5317	8	1.512	4	0.081
HD 118006	V	3778	0	-36.779	1	...
HIP 66222	M	5216	449	14.986	7	0.130
HD 117987	V	3725	0	-74.955	1	...
HD 118082	V	4799	1103	-26.805	8	0.129
HIP 66283	V	5327	31	7.892	5	0.100
HIP 66459	M	4066	1618	-14.518	11	0.124
HD 118722	V	3780	0	0.927	1	...
HD 118744	V	5017	1159	-0.025	15	0.107
HD 118914	V	3441	85	16.680	2	0.140

TABLE 3 — *Continued*

Star Name	Template <sup>a</sup>	<JD> -2450000	$\Delta T$ (days)	<RV> (km s <sup>-1</sup> )	Obs	$\sigma_{RV}$ (km s <sup>-1</sup> )
HAT-P-3	V	4305	1134	-23.372	11	0.155
HD 119824	V	3778	0	-2.630	1	...
HD 119850	M	4405	1291	15.778	20	0.110
HIP 67164	M	4090	1121	5.389	4	0.325
HD 120066	V	4604	1772	-30.559	3	0.045
HD 120528	V	4048	473	-22.803	7	0.181
G.J 528b	V	4412	1922	-22.549	5	0.180
HD 120476a	V	4037	1833	-20.238	3	0.106
HD 120531	V	4840	1069	24.663	9	0.278
HD 120467	V	4530	1979	-37.628	23	0.121
HD 120636	V	5334	89	-13.517	2	0.096
HD 120666	V	3780	3	-1.675	2	0.016
HIP 67691	V	4991	455	-45.112	8	0.246
HD 121135	V	4258	0	125.174	1	...
HD 121151	V	3778	0	-37.437	1	...
HIP 67842	M	5351	58	1.053	4	0.126
HD 121320	V	4275	1959	-11.944	5	0.079
HD 121550	V	4439	1085	-11.057	35	0.094
HD 121579	V	3670	1151	13.162	5	0.097
HD 122064	V	3950	2076	-26.524	85	0.120
HAT-P-12	V	4442	1135	-40.639	24	0.125
HD 122120	V	4305	1884	-57.442	45	0.105
HD 122253	V	4679	1098	-9.990	7	0.106
HD 122255	V	3389	29	25.546	3	0.103
HIP 68461	V	3870	185	15.141	2	0.097
HD 122303	M	4335	1895	-25.825	24	0.096
HD 122517	V	5366	23	-12.121	3	0.013
HD 122652	V	4235	1806	1.484	5	0.107
HD 122563	V	4258	0	-26.508	1	...
HD 122683	V	3495	206	6.077	3	0.065
HD 122973	V	4014	617	-11.875	9	0.138
HD 123265	V	4088	647	-41.642	4	0.052
HD 123239	V	4764	1025	41.990	8	0.090
HD 123613	V	3601	350	-1.890	2	0.119
HD 123812	V	4377	389	23.502	3	0.115
HD 124257b	V	3671	559	3.091	4	0.098
HD 124257a	V	3566	416	3.135	3	0.071
HD 124106	V	4765	1915	3.352	8	0.046
HD 124292	V	4711	1832	37.725	39	0.133
HD 124641	V	5049	743	11.842	5	0.424
HD 124642	M	3560	350	-16.049	3	0.105
HD 125184	V	3701	746	-12.331	12	0.117
HD 125390	V	4830	1162	-76.758	7	0.222
HD 125217	V	4778	1122	-6.304	8	0.430
HD 125455	V	4402	1979	-9.856	28	0.114
HD 125612	V	4671	1776	-18.255	42	0.107
G.J 546	V	4046	1806	-36.783	3	0.180
HD 126053	V	4385	1898	-19.287	43	0.121
HD 126203	V	3763	849	-29.360	10	0.090
HD 126532	V	3589	375	22.344	2	0.002
HD 126583	V	3512	416	0.702	5	0.090
HD 126631	V	4258	0	-19.112	1	...
HD 126614	V	4713	1537	-32.896	49	0.174
HD 126990	V	5288	54	7.697	2	0.242
HD 126991	V	4792	1097	-94.578	9	0.112
HD 126831	V	3456	55	19.391	2	0.104
HD 128642	V	3429	3	-35.902	6	0.723
HIP 70865	M	4600	1865	7.867	12	0.275
HD 127334	V	4678	1445	-0.401	51	0.118
HIP 70975	M	4120	1243	-1.351	4	0.351
HD 127374	V	4765	1027	-35.966	20	0.122
HD 127741	V	5320	0	9.336	1	...
WASP14	V	4843	348	-5.627	4	0.318
HD 128165	M	3560	350	11.441	3	0.218
HIP 71253	M	4223	459	-1.638	7	0.111
HD 128095	V	4861	1162	28.952	9	0.309
HD 128311	V	4368	2137	-9.521	38	0.191
HD 128720	V	4896	1122	16.832	8	0.100
HD 129333	V	4246	1771	-20.044	10	0.677
HD 128987	V	3961	1768	-22.948	7	0.073
HD 129010	V	3634	417	-7.671	2	0.602
HD 129191	V	3634	416	12.673	2	0.076
HD 129601	V	4892	1162	-14.491	8	0.150
HIP 71898	M	4549	1864	18.687	12	0.082
HD 129471	V	3925	643	26.166	2	0.073
HD 129814	V	3541	602	6.501	2	0.076

TABLE 3 — *Continued*

Star Name	Template <sup>a</sup>	<JD> -2450000	$\Delta T$ (days)	<RV> (km s <sup>-1</sup> )	Obs	$\sigma_{RV}$ (km s <sup>-1</sup> )
HD 130004	M	3537	347	-9.531	6	0.124
HD 130087	V	3634	416	-15.624	2	0.143
HD 130048	V	5320	0	-20.891	1	...
HD 130307	M	3455	58	12.844	2	0.160
HD 130322	V	4675	1952	-12.503	5	0.113
HD 130666	V	4250	3	-49.056	3	0.142
HD 130672	V	3604	0	-30.798	1	...
HD 130871	V	3426	0	-32.318	1	...
HD 131156b	V	4839	0	2.610	1	...
HD 131156	V	4998	322	1.762	3	0.088
HD 130992	V	4264	1537	-57.193	51	0.127
HD 131117	V	3634	416	-28.754	2	0.139
HD 131183	V	4437	1627	-26.414	8	0.076
HD 131580	V	3778	0	-31.124	1	...
HD 131509	V	3503	603	-44.749	3	0.167
HD 131496	V	4983	1122	1.146	14	0.131
GJ 569a	M	4307	1894	-7.217	4	0.246
HD 132142	V	4628	2106	-14.789	32	0.104
HD 132130	V	3778	0	11.222	1	...
HD 131977	V	4461	1388	27.063	3	0.140
HD 132133	V	3604	0	-30.056	1	...
HIP 73302	V	3778	0	-7.481	1	...
HD 132425	V	3763	29	-10.219	2	0.222
HD 132505	V	3426	0	-15.563	1	...
HIP 73427	V	5119	452	-26.337	6	0.133
HD 133125	V	3992	320	-14.263	5	0.050
HD 133233	V	3876	431	1.537	18	0.133
HD 133295	V	4354	1989	-2.174	6	0.208
HD 134319	V	4396	1805	-6.357	5	0.110
HD 134047	V	3842	0	3.039	1	...
HD 134048	V	3574	6	13.608	3	0.107
HD 135143	V	3778	0	-4.299	1	...
HD 134353	V	3651	350	-24.131	3	0.064
HD 134440	V	3427	0	310.001	1	...
HD 134439	V	3427	0	309.433	1	...
HIP 74346	V	5331	67	-69.158	4	0.132
HD 135101a	V	4891	1719	-38.885	13	0.122
s101438b	V	3501	599	-38.877	3	0.110
HD 135148	V	4258	0	-96.007	1	...
HD 134987	V	4523	1948	5.068	29	0.111
HD 238433	V	5046	1162	9.244	5	0.784
HD 135446	V	3562	30	-9.102	12	0.110
HD 135724	V	3778	0	12.252	1	...
HD 135872	V	5335	31	-20.488	2	0.108
HD 136159	V	5330	115	-11.975	3	0.070
HD 136028	V	3842	0	-13.813	1	...
HD 136274	V	3732	536	-30.515	3	0.125
HD 136418	V	5004	1158	-34.407	28	0.197
HIP 74995	M	4555	2136	-9.523	150	0.132
HAT-P-5	V	5055	1103	-1.317	47	0.093
HD 136442	V	4259	1960	-46.986	37	0.102
HD 136513	V	4972	1094	-59.606	15	0.152
HD 136618	V	3604	0	-18.962	1	...
HD 136352	V	4340	1039	-68.923	37	0.083
HD 136713	V	4446	2017	-6.052	93	0.127
HD 136834	V	3534	695	-26.417	3	0.018
HD 136925	V	3680	509	-49.011	2	0.028
HD 137368	V	5288	54	-8.820	2	0.146
HD 137631	V	3604	0	-50.093	1	...
HD 137778	V	4093	2082	7.911	6	0.295
HD 137985	V	3624	154	-0.660	3	0.100
HD 139813	V	4193	1805	-15.787	5	0.216
HD 138278	V	3399	1	-12.712	2	0.087
HD 138549	V	3774	534	11.927	3	0.038
HD 138600	V	3552	24	-37.465	7	0.085
HD 138776	V	3633	411	10.632	2	0.144
HD 139477	V	4370	1782	-8.630	2	0.077
HD 139323	V	4593	2135	-67.105	124	0.131
HD 139457	V	3534	695	37.592	3	0.049
HD 139907	V	3905	978	-29.394	5	0.171
HD 140025	V	4881	976	30.158	9	0.103
HD 140296	V	3778	0	-10.063	1	...
HD 139879	V	3604	0	-8.865	1	...
HD 140538a	V	4181	2075	19.021	131	0.105
HD 141186	V	3633	236	-39.418	4	0.116
HD 141004	V	4211	1914	-66.390	179	0.126



TABLE 3 — *Continued*

Star Name	Template <sup>a</sup>	<JD> -2450000	$\Delta T$ (days)	<RV> (km s <sup>-1</sup> )	Obs	$\sigma_{RV}$ (km s <sup>-1</sup> )
HD 141399	V	5051	1954	-21.912	49	0.129
HD 141085	V	3604	0	-44.352	1	...
HD 141272	V	3878	1743	-26.394	7	0.076
HD 141712	V	4685	1121	-23.235	13	0.144
HD 141680	V	3842	0	-3.770	1	...
HD 142091	V	5330	116	-25.107	3	0.110
HD 141937	V	4391	2112	-2.815	14	0.135
HD 141885	V	3594	380	-15.963	3	0.106
HD 142245	V	4907	1122	6.708	12	0.117
HD 142626	V	3733	537	9.116	3	0.141
HD 142229	V	4199	1002	-22.315	5	0.221
HD 141943	V	4838	296	-0.907	2	0.369
HIP 77908	V	4929	1	5.462	2	0.026
HD 143174	V	4542	1806	-43.590	52	0.133
HD 142943	V	3399	1	-16.177	2	0.118
HD 143291	V	3502	598	-72.594	3	0.091
HD 143006	V	3809	1775	-1.800	14	0.167
pz99_j155847	V	4690	0	-7.436	1	...
WASP17	V	5232	0	-49.251	1	...
HD 143332	V	3472	149	-30.485	9	0.114
HIP 78423	V	5034	445	-35.942	5	0.136
rx_j1600	V	4689	0	-0.901	1	...
HD 143761	V	5178	1449	17.873	79	0.111
XO-1	V	5232	0	1.972	1	...
HD 144287	V	4128	1297	-49.293	35	0.259
HD 144579	V	3919	2076	-59.457	61	0.099
HD 144585	V	4072	1055	-14.014	17	0.116
HD 145224	V	3778	0	-27.545	1	...
HD 145229	V	5026	542	-36.103	4	0.045
HD 144988	V	3335	191	-53.220	2	0.058
HD 145675	V	4515	2141	-13.803	90	0.124
HD 145331	V	3604	0	-58.052	1	...
HIP 79308	V	3744	534	-50.240	3	0.103
HIP 79431	M	5109	451	-4.656	21	0.196
HD 145934	V	4496	1916	-28.013	14	0.214
HD 145958b	V	4144	1484	18.426	46	0.100
HD 145958a	V	4244	1690	18.308	70	0.103
HD 145809	V	3425	365	21.158	3	0.027
HD 146278	V	4834	976	11.352	8	0.085
HD 146050	V	3729	392	-0.702	4	0.087
HD 146362b	V	4509	1952	-14.828	37	0.107
HD 147231	V	3547	0	-16.654	1	...
pz99_j161459	V	4689	0	-0.987	1	...
HD 146233	V	4245	1901	11.756	117	0.128
HIP 79698	V	5007	451	-45.404	7	0.139
pz99_j161618	V	4690	0	-8.416	1	...
HD 146434	V	3604	0	-52.566	1	...
HD 147379a	M	4128	1585	-18.864	8	0.060
HD 147379b	M	4365	1556	-18.460	5	0.148
HD 146775	V	3400	240	-30.111	3	0.061
HD 147062	V	3604	0	-46.978	1	...
HD 147506	V	4274	1369	-19.930	119	0.305
HIP 80096	V	5329	32	-73.034	4	0.080
HD 147750	V	3642	723	-37.053	4	0.041
HD 148238	V	3778	0	-16.948	1	...
HD 147719	V	3571	0	14.619	1	...
HIP 80295	V	3516	178	-17.445	2	0.100
HD 147752	V	3928	6	-35.016	5	0.025
HD 147887	V	3604	0	6.721	1	...
HD 147776	V	4418	1743	7.218	2	0.060
G.J 625	M	4310	1915	-13.063	34	0.139
HD 148164	V	4150	1833	-64.494	13	0.132
HD 148284	V	4622	1751	-36.083	13	0.212
sr21	V	4690	0	-26.537	1	...
HD 148467	V	4671	1569	-36.189	23	0.090
HD 148428	V	3604	0	-23.092	1	...
HIP 80824	M	4507	1300	-21.249	36	0.115
HD 149026	V	3741	1924	-18.057	46	0.107
HD 150706	V	4402	1805	-17.191	7	0.114
HD 148979	V	5335	31	7.133	2	0.046
HD 234314	V	3845	680	-22.113	5	0.230
HD 149143	V	3970	1953	12.266	32	0.167
HD 149750	V	3962	978	15.330	6	0.213
HD 149661	V	4264	1896	-12.794	5	0.295
HD 149724	V	3682	504	-33.541	2	0.109
HD 149907	V	5333	86	-9.995	2	0.041

TABLE 3 — *Continued*

Star Name	Template <sup>a</sup>	<JD> -2450000	$\Delta T$ (days)	<RV> (km s <sup>-1</sup> )	Obs	$\sigma_{RV}$ (km s <sup>-1</sup> )
HD 149806	V	4530	1425	10.471	38	0.114
HD 149760	V	3604	0	9.309	1	...
HD 150122	V	3399	3	-58.657	3	0.096
HD 150237	V	3573	5	-46.708	2	0.198
HD 150554	V	4297	1804	-18.379	10	0.188
HD 150433	V	3360	240	-40.119	2	0.204
HD 150331	V	3818	744	-6.637	15	0.129
HD 150437	V	3360	240	14.142	2	0.128
HD 150420	V	3509	568	-11.217	3	0.181
HD 151541	V	4290	2141	9.473	41	0.136
HD 150698	V	3360	240	48.248	2	0.073
HD 151522	V	4469	670	-45.210	7	0.472
HD 150936	V	3604	0	-37.219	1	...
HD 151288	M	4926	1913	-31.349	33	0.132
HD 151329	V	3577	444	-26.417	5	0.482
HD 151627	V	3842	0	-14.058	1	...
HD 151504	V	4224	1128	-75.510	22	0.098
HD 151877	V	3938	1116	2.117	3	0.345
HD 152125	V	3960	680	-25.716	7	0.171
HD 151852	V	4823	1001	-38.440	7	0.157
HD 151995	V	3430	0	-5.554	1	...
HIP 82408	V	5380	0	-0.461	1	...
HD 152733	V	4693	1054	-27.517	9	0.113
HD 152792	V	3767	505	4.624	3	0.131
HD 152581	V	4902	1116	3.739	12	0.111
HD 152555	V	4337	1992	-15.891	5	0.241
HD 153525	V	4404	1886	-7.339	5	0.108
HD 153557	V	4187	1861	-6.564	3	0.020
HIP 83043	M	4726	1914	4.145	25	0.101
HD 153378	V	3803	1143	-24.765	9	0.083
HD 153458	V	3535	695	0.591	3	0.073
HD 154345	V	4456	1945	-46.945	89	0.121
HD 154325	V	3845	680	-28.603	5	0.206
HD 154144	V	3883	1002	-19.163	23	0.148
HD 154088	V	4463	2136	14.163	167	0.102
HD 154363	V	4478	1811	34.095	34	0.118
HAT-P-18	V	4790	863	-11.250	29	0.129
HD 154656	V	4121	648	-22.618	5	0.070
HIP 83762	M	3872	484	-50.725	6	0.172
HD 154697	V	3604	0	-33.717	1	...
HD 154994	V	4142	648	-58.311	6	0.051
HD 155456	V	3745	535	-59.531	3	0.125
HD 155524	V	5320	0	-6.037	1	...
HIP 84099	M	3551	696	-44.404	3	0.323
HD 155413	V	3955	142	-23.274	10	0.105
HD 156279	V	4908	2134	-20.670	36	0.289
HD 155415	V	3604	0	-5.489	1	...
HD 155712	V	4373	1923	19.778	54	0.108
HD 155817	V	3605	0	-54.182	1	...
HD 155968	V	3927	646	-29.848	2	0.025
HD 156026	V	4288	1896	0.061	5	0.179
HD 156079	V	3926	645	-103.318	2	0.085
HD 156342	V	4545	1174	-63.164	17	0.084
HD 156668	V	5042	1832	-44.547	254	0.110
HD 156985	V	4736	1950	-4.805	84	0.105
HD 156365	V	3360	240	-13.057	2	0.122
HD 156549	V	3552	24	16.765	7	0.123
GJ 667c	M	4346	1688	6.448	7	0.202
HIP 84790	M	3479	0	-19.189	1	...
HD 156826	V	3422	366	-32.685	2	0.017
HAT-P-14	V	5180	715	-20.393	59	0.095
HD 156846	V	5071	419	-68.386	55	0.242
HD 157214	V	4511	1923	-78.559	40	0.119
HD 157481	V	5320	0	-52.955	1	...
HD 157261	V	5336	32	-1.087	2	0.004
HD 157172	V	3360	240	-78.978	2	0.057
HD 157299	V	3604	0	-47.361	1	...
HD 157347	V	4257	2081	-35.854	99	0.126
HD 157338	V	3718	1569	-24.248	18	0.110
HD 158633	V	4366	1915	-38.564	31	0.113
HD 158259	V	4405	1712	13.605	2	0.078
HD 157881	M	4119	1840	-23.118	4	0.217
HD 158038	V	4945	1121	19.632	14	0.159
HD 157719	V	4664	1042	-76.728	5	0.983
HD 158210	V	3573	5	-20.555	2	0.135
HD 158173	V	3604	0	-62.633	1	...

TABLE 3 — *Continued*

Star Name	Template <sup>a</sup>	<JD> -2450000	$\Delta T$ (days)	<RV> (km s <sup>-1</sup> )	Obs	$\sigma_{RV}$ (km s <sup>-1</sup> )
HD 158449	V	4807	1065	-26.926	8	0.098
HIP 85582	V	4751	238	-8.080	8	0.149
HD 159062	V	4188	1527	-83.967	40	0.115
s122446	M	4483	1536	-12.468	23	0.110
HD 159063	V	3431	0	-6.176	1	...
HD 159222	V	4148	1706	-51.556	90	0.121
HIP 85977	V	4749	209	-94.063	8	0.130
HD 159798	V	5320	0	-47.048	1	...
GJ 687	M	4339	1537	-28.720	73	0.109
HD 160215	V	4718	1087	-59.230	11	0.087
HD 160013	V	3635	415	1.327	2	0.250
GJ 686	M	4324	1434	-9.499	37	0.112
HD 160247	V	5312	0	-8.367	1	...
HD 159868	V	4297	89	-23.525	33	0.092
HD 160693	V	3683	505	33.975	2	0.176
HD 161284	V	4071	474	-7.570	13	0.145
HD 160371	V	5379	0	-8.715	1	...
HD 161897	V	4389	1587	-16.653	3	0.171
GJ 694	M	4487	1292	-14.328	14	0.084
HD 161131	V	5312	0	5.747	1	...
HD 161424	V	3604	0	-49.070	1	...
HIP 86961	M	4626	1842	-28.929	8	0.095
HD 161797	V	4843	587	-17.576	25	0.092
HD 161622	V	5379	0	-6.795	1	...
HIP 87062	V	3360	239	84.660	2	0.298
HD 161848	V	3551	696	-94.955	3	0.124
HIP 87123	V	4658	1064	-66.098	8	0.104
HD 162232	V	4550	1771	-72.674	20	0.083
TrES3	V	4343	1073	9.647	19	0.136
HIP 87464	V	4719	2	-24.462	4	0.061
HD 162808	V	3576	0	-30.173	1	...
TrES4	V	4829	913	-15.865	2	0.158
HD 162587	V	5379	0	-16.157	1	...
HD 163607	V	4791	1803	-10.118	38	0.142
HD 163528	V	4708	1122	-65.155	16	0.197
HD 163589	V	3966	824	-36.033	4	0.091
HD 163153	V	3532	364	-72.845	14	0.086
HD 163489	V	4320	1556	-49.414	18	0.144
HD 164330	V	3912	680	-12.803	4	0.694
GJ 699	M	4192	1692	-110.416	74	0.130
HD 164213	V	5320	0	-4.060	1	...
HD 164595	V	3724	490	2.120	2	0.340
HD 164507	V	3943	793	5.310	2	0.108
HD 164509	V	4810	1810	13.640	36	0.119
HD 165109	V	5330	116	-4.620	3	0.158
HD 164651	V	3393	308	-80.539	2	0.005
HD 164922	V	4151	2137	20.236	100	0.098
HD 165173	V	3583	725	0.164	3	0.061
HD 165222	M	4561	2142	32.621	62	0.141
HD 165401	V	4264	1710	-118.491	8	0.244
HD 165269	V	3490	118	-0.814	2	0.270
HD 165672	V	3604	0	-5.497	1	...
HD 166494	V	4594	1028	-30.304	10	0.147
HD 166435	V	3550	0	-14.487	1	...
HD 166620	V	4342	1992	-19.465	41	0.101
HD 167042	V	5317	121	-18.181	2	0.093
HIP 89087	V	4719	2	-39.517	4	0.135
HIP 89215	V	3394	306	-0.842	2	0.366
HD 167215	V	3696	292	-41.855	2	0.129
HD 167216	V	3561	721	-42.731	3	0.266
HD 167389	V	3720	483	-5.395	2	0.259
GJ 708	V	4279	0	2.332	1	...
HD 168009	V	4631	1380	-64.634	29	0.118
HD 167665	V	3852	1486	8.523	4	0.039
LHS 462	M	3706	454	0.491	2	0.252
HD 168603	V	3949	29	-32.771	2	0.007
HD 168443	V	4649	2140	-48.446	24	0.328
HD 168874	V	3550	0	-20.092	1	...
HD 168723	V	5218	377	9.219	4	0.086
HD 168746	V	4265	1437	-25.604	2	0.075
HD 168960	V	3678	258	-9.966	2	0.078
HIP 90075	V	3576	0	-36.087	1	...
HD 170003	V	5320	0	-3.058	1	...
HD 169889	V	3832	437	-17.691	3	0.031
HIP 90376	V	4719	2	-23.264	4	0.141
HD 169830	V	4583	1834	-17.197	18	0.133

TABLE 3 — *Continued*

Star Name	Template <sup>a</sup>	<JD> -2450000	$\Delta T$ (days)	<RV> (km s <sup>-1</sup> )	Obs	$\sigma_{RV}$ (km s <sup>-1</sup> )
HD 170174	V	3394	306	-28.564	2	0.519
HD 170469	V	4128	1827	-59.340	18	0.117
HD 170512	V	3830	1127	-36.281	11	0.107
HD 170493	V	4382	1466	-54.776	44	0.109
HD 170657	V	4212	2082	-43.137	13	0.161
HD 171010	V	5320	0	-33.552	1	...
g205-028	M	3721	483	-18.890	2	0.337
HD 171067	V	3754	414	-46.246	2	0.025
WASP-3	V	4655	350	-5.409	28	0.126
GJ 4063	M	3707	456	12.618	2	0.255
HD 171238	V	3604	0	21.446	1	...
HD 172043	V	5320	0	3.164	1	...
HD 171665	V	3393	307	-23.279	2	0.005
HD 171918	V	3393	307	-67.213	2	0.058
HD 171999	V	3604	0	-51.888	1	...
HD 172310	V	3661	363	31.210	2	0.146
HD 172051	V	4237	1898	37.095	41	0.110
HD 172365	V	5379	0	-20.204	1	...
HIP 91699	M	3758	421	-31.873	2	0.060
HD 172513	V	3547	0	-11.558	1	...
HD 173739	M	4325	1436	-0.794	31	0.122
HD 173740	M	4341	1436	1.118	30	0.135
HD 173701	V	4285	1439	-45.630	31	0.093
Kepler-8	V	5050	152	-52.890	36	0.355
HD 173818	V	3717	2084	15.468	5	0.059
HD 174080	V	3942	789	-7.083	2	0.016
HD 174622	V	3828	767	-49.990	3	0.130
HIP 92403	M	3575	695	-10.535	3	0.060
HD 175441	V	3574	6	-21.276	3	0.094
HD 174719	V	3944	786	-17.270	2	0.036
HD 175425	V	3845	680	-67.588	5	0.190
HD 175541	V	4592	2141	19.674	42	0.114
HIP 92922	V	4010	680	-39.302	8	0.203
HIP 93119	V	4720	4	-14.846	5	0.138
HD 176377	V	4845	1831	-40.681	71	0.096
HD 177274	V	4230	1067	-5.141	7	0.215
HD 176414	V	3539	98	33.544	9	0.108
HD 230409	V	3785	477	-2.415	2	0.064
HD 176650	V	5322	0	29.613	1	...
KIC 3323887	V	5359	35	2.187	10	0.100
Kepler-4	V	5075	93	-60.975	23	0.168
HD 176982	V	3604	784	-6.825	3	0.062
HD 177033	V	3604	0	-46.802	1	...
TrES1	V	4053	2052	-20.569	14	0.195
HD 177572	V	3720	483	-10.245	2	0.191
HIP 93703	V	5347	69	-41.083	15	0.086
HD 177830	V	4573	1841	-72.083	53	0.153
HIP 93871	V	4719	2	9.032	4	0.065
GJ 745a	M	4555	845	32.263	8	0.106
GJ 745b	M	4629	440	31.940	5	0.093
TrES2	V	4260	799	-0.640	63	0.059
g207-019	M	3757	410	-1.750	2	0.117
HD 178251	V	4805	982	91.769	14	0.118
HD 178911b	V	4733	1770	-40.551	16	0.345
HD 179306	V	5347	69	5.136	15	0.107
HD 179079	V	4457	1715	19.440	70	0.107
HD 179152	V	5322	0	-20.725	1	...
HD 179957	V	4242	1871	-41.824	79	0.119
HD 179958	V	4271	1560	-41.162	75	0.125
HD 180161	V	4185	1738	-27.036	4	0.130
HD 179596	V	3480	1	-4.219	2	0.105
HD 180053	V	4999	1164	-5.874	84	0.135
Kepler-7	V	5134	1	0.222	2	0.575
KIC 10723750	V	5352	0	-12.784	1	...
HD 230999	V	3585	722	-81.456	3	0.192
HD 179949	V	4640	1468	-24.350	4	0.178
HD 180684	V	3632	783	-2.002	2	0.233
HD 180617	M	4668	1829	35.730	100	0.154
HD 181253	V	3768	1195	-28.168	21	0.153
HD 180902	V	4944	1041	-4.651	17	0.176
HD 231157	V	3604	0	-43.279	1	...
HD 181234	V	3604	784	-46.730	3	0.051
HD 181342	V	4952	1041	-0.837	21	0.135
HD 182488	V	4838	1448	-21.485	56	0.138
HD 182407	V	3654	1196	-30.323	11	0.122
HD 182619	V	3826	412	8.280	3	0.106

TABLE 3 — *Continued*

Star Name	Template <sup>a</sup>	<JD> -2450000	$\Delta T$ (days)	<RV> (km s <sup>-1</sup> )	Obs	$\sigma_{RV}$ (km s <sup>-1</sup> )
HD 182572	V	3886	2081	-100.289	60	0.125
HD 183298	V	5345	69	-19.122	16	0.071
COROT2	V	5286	0	23.603	1	...
HD 183473	V	4753	1123	-46.421	10	0.089
HD 183263	V	4530	1831	-50.240	29	0.107
HAT-P-7	V	4947	1039	-10.525	35	0.212
HD 183650	V	3584	723	-9.752	3	0.031
HD 183216	V	4852	326	-43.069	2	0.024
HD 183756	V	5322	0	-5.083	1	...
HD 183658	V	3570	784	58.219	9	0.089
HD 231701	V	4159	1748	-63.476	16	0.098
HD 183870	V	4025	2049	-48.823	4	0.304
KIC 7825899	V	5351	0	-21.275	1	...
HD 185144	V	4297	2138	26.620	424	0.112
KIC 7287995	V	5351	0	0.533	1	...
HD 185414	V	4461	1826	-15.771	36	0.189
HD 185269	V	5101	575	0.620	26	0.112
HD 185295	V	3758	422	-18.710	2	0.020
KIC 5972334	V	5352	0	-62.979	1	...
HD 186408	V	4692	1391	-27.391	49	0.122
HD 186427	V	4841	1423	-27.859	62	0.147
HD 186104	V	3604	0	-61.389	1	...
HIP 97051	V	5057	660	-12.314	15	0.127
HD 187091	V	5314	9	-14.941	6	0.050
HD 186932	V	3604	0	-57.813	1	...
HD 187123	V	4404	2105	-16.896	30	0.099
Kepler-6	V	5003	59	-49.222	11	0.107
HD 187237	V	3773	1098	-32.797	4	0.215
HD 187748	V	3944	789	-5.456	2	0.135
HAT-P-11	V	4885	1040	-63.511	114	0.101
HD 187944	V	3480	1	-12.006	2	0.130
HD 187923	V	4231	2079	-20.619	99	0.138
HD 188015	V	4201	2141	0.060	10	0.075
HD 187897	V	4749	120	-37.507	2	0.044
GJ 1245b	M	4242	1434	5.081	10	0.178
HD 188345	V	4124	824	-85.627	3	0.073
HD 188268	V	4121	648	9.295	5	0.105
HD 188311	V	4121	648	9.773	5	0.114
HD 188386	V	5068	1041	-73.744	22	0.145
HD 188510	V	3604	729	-192.628	2	0.175
HD 188512	V	4401	1452	-40.074	21	0.119
HD 188298	V	3604	0	33.769	1	...
HD 188376	V	3936	1768	-16.090	5	0.122
HD 189087	V	3945	787	-30.109	2	0.203
Kepler-5	V	5020	125	-18.527	9	0.113
HD 189186	V	5322	0	56.577	1	...
HD 189733	V	3983	1618	-2.570	86	0.143
HD 189625	V	3752	544	-28.176	2	0.064
HD 189627	V	3604	0	-14.995	1	...
KIC 8394721	V	5351	0	-23.258	1	...
HD 190067	V	4207	1472	20.375	96	0.126
HD 190007	V	3761	1828	-30.270	11	0.105
HD 190228	V	4631	1827	-50.196	8	0.114
HD 190360	V	3979	2135	-45.253	88	0.141
HD 190404	V	4255	1777	-2.535	29	0.157
HD 190406	V	4549	1768	4.617	46	0.125
HD 190571	V	5321	2	37.432	2	0.101
HD 190594	V	4281	1086	-33.632	20	0.129
HD 190821	V	4024	1089	-8.951	12	0.128
HD 191067	V	5332	84	-3.437	2	0.120
HIP 99205	V	4822	311	-33.930	6	0.101
HD 190931	V	4397	1072	-25.905	10	0.098
HD 191359	V	5322	0	27.090	1	...
HIP 99332	V	4896	326	-7.735	9	0.124
HIP 99385	V	4719	1	21.998	3	0.043
bd+23 3912	V	3552	0	-115.163	1	...
HD 193202	V	4494	1791	-1.675	51	0.111
HD 191785	V	4335	1872	-49.289	27	0.121
HD 191408	V	4096	2113	-129.355	78	0.121
HD 192020	V	3755	415	-11.537	2	0.142
HD 192148	V	3576	0	-26.591	1	...
HD 191957	V	3271	62	-24.506	2	0.041
HD 355183	V	4161	1120	-16.025	24	0.107
HD 192153	V	4830	1034	-37.994	10	0.106
HD 192263	V	4122	1804	-10.853	5	0.153
HD 192343	V	3758	422	-0.611	2	0.035

TABLE 3 — *Continued*

Star Name	Template <sup>a</sup>	<JD> -2450000	$\Delta T$ (days)	<RV> (km s <sup>-1</sup> )	Obs	$\sigma_{RV}$ (km s <sup>-1</sup> )
HD 192344	V	3688	422	-0.546	3	0.032
HD 192310	V	4872	2143	-54.374	103	0.118
HD 193342	V	4699	1085	-24.246	9	0.128
HIP 100040	V	3573	5	-98.254	2	0.099
HD 193391	V	4998	1041	-41.912	14	0.095
HD 193795	V	3754	415	6.833	2	0.080
HD 193728	V	3603	0	-21.142	1	...
HD 193690	V	4469	1038	-1.419	13	0.098
HD 194110	V	5322	0	-20.027	1	...
HD 193901	V	3604	784	-171.504	3	0.113
HD 194080	V	3888	420	2.383	4	0.025
HAT-P-23	V	4840	556	-14.356	15	0.263
HD 194541	V	4650	1064	-20.453	12	0.124
HD 194913	V	3573	5	8.423	2	0.135
HD 195034	V	4049	1565	-0.857	5	0.249
HD 195019b	M	4256	1177	-89.211	5	0.254
HD 195019	V	4555	1832	-91.443	19	0.253
GJ 793	M	4224	1088	10.429	5	0.083
HD 195787	V	4314	82	-10.278	4	0.481
WASP-2	V	4675	0	-27.958	1	...
19164495-1717074 <sup>b</sup>	V	5851	0	41.410	1	...
HIP 101262	V	5203	352	-26.987	2	0.046
HD 195564	V	4070	1827	9.460	24	0.138
HD 195824	V	4851	1038	7.740	9	0.129
19164725-1604093 <sup>b</sup>	V	5851	0	41.500	1	...
HD 196199	V	3479	0	-27.296	1	...
HD 196124	V	4554	1686	-42.450	59	0.108
HD 196201	V	3550	0	-19.175	1	...
HD 196645	V	4912	1012	-33.297	12	0.114
HD 196850	V	3337	487	-21.107	90	0.090
HD 196676	V	5363	23	-0.545	2	0.150
HD 196761	V	4013	2136	-41.930	46	0.115
HD 197162	V	4676	1094	-139.688	18	0.135
HD 197076	V	4518	1738	-35.402	160	0.110
HIP 102332	V	5028	2	-73.673	2	0.312
HD 197623	V	4153	825	-69.405	3	0.059
GJ 806	M	4715	1468	-24.697	41	0.116
GJ 803	M	4180	1089	-4.499	14	0.155
HD 197964	V	5290	0	-6.208	1	...
HD 335129	V	3573	5	-49.255	2	0.112
HD 198425	V	4212	1828	10.659	4	0.044
HD 199019	V	4357	1651	-11.467	4	0.134
HD 198483	V	3605	0	-19.338	1	...
HIP 102870	V	4720	1	-52.510	3	0.049
HD 198683	V	3604	0	-30.569	1	...
HD 199476	V	4503	1469	-30.335	24	0.140
HD 198599	V	3922	299	20.713	14	0.128
HD 198802	V	4261	2134	-3.102	5	0.089
HD 199305	M	4498	1434	-17.144	19	0.133
HD 199100	V	3605	0	-25.874	1	...
HD 199178	V	5322	0	-10.198	1	...
HD 199086	V	3970	734	15.766	2	0.034
HIP 103256	V	4719	2	-39.414	4	0.129
HIP 103269	V	3585	721	-130.498	3	0.276
HD 199255	V	5322	0	21.641	1	...
HD 199260	V	4838	326	-15.836	3	0.155
HD 199381	V	5363	22	49.179	2	0.084
HD 199580	V	5322	0	-20.795	1	...
HD 199683	V	3604	0	-11.223	1	...
HIP 103650	V	4918	365	-29.652	10	0.166
HD 199960	V	4658	1825	-17.526	5	0.237
HD 200078	V	3604	0	-60.325	1	...
HD 200156	V	3604	0	-5.215	1	...
HD 200491	V	4743	1121	-7.484	8	0.157
HD 200565	V	4136	1173	-3.857	2	0.214
HD 200538	V	3786	475	15.455	2	0.185
HIP 104092	V	4719	2	-66.502	4	0.102
HD 200625	V	3787	473	5.300	2	0.187
HD 200964	V	4978	974	-71.884	40	0.148
HD 201091	V	4529	1960	-65.841	104	0.137
HD 201092	V	4312	1960	-64.420	93	0.134
HD 201651	V	3929	1191	-12.775	6	0.072
HD 200968	V	3737	1805	-32.680	12	0.117
HD 201219	V	4341	1468	4.919	6	0.109
HD 201203	V	3549	0	-16.550	1	...

TABLE 3 — *Continued*

Star Name	Template <sup>a</sup>	<JD> -2450000	$\Delta T$ (days)	<RV> (km s <sup>-1</sup> )	Obs	$\sigma_{RV}$ (km s <sup>-1</sup> )
HIP 104432	M	4579	1178	-58.200	20	0.147
HD 201378	V	3604	0	-30.698	1	...
HD 201924	V	4067	884	-49.826	5	0.071
HD 201989	V	4517	1439	-23.863	4	0.097
HD 202575	V	4298	1826	-18.263	3	0.109
HD 202696	V	4929	1085	-34.433	32	0.125
HD 202560	V	4673	8	20.932	5	0.117
HD 202751	V	4505	1257	-27.448	39	0.104
HD 202867	V	4753	1067	14.212	8	0.109
HD 203030	V	4251	1259	-16.696	4	0.043
HIP 105341	V	4719	2	18.079	4	0.120
HD 202917	V	3845	473	-1.499	3	0.533
HD 203471	V	4751	1034	23.620	14	0.126
HD 203473	V	4226	404	-61.949	2	0.081
HIP 105904	V	3878	768	-64.110	4	0.177
HD 204277	V	4616	1238	9.390	6	0.100
HD 204814	V	3977	878	-87.086	4	0.093
HD 204587	V	4492	1533	-84.103	20	0.111
HD 205163	V	4858	1068	50.098	10	0.097
HD 205351	V	3724	453	-17.932	3	0.142
HD 205353	V	4180	313	6.028	2	0.191
HD 205855	V	4513	666	7.125	20	0.086
HAT-P-17	V	4797	955	20.094	37	0.113
HD 205905	V	4270	1748	-17.076	6	0.227
HD 206116	V	4293	405	-6.512	3	0.080
HD 206332	V	4346	0	-44.428	1	...
HD 207897	V	3843	361	-6.551	3	0.060
HIP 107062	V	5029	0	-51.449	1	...
HD 206374	V	4220	1776	-42.981	6	0.197
HD 206387	V	3600	718	-7.438	2	0.508
HD 206658	V	4286	1322	6.091	36	0.112
HD 206610	V	4961	1065	-18.658	26	0.104
HD 206635	V	4749	1037	-40.357	8	0.108
HD 206993	V	5348	52	-3.681	2	0.097
HD 207485	V	3864	421	-19.099	3	0.043
HD 207077	V	4709	1060	-20.370	7	0.090
HD 207583	V	3962	715	21.955	2	0.073
HD 207839	V	4072	827	-29.891	5	0.091
HD 207966	V	3241	0	-24.701	1	...
HD 207874	V	4017	826	-26.747	2	0.143
HD 207978	V	4086	0	19.053	2	0.055
HD 207832	V	4486	1445	-16.682	51	0.102
HD 207994	V	3620	454	-29.755	9	0.156
HD 208038	V	4226	1773	13.536	4	0.042
HIP 108056	V	3724	453	-97.943	3	0.167
HD 208313	V	4673	1185	-13.228	28	0.107
HD 208585	V	4845	1062	-26.979	9	0.143
HIP 108388	V	3574	5	-16.960	2	0.132
HD 208801	V	4072	2135	-50.081	3	0.067
HD 208897	V	5322	0	-14.780	1	...
HD 208880	V	3784	360	-15.791	2	0.019
HD 209203	V	3759	335	9.381	5	0.116
HD 209340	V	3724	453	-33.511	4	0.186
HD 209393	V	4427	1412	5.032	5	0.125
HD 209290	M	4326	1123	18.275	36	0.120
HD 209253	V	4389	1057	16.519	6	0.145
HD 209458	V	4070	1951	-14.691	28	0.114
HD 209706	V	3759	335	-19.446	5	0.140
HIP 108940	V	4722	10	-24.619	6	0.062
HD 209599	V	4062	881	-0.117	5	0.101
HD 210011	V	3669	510	-10.319	10	0.070
HD 209875	V	3604	0	-40.972	1	...
HD 210144	V	4090	828	-33.433	5	0.054
HD 211681	V	4319	1413	-40.288	3	0.282
HD 210323	V	3759	335	-17.431	5	0.147
HD 210312	V	3604	0	16.476	1	...
HD 210277	V	4358	2142	-20.844	89	0.126
HD 210373	V	5381	0	-40.170	1	...
HIP 109388	M	4550	2137	-15.334	46	0.155
HD 210320	V	4024	0	30.523	1	...
HD 210302	V	4331	1584	-16.154	36	0.194
HD 210392	V	3604	0	-1.541	1	...
HD 210460	V	4041	1858	20.381	4	0.047
HD 210521	V	4568	451	-13.818	5	0.135
HIP 109555	M	4194	1064	-51.312	5	0.087
HD 210702	V	5270	164	16.340	2	0.166

TABLE 3 — *Continued*

Star Name	Template <sup>a</sup>	<JD> -2450000	$\Delta T$ (days)	<RV> (km s <sup>-1</sup> )	Obs	$\sigma_{RV}$ (km s <sup>-1</sup> )
HD 211038	V	3421	365	10.331	2	0.065
HD 211080	V	3604	0	8.305	2	0.021
HIP 109980	V	4921	472	-4.563	14	0.150
HD 211810	V	4285	1484	-36.581	16	0.088
HD 211567	V	3624	154	-46.834	3	0.146
v383lac	V	4355	1412	-18.624	4	0.950
HD 212315	V	3466	177	-10.645	3	0.614
HD 212291	V	4059	2013	-5.589	39	0.100
HD 212585	V	3693	7	-16.314	4	0.129
HD 212733	V	3843	361	6.913	3	0.302
HIP 110750	V	4927	470	-20.659	10	0.101
HIP 110774	V	4837	471	0.802	4	0.078
HD 212771	V	4954	1041	14.863	22	0.122
HD 212801	V	3767	434	-8.588	2	0.015
HD 239960	M	4502	1568	-34.536	27	0.097
HD 213066	V	4226	405	-39.161	2	0.034
HD 213042	V	4398	1533	5.632	47	0.157
HD 213278	V	4633	817	-53.476	7	0.077
HD 213472	V	3603	0	16.907	1	...
HD 213519	V	3603	0	-31.688	1	...
HD 213329	V	4226	405	-12.736	2	0.106
HD 213628	V	3604	0	-50.513	1	...
HD 214683	V	3846	365	23.821	3	0.039
HD 214823	V	4281	1564	-44.542	14	0.230
HD 214749	V	4304	744	-0.011	4	0.101
HD 214759	V	4322	30	-20.153	7	0.053
HD 215032	V	3898	1602	21.062	13	0.083
HD 215049	V	4668	795	-29.844	5	0.130
HD 215152	V	4359	1524	-13.842	39	0.121
HD 215274	V	3931	6	-9.418	4	0.138
HD 215500	V	4082	828	-45.555	5	0.064
HD 215578	V	4294	1951	-20.817	4	0.429
HD 215704	V	4154	828	-51.527	8	0.092
HIP 112460	M	4210	1086	0.192	3	0.041
HD 215625	V	3604	0	8.439	1	...
HIP 112496	V	5083	163	-23.929	5	0.151
HD 216520	V	4935	2040	-18.720	94	0.113
HD 215908	V	4636	705	6.348	7	0.092
HD 216083	V	3575	6	-6.312	3	0.214
HD 216175	V	3759	335	-41.508	5	0.128
HD 216191	V	4125	828	18.901	6	0.110
HD 216275	V	4426	1412	13.676	5	0.152
HD 216320	V	3793	381	-18.997	2	0.984
HD 216259	V	4389	1257	1.241	63	0.125
HIP 112918	V	4813	472	-7.787	5	0.119
HAT-P-8	V	4506	1039	-22.143	14	0.168
GJ 876	M	4312	1860	-1.519	50	0.157
HIP 113026	V	4719	2	-17.765	4	0.137
HD 216722	V	5378	0	-45.529	1	...
HIP 113207	V	3817	680	-22.104	5	0.177
HD 216834	V	4537	472	-32.615	7	0.276
HD 216803	V	4274	1619	7.152	4	0.086
HD 216899	M	4495	1257	-27.255	23	0.141
HD 217014	V	4637	1452	-33.118	36	0.128
HAT-P-1	V	4278	1449	-2.698	72	0.156
HD 217004	V	3604	0	0.298	1	...
HIP 113409	V	4944	470	10.016	10	0.148
HD 217107	V	4353	2135	-13.269	50	0.132
HD 217165	V	4707	141	13.225	8	0.147
HD 217523	V	3759	335	-15.383	5	0.075
HD 217357	M	4384	1765	16.461	49	0.203
HD 217496	V	4678	854	-2.206	6	0.128
HD 217591	V	4877	1062	-9.106	18	0.149
HD 217681	V	4685	796	-0.257	6	0.079
HD 217850	V	4516	1810	7.224	17	0.177
HD 217877	V	4197	1416	-12.738	3	0.100
HD 218168	V	3794	381	2.673	2	0.148
HD 218209	V	3793	381	-16.058	2	0.006
HD 218133	V	3563	630	-48.818	4	0.165
HD 217987	M	4485	1846	8.759	32	0.165
HD 218354	V	3867	592	-10.368	5	0.097
HIP 114156	V	4839	467	15.298	4	0.031
HD 218445	V	3795	858	27.606	7	0.199
HD 218566	V	4548	1595	-37.825	31	0.119
HIP 114411	M	4067	793	-6.676	7	0.131
HD 218868	V	4420	1245	-30.613	70	0.101



TABLE 3 — *Continued*

Star Name	Template <sup>a</sup>	<JD> -2450000	$\Delta T$ (days)	<RV> (km s <sup>-1</sup> )	Obs	$\sigma_{RV}$ (km s <sup>-1</sup> )
HD 218935	V	5376	0	-9.811	1	...
HD 219396	V	3822	650	-46.903	5	0.119
HIP 114587	V	3937	680	2.493	6	0.180
HD 219134	V	4023	2135	-18.560	151	0.127
HD 219428	V	3978	769	-6.478	10	0.154
HD 219498	V	4461	1238	-9.499	6	0.087
HD 219538	V	4367	1506	9.967	45	0.109
HIP 114914	V	3603	0	-12.124	1	...
HD 219542	V	3421	364	-10.995	2	0.005
HD 219623	V	4975	510	-27.153	5	0.114
HD 219553	V	4533	451	3.458	5	0.101
HIP 115004	V	5193	10	27.132	3	0.080
HD 219770	V	4226	405	8.483	2	0.013
HD 219781	V	3832	679	-20.145	8	0.234
HD 219828	V	3867	592	-24.104	7	0.075
HD 219834b	V	4395	1432	10.752	29	0.097
HD 219953	V	3793	381	-48.231	2	0.047
HD 220122	V	4865	859	-46.327	13	0.124
HD 220182	V	3972	734	3.437	2	0.292
HIP 115332	M	4092	733	-6.504	3	0.034
HD 220221	V	4120	1771	-13.568	4	0.123
HD 220339	V	4633	1621	33.984	41	0.112
HIP 115562	M	3967	2137	-33.184	7	0.071
HD 220845	V	3749	4	-7.269	4	0.076
HD 220908	V	4014	650	-13.666	2	0.067
HD 220952	V	4686	932	-15.604	9	0.115
HD 221149	V	4226	405	-7.161	2	0.055
HD 221354	V	4380	2039	-25.113	186	0.122
HD 221356	V	4705	1649	-12.625	3	0.081
HIP 116215	V	4722	2	-0.640	4	0.127
HD 221504	V	4668	796	-1.391	5	0.133
HD 221561	V	4024	0	18.685	1	...
WASP4	V	5378	0	57.414	1	...
HD 221822	V	3722	148	-12.709	5	0.142
HD 221851	V	4177	1771	-21.201	4	0.058
HD 221974	V	4293	405	-26.035	3	0.074
HD 222038	V	3753	393	-22.881	3	0.019
HD 222089	V	5377	0	-3.161	1	...
HD 222112	V	4632	854	-12.685	7	0.076
HAT-P-6	V	4319	1353	-22.390	18	0.104
HD 222404	V	4371	0	-44.036	2	0.024
HD 222335	V	4322	30	-7.296	7	0.072
HD 222368	V	4085	0	5.846	2	0.019
HD 222391	V	3803	768	-2.850	4	0.118
HIP 116838	V	4783	364	-18.154	6	0.121
HD 222582	V	4809	1035	12.032	7	0.117
GJ 905	M	4581	745	-77.715	8	0.124
HD 222697	V	3954	766	14.534	2	0.106
HD 222986	V	3829	748	-3.355	11	0.082
HIP 117197	V	4888	469	-20.792	19	0.116
HD 223171	V	4256	0	14.836	2	0.013
HD 223205	V	3695	2	-43.921	3	0.079
HD 223238	V	3571	0	-15.254	1	...
HIP 117386	V	3695	2	-10.935	3	0.128
HD 223315	V	3974	739	0.017	2	0.236
GJ 908	M	4469	1801	-71.084	52	0.169
HIP 117492	V	4816	469	-12.262	5	0.173
HD 223498	V	4119	1289	-24.005	3	0.037
HIP 117559	V	5164	324	-3.701	7	0.182
HD 223627	V	4755	736	-52.620	5	0.134
HD 223691	V	3422	367	1.494	2	0.146
HD 223869	V	5381	0	15.833	1	...
HD 224040	V	4226	405	9.641	2	0.011
HIP 117886	M	4565	1422	-1.903	19	0.141
HIP 117946	V	4972	657	-11.442	9	0.114
HD 224383	V	3598	746	-31.245	3	0.110
HIP 118261	V	5054	657	1.702	28	0.131
HD 224601	V	4219	405	-49.248	4	0.067
HD 224619	V	4367	424	21.009	31	0.108
HIP 118310	V	5189	3	6.494	3	0.037
HD 224679	V	4684	817	-17.394	9	0.114
HD 224693	V	3885	1830	1.396	29	0.113

<sup>a</sup> We used the Vesta spectrum as a template when V is listed, and a spectrum for HIP 80824 as a template when M is listed.<sup>b</sup> 2MASS IDs.



TABLE 4  
 RADIAL VELOCITIES DIFFERENT BY OVER 2 KM S<sup>-1</sup> FROM PULKOVA

HD	HIP	Present	Pulkova	Comment
1293	1365	45.14	42.9	PRV var: +0.080 km/s/yr
3795	3185	-45.481	-47.4	PRV var: +0.12 km/s/yr
11616	8872	-11.79	35.5	Double line, SB2: ~50 km/s
11970	9199	-14.377	-7.2	SB1, K=5km/s, P=25yr
—	13447	-1.291	14	No PRV
27990	20679	42.593	37.9	No PRV
28192	20752	-4.138	-6.2	No PRV
30649	22596	32.241	28.7	SB1 binary: K=1.5 km/s, P=24yr
31412	22919	42.118	47	SB1 binary: K=5.9 km/s, P=42yr, e=0.90
31543	22960	-6.94	-9.3	SB1 binary: K=0.7 km/s, P=4.5yrs
38308	27153	43.522	28	No PRV
39251	27791	-9.594	-16.9	No PRV
61364	37337	-10.536	-13.8	No PRV; Known double star
64730	38730	15.976	18.8	PRV var: K = 0.14 km/s
—	41443	55.036	34.4 9	PRV: sigma=0.005 km/s (constant) during 1.2 yr. Long Period binary?
76078	43870	-34.605	-18	GCS ;No PRV
88638	50180	49.355	38.1	No PRV
96626	54428	23.107	-3.1	No PRV
100069	56185	-7.674	-20.8	No PRV
—	62794	9.818	-4.5	double line spectroscopic binary
—	63510	-13.74	-11.2	binary, K=1.2 km/s, P=15 yr
117987	66229	-74.955	-71.9	No PRV
126831	70776	19.391	21.5	No PRV
128642	70857	-35.902	-50.3	known spectroscopic binary
132425	73314	-10.219	-15.3	No PRV
133233	73652	1.537	-7.6	known probable binary
134439	74235	-119.632	310.4	Companion to HIP 74234
135148	74491	-96.007	-90.9	No PRV
137631	75663	-50.093	-58.3	No PRV
138278	75881	-12.712	-8.6	No PRV
146434	79749	-52.566	-34.6	No PRV
150122	81476	-58.657	-37.1	SB2 spectroscopic binary
158038	85294	19.632	13.5	binary, +0.1km/s/yr
180053	94465	-5.874	10	PRV: planet, k=.05km/s
182407	95401	-30.323	-27.7	known binary, +0.3km/s/yr
187091	97279	-14.941	0.0	double line binary; (Welsh et al. 2011; Burkart et al. 2012)
193342	99987	-24.246	-18.9	known binary, k=0.5km/s, p=5yr
199178	103144	-10.198	-26	probable binary, 0.5km/s/yr
—	112918	-7.787	-4.2	HIC ;precise RVs agree
223171	117320	14.836	32.6	Known Binary, K=3.6 km/s, P=0.7yr

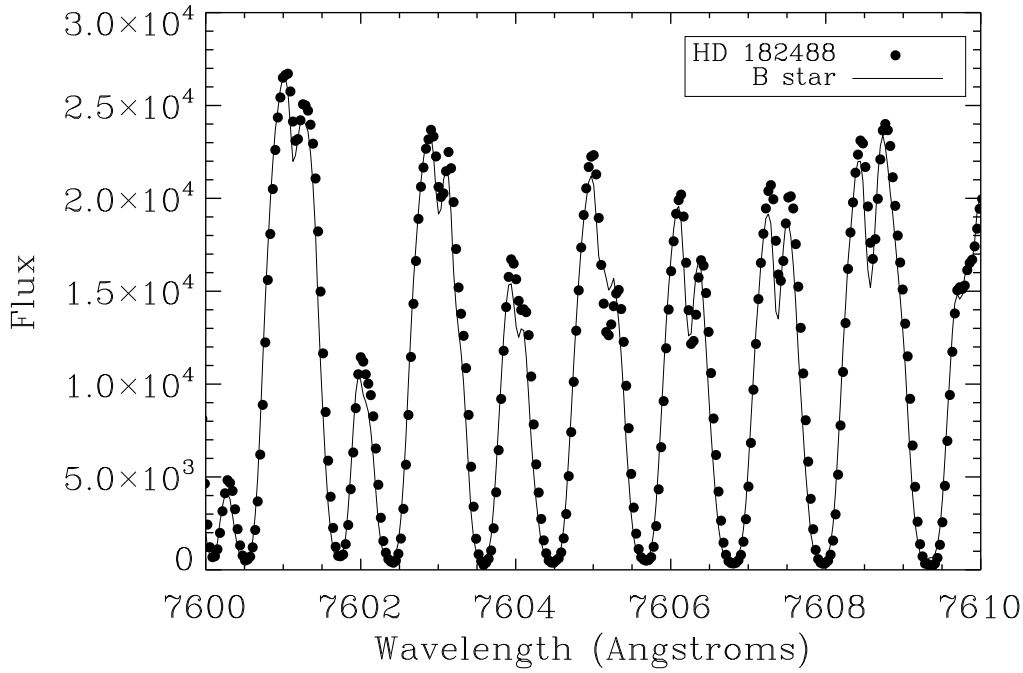


FIG. 1.— Telluric A band seen in both the reference B star, HD 79439 (solid line) and the program star, HD 182488 (dots). Careful inspection shows that the telluric lines in the spectrum of the program star are slightly displaced redward of those in the B star by 0.437 pixels, due primarily to a difference in the zero-points of the two wavelength scales caused by instrumental effects. We remove these differences in wavelength zero-point to within a hundredth of a pixel by  $\chi^2$  fitting of one spectrum to the other, with the displacement the free parameter. This yields final radial velocities precise to better than  $0.1 \text{ km s}^{-1}$ .

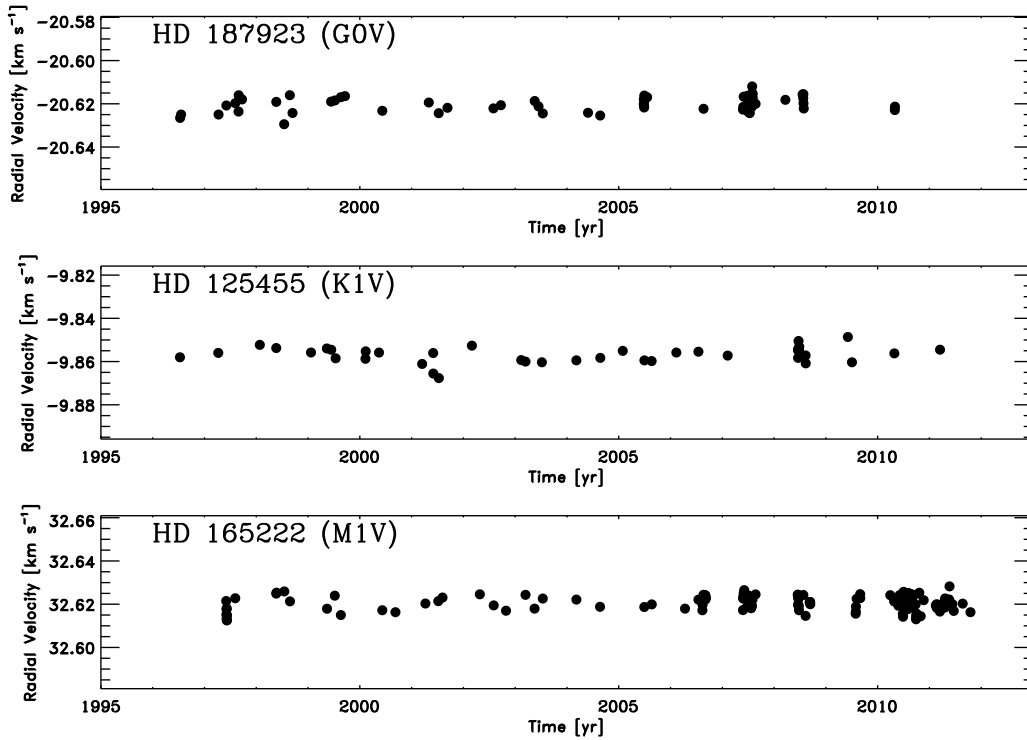


FIG. 2.— Precise measurements of barycentric radial velocity vs. time for three representative standard stars listed in Tables 1 and 2. These relative radial velocities are measured using iodine gas in absorption at the telescope, providing the wavelength scale superimposed directly on the stellar lines (Marcy & Butler 1992), and yield a typical precision of  $0.002 \text{ km s}^{-1}$  ( $2 \text{ m s}^{-1}$ , RMS). The zero-point of these velocities is determined using the present technique that employs telluric lines, and the relative velocities come from the iodine-based measurements. The three standard stars exhibit velocity variation of less than  $0.020 \text{ km s}^{-1}$  (RMS) during a time span of over 10 years, meeting the criteria for status as a standard star in this paper.

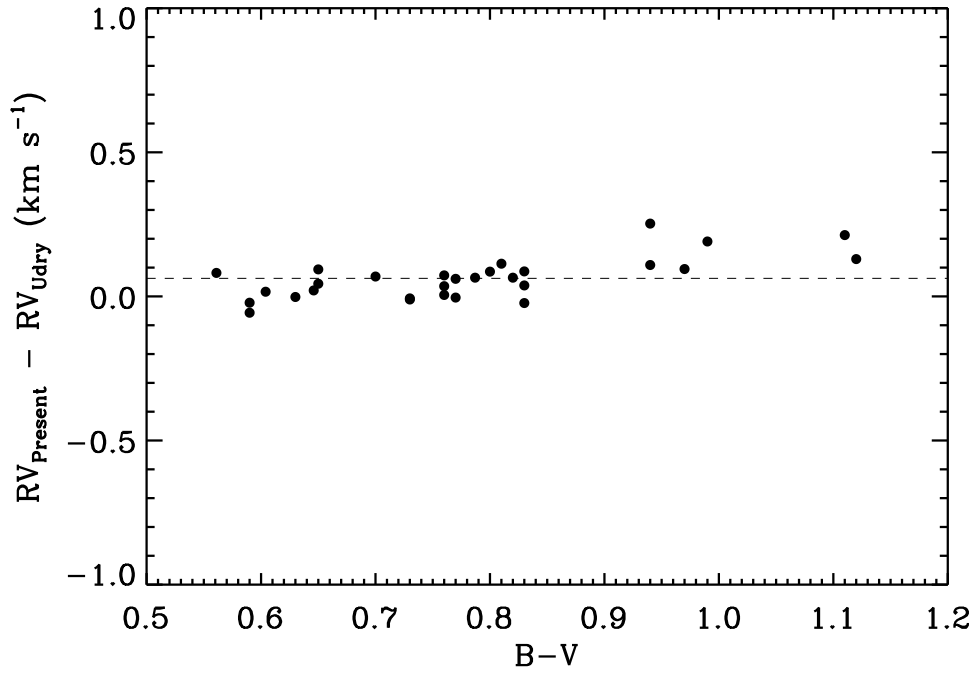


FIG. 3.— Difference in radial velocities of standard stars between those measured here and those from Udry et al. (1999a), for all stars in common, as a function of B-V color. The RMS scatter is  $0.072 \text{ km s}^{-1}$ , and the means of the two sets of radial velocities differ by, (present-Udry) =  $0.063 \text{ km s}^{-1}$ . However, there is clear evidence of a systematic trend in the difference in the velocity zero-points with stellar color such that the present-Udry velocities increase by  $0.15 \text{ km s}^{-1}$  between G0 and M0 stars. The origin of this difference is difficult to trace.

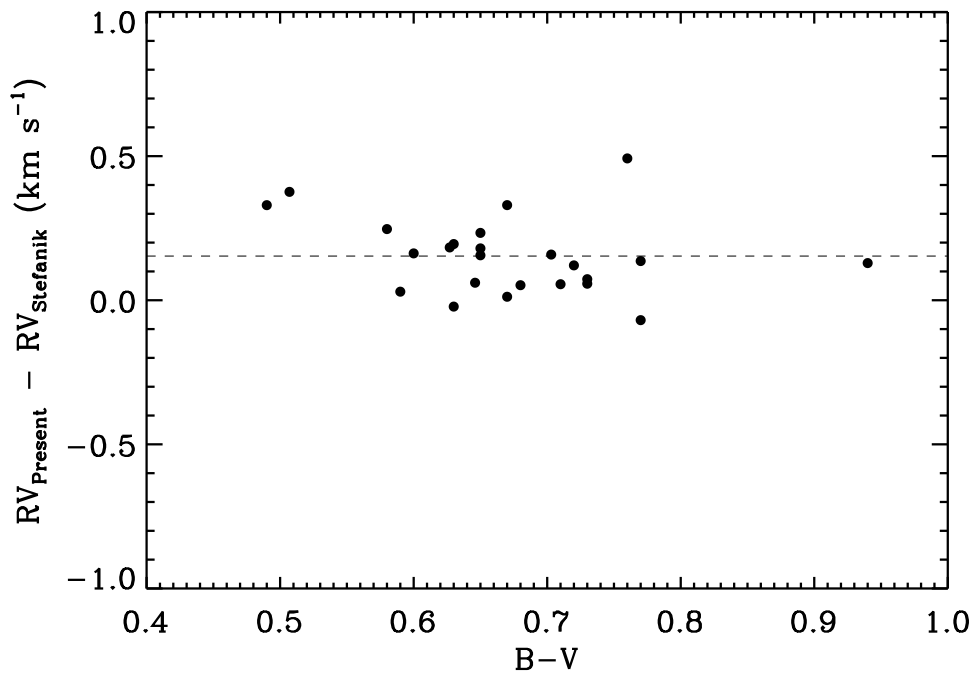


FIG. 4.— Difference in radial velocities of standard stars between those measured here and those from Stefanik et al. (1999), for 25 standards in common. The RMS scatter is  $0.13 \text{ km s}^{-1}$  and the means of the two sets of radial velocities differ by (present-Stefanik) =  $+0.15 \pm 0.026 \text{ km s}^{-1}$ . Apparently these two sets of standard stars have velocities consistent at the level of  $0.15 \text{ km s}^{-1}$ . Doppler measurements of asteroids raises the CfA zero-point by  $0.139 \text{ km s}^{-1}$ , bringing the two zero-points to agreement within  $0.01 \text{ km s}^{-1}$ .

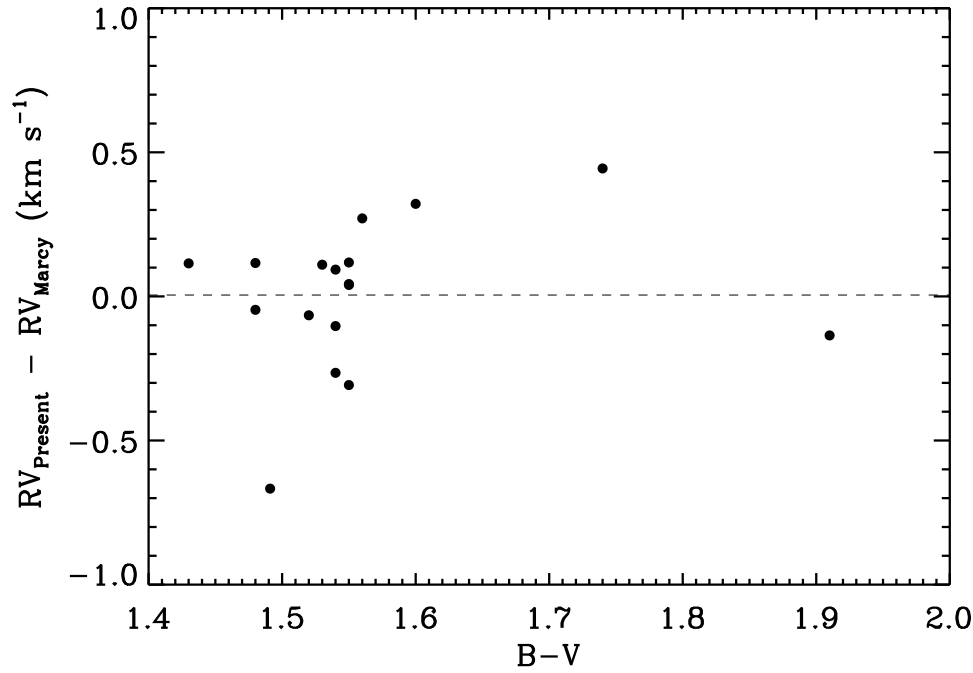


FIG. 5.— Difference in radial velocities of M dwarfs deemed standard stars between the velocities measured here and those from Marcy et al. (1987). The differences have an RMS scatter of  $0.26 \text{ km s}^{-1}$  and a zero-point difference of  $+0.007 \text{ km s}^{-1}$  which is insignificant. The level of agreements between these sets of velocities implies errors of no more than  $0.26 \text{ km s}^{-1}$ , most of which likely comes from velocity errors in Marcy et al. (1987)

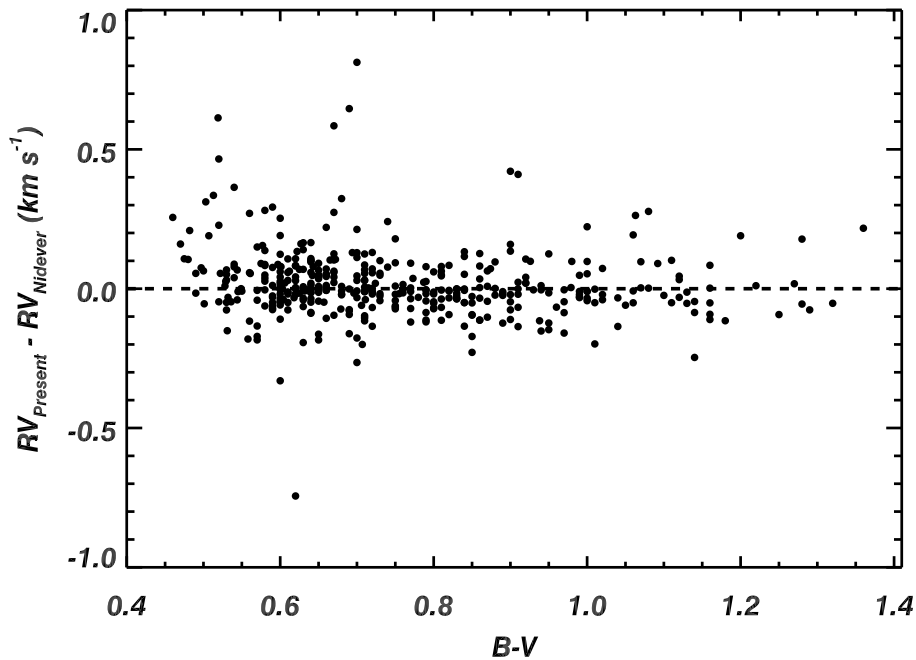


FIG. 6.— Difference between present velocities and those of Nidever et al. (2002) for all 428 F,G, and K stars in common plotted versus  $B-V$ . The scatter of  $0.1 \text{ km s}^{-1}$  demonstrates that the present velocities agree with those of Nidever et al. (2002) with a joint RMS of  $0.1 \text{ km s}^{-1}$ , and that they share a common zero-point and velocity scale. There are six stars with a velocity difference (present minus Nidever et al.) larger than  $0.5 \text{ km s}^{-1}$  namely HD 87359 ( $+0.81 \text{ km s}^{-1}$ ), HD 114174 ( $+0.58 \text{ km s}^{-1}$ ), HD 180684 ( $+0.61 \text{ km s}^{-1}$ ), HD 196201 ( $+0.65 \text{ km s}^{-1}$ ), and HD 91204 ( $-0.74 \text{ km s}^{-1}$ ), and HD217165 ( $-2.2 \text{ km s}^{-1}$ ). All are clearly binary stars as confirmed by coherent variations of over  $0.5 \text{ km s}^{-1}$  in our iodine-based *relative* RV measurements for each of them.

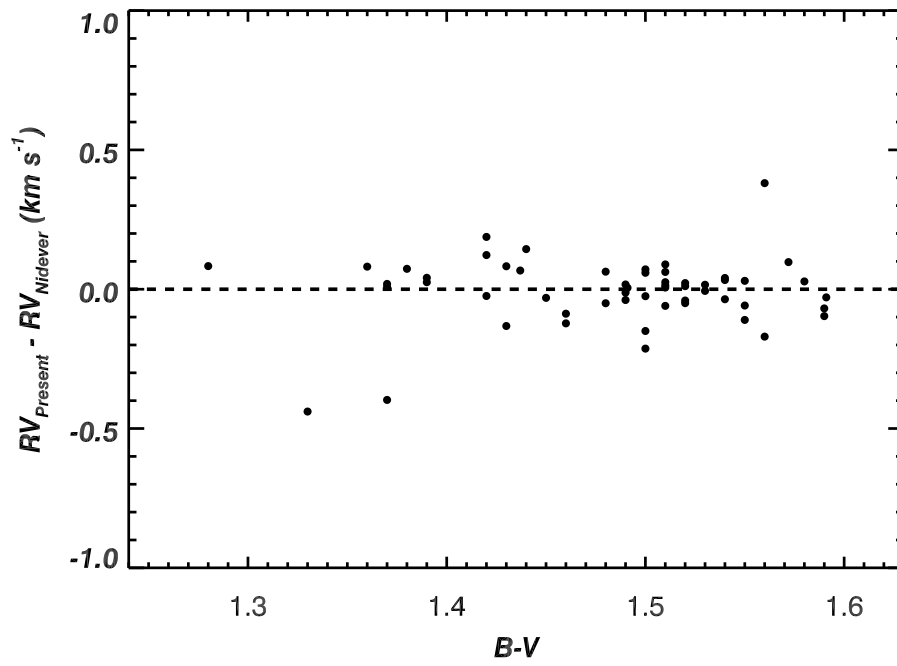


FIG. 7.— Difference between present velocities and those of Nidever et al. (2002) for all 52 M dwarfs in common. The RMS of  $0.13 \text{ km s}^{-1}$  implies errors of no more than that magnitude for the M dwarfs in both sets.

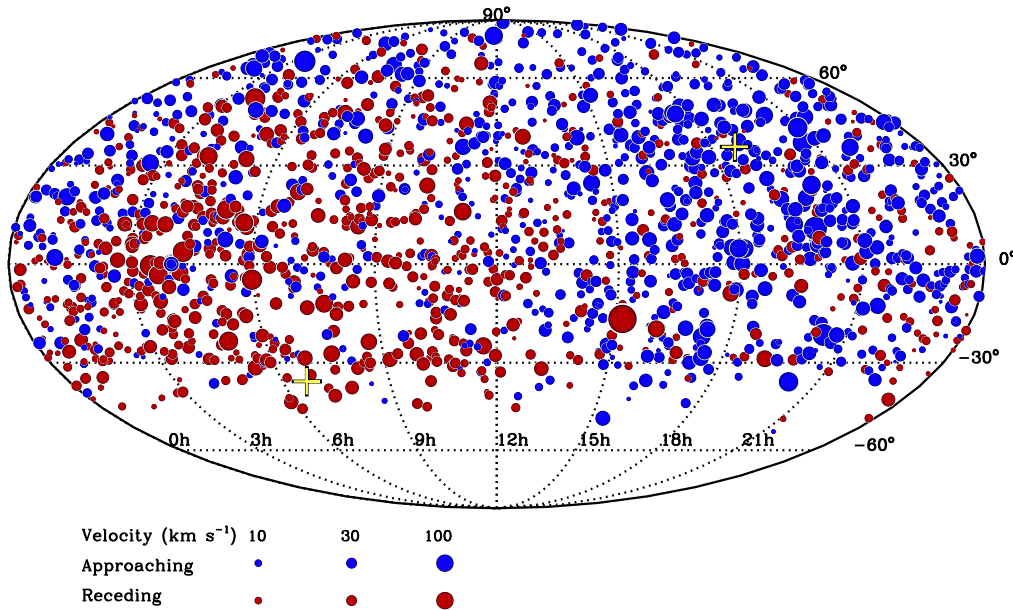


FIG. 8.— Location on the celestial sphere and the radial velocities relative to the barycenter of the Solar System of the 2046 FGKM stars in the Solar neighborhood presented here. The radial velocities are color-coded, with blue and red corresponding to approaching and receding stars, respectively, relative to the solar system barycenter. The diameter of the dot is proportional to the square root of the absolute value of the radial velocity (see the key). The coordinates are equatorial in a Mollweide projection. Stars are located at all RA and northward of Dec = -50 deg. The large number of stars near the equator, as well as in the north and south, offers a variety of different spectral types as reference stars accessible from ground-based observatories worldwide. The Solar Apex is marked with a cross at RA = 18 hr 40 min, DEC = +35 deg 58 min, indicating the direction of the Sun's velocity vector relative to nearby G dwarfs (Abad *et al.* 2003). The solar antapex is also marked. The large red dot at RA~15hr 10 min and DEC~-16 deg represents two stars, HD 134439, HD 134440 (both metal poor halo stars) receding at 309.4 and 310.0 km s<sup>-1</sup>, respectively, approaching the escape velocity (550 km s<sup>-1</sup>) of the Milky Way Galaxy. The star with the greatest blueshift is HD 188510 (RA = 19 55 9.6, DEC = +10 44 27), approaching at 192.6 km s<sup>-1</sup>.